

**BINDING CHARACTERIZATION OF SULFONAMIDE ANTIBIOTICS  
AND POLYCYCLIC AROMATIC HYDROCARBONS TO MICELLES  
USING SEMI-EQUILIBRIUM DIALYSIS (SED) AND  $^1\text{H}$  NMR  
SPECTROSCOPY**

by

Ashish Kumer Sarker

A thesis submitted to the Department of Chemistry

In conformity with the requirements of the

degree of Doctor of Philosophy

Queen's University

Kingston, Ontario, Canada

March, 2016

Copyright ©Ashish Kumer Sarker, 2016

## Abstract

Micellar enhanced ultrafiltration (MEUF) has been shown to be an effective removal technique for a variety of trace contaminants in wastewater, especially for low molecular weight organic contaminants. In MEUF, contaminants first partition into surfactant micelles prior to removal by ultrafiltration, where the contaminants are below the molecular weight cut-off of the ultrafiltration membrane but the micelles are above the cut-off. To predict the removal efficiency of MEUF, it is important to measure of extent to which a species will bind to a micelle as well as to develop an understanding of the dynamics of the binding interactions. Herein, we report micellar binding constants for a series of sulfonamide antibiotics (sulfadoxine, sulfathiazole, sulfamethoxazole, sulfamerazine, sulfadiazine, sulfamethazine, sulfacetamide, sulfaguanidine, and sulfanilamide) with CTABr micelles, as determined using semi-equilibrium dialysis and  $^1\text{H}$  NMR methods. We also report the binding constant measurements for polycyclic aromatic hydrocarbons (PAHs), including phenanthrene, naphthalene, pyrene and fluorene, to several micelle types. Unlike the antibiotics, where charge-charge interactions determined binding to CTABr micelles, the neutral PAHs show strong binding with micelles because of hydrophobic interactions. Our results enabled us to develop a relationship between binding constant ( $\text{Log } K_B$ ) and  $\text{Log } K_{OW}$  for both charged and neutral compounds, which will be useful for predicting MEUF performance for removal of organic micro contaminants from wastewater.

## **Co-Authorship**

All the work contained in this thesis was done by the author in the Department of Chemistry at Queen's University under the supervision of Dr. Stephen Brown. In chapter 3, data for the free sulfonamide equilibration experiment was collected from the work done by Hilary Chung. In chapter 4, NMR data of the six sulfonamides were collected from the work done by Patrick J. Cashin. Only three sulfonamides (sulfanilamide, sulfadoxine and sulfamethazine) pertaining to NMR experiments were done by the author. Dr. Stephen Brown has reviewed all the data and aided in preparing manuscripts.

## Acknowledgements

I humbly express my deepest sense of gratitude to my supervisor, Dr. Stephen Brown for his amicable, friendly and thoughtful supervision. His encouragement, consistent support and positive comments paved the way in materializing my dream into reality.

I am also grateful to Dr. Philip Jessop and Dr. Erwin Buncel for their serving on my supervisory committee member. I would also like to thank Dr. Franciose Saurial and Dr. Igor Kozin for their training and support in using NMR spectroscopy and HPLC respectively. I would also like to thank Dr. Fern McSorley for her initial help to set up spectrofluorometer, and Dr. David Zechel for his support in using spectrofluorometer. I would also like to thank Dr. Vimal K. Balakrishnan and Dr. Kirsten Exall of Environment Canada for their advice and suggestions relevant to this project.

I would also like to thank Dr. Michelle Douma, Dr. Ray Bowers and all other group members of Dr. Brown for their help and co-operation. I would also like to acknowledge Environment Canada and Queen's University School of Graduate Studies and Research, and the Department of Chemistry for their financial support.

I would like to acknowledge my parents for their encouragement and support throughout this study. I would also like to express my greatest acknowledgement to my wife Anupama Biswas for her support in each and every critical stage of this journey. Finally, I would like to express my deepest acknowledgment to my little son Aditya and my daughter Nabonita whose relentless love and smile were the potential sources of strength, dedication and motivation in order to achieve this goal.

## **Statement of Originality**

I hereby certify that all of the work described within this thesis is the original work of the author. Any published (or unpublished) ideas and techniques from the work of others are fully acknowledged in accordance with the standard referencing practices

(Ashish Kumer Sarker)

(March, 2016)

# Table of Contents

<b>Abstract</b>	<b>ii</b>
<b>Co-Authorship</b>	<b>iii</b>
<b>Acknowledgements</b>	<b>iv</b>
<b>Statement of Originality</b>	<b>v</b>
<b>List of Figures</b>	<b>xi</b>
<b>List of Tables</b>	<b>xiv</b>
<b>List of Abbreviations</b>	<b>xv</b>

## Chapter 1-Introduction

1.1 General Introduction	1
1.2 Organic contaminants in the wastewater	3
1.2.1 Sulfonamides	4
1.2.2 Polycyclic Aromatic Hydrocarbons (PAHs)	6
1.3 Conventional wastewater treatment options	7
1.3.1 Primary treatment (mechanical)	12
1.3.2 Secondary treatment (biological)	12
1.3.3 Tertiary treatment (chemical)	14
1.3.4 Limitations for Sulfonamides and PAHs	14
1.4 Oil-sands produced water (OSPW)	15
1.4.1 Conventional OSPW treatment process	16
1.4.2 Limitations for OSPW	17
1.5 Advanced wastewater treatment by filtration	18
1.5.1 Limitation of membrane filtration	20
1.5.2 Micellar Enhanced Ultrafiltration (MEUF)	21
1.6 Objective of the research	22
1.7 Scope of the research	23
1.8 References	24

## Chapter 2-Literature review

2.1 Surfactant and micelle formation-----	33
2.1.2 Classification of surfactants-----	37
2.1.2.1 MEUF using cationic surfactant -----	38
2.1.2.2 MEUF using anionic surfactant-----	40
2.1.2.3 MEUF using, switchable surfactant-----	40
2.2 Binding of contaminants to micelles-----	41
2.2.1 Separation of bound contaminants using MEUF-----	42
2.3 Measuring of binding constants-----	43
2.3.1 Binding constant by Fluorometer-----	45
2.3.2 Binding constant by micellar High Performance Liquid Chromatography-----	47
2.3.3 Binding constant by micellar electrokinetic chromatography-----	49
2.3.4 Binding constant by SED-----	52
2.3.5 Binding constant by <sup>1</sup> H NMR spectroscopy-----	56
2.4 Characterizing of binding constant-----	58
2.4.1 Binding constant (Log $K_B$ ) and its co-relation with Octanol-Water (Log $K_{OW}$ )-----	59
2.4.2 Binding constant (Log $K_B$ ) and its co-relation with Free energy-----	61
2.5 References-----	62

## Chapter 3- Determining binding of sulfonamide antibiotics to CTABr micelles using semi-equilibrium dialysis techniques

3.1 Introduction -----	71
3.2 Materials and methods-----	73
3.2.1 Materials -----	73
3.2.2 Semi-equilibrium dialysis method-----	73
3.2.3 Sample preparation-----	74
3.2.4 Analysis procedure-----	75
3.2.5 CMC determination -----	75
3.2.6 Characterizing the SED method -----	76
3.3 Results and discussion-----	78

3.3.1 Determination of binding constants by SED-----	78
3.3.2 Physico-chemical applications of micellar binding constants -----	83
3.3.3 Use of micellar binding constants to describe MEUF potential-----	87
3.4 Conclusions -----	87
3.5 References-----	88

**Chapter 4- Understanding binding of sulfonamide antibiotics to CTABr micelles using <sup>1</sup>H NMR spectroscopy**

4.1 Introduction-----	91
4.2 Materials and methods-----	93
4.2.1 Materials-----	93
4.2.2 Sample preparation-----	94
4.2.3 <sup>1</sup> H NMR studies-----	94
4.2.4 CMC determination-----	95
4.3 Results and discussion-----	96
4.3.1 NMR spectra in D <sub>2</sub> O with CTABr-----	96
4.3.2 Determining Locus and orientation of the sulfonamide-----	99
4.3.3 Determination of binding constant of sulfonamides with CTABr micelles -----	102
4.4 Conclusions-----	106
4.5 References -----	107

**Chapter 5- Determining binding of polycyclic aromatic hydrocarbons to CTABr micelles using semi-equilibrium dialysis techniques**

5.1 Introduction-----	109
5.2 Experimental -----	111
5.2.1 Materials and methods-----	111
5.2.2 Spectrofluorometric measurement-----	113
5.2.3 Conductivity measurement-----	114
5.2.4 Characterizing SED method-----	115
5.3 Results and discussion -----	116



5.3.1 Surfactant concentration, CMC and PAH concentrations-----	116
5.3.2 Determination of MDL and LOQ-----	118
5.3.3 Determination of the binding constant of PAH-----	119
5.3.4 Statistical analysis of the variances of binding constant-----	124
5.4 Conclusions-----	126
5.5 References -----	126

**Chapter 6- Determining binding of polycyclic aromatic hydrocarbons to micelle formed by SDS and SOL using semi-equilibrium dialysis**

6.1 Introduction-----	128
6.2 Experiment-----	131
6.2.1 Materials and methods-----	131
6.2.2 Spectrofluorometric measurement-----	133
6.2.3 Conductivity measurement-----	133
6.2.4 Characterizing SED method-----	134
6.3 Results and discussion-----	136
6.3.1 Surfactant concentration, CMC and PAH concentrations-----	136
6.3.2 Determination of the binding constant of PAH-----	137
6.4 Conclusions-----	141
6.5 References -----	142

**Chapter 7 - Summary and Future Work**

7.1 Summary of chapters-----	144
7.2 General conclusions-----	145
7.3 Future work-----	147
7.4 References -----	150

**Appendix**

Appendix A: Additional data for chapter 3 -----151  
Appendix B: Additional data for chapter 4-----155  
Appendix C: Additional data for chapter 5-----160  
Appendix D: Additional data for chapter 6 -----166

## List of Figures

<b>Fig. 1.1.</b> Various pathways of pharmaceutical residues in the aquatic environment-----	5
<b>Fig. 1.2.</b> Generic wastewater collection and treatment system-----	8
<b>Fig. 1.3.</b> Flow diagram of the conventional wastewater treatment system-----	13
<b>Fig. 1.4.</b> Effective size ranges of different filtration systems-----	19
<b>Fig. 1.5. (a)</b> Structure of a Surfactant <b>(b)</b> Micellar enhanced ultra filtration-----	22
<b>Fig. 2.1.</b> Micelle formation process: a) A surfactant as dissolved substance b) Adsorption of surfactant at the air-water interface c) a monolayer of surfactants is formed at the interfaces d) formation of micelles-----	33
<b>Fig. 2.2.</b> Thermodynamic cycle of micelle formation-----	35
<b>Fig. 2.3.</b> Diagram of the apparatus of measuring substrate binding by rate of dialysis-----	44
<b>Fig. 2.4.</b> Effect of the Triton X-100 concentration on the fluorescence emission of PAS-S at an excitation wavelength of 412 nm and 1 M HCl media-----	47
<b>Fig. 2.5.</b> Variation of $1/k'$ vs micellized SDS concentration in solution. Mobile phase phase: 0.1M NaCl/SDS (a) benzene derivatives (b) naphthalene derivatives-----	49
<b>Fig. 2.6.</b> Variation of the capacity factor ( $k'$ ) for benzene derivatives as a function in 0.05 M CHES buffer modified with 3% n-propanol-----	51
<b>Fig. 2.7.</b> Cross-sectional representation of a CTABr Micelle-----	53
<b>Fig. 2.8.</b> In house prepared SED cell-----	54
<b>Fig. 2.9.</b> Schematic diagram of the Semi Equilibrium Dialysis (SED) process-----	55
<b>Fig. 2.10.</b> Binding curve of $\alpha$ -Cyclodextrin. The filled circles correspond to the experimental data points; the smooth curve is the best (spline-smoothed) fit of the data point-----	58
<b>Fig. 3.1.</b> (a) Semi-equilibrium dialysis cell and (b) illustration of separation behaviour across the dialysis membrane -----	74
<b>Fig. 3.2.</b> Conductivity of CTABr solutions. The discontinuity between two linear ranges indicates the CMC value of CTABr (0.92 mM)-----	76

<b>Fig. 3.3.</b> Concentration of sulfadiazine on permeate side of SED cell to confirm equilibration of free sulfadiazine by 24 h. Sulfadiazine concentration was determined by HPLC with UV detection-----	77
<b>Fig. 3.4.</b> Conductivity measurement over time showing diffusion of CTABr surfactant in the SED cell from the Retentate to the Permeate. The surfactant concentration in the permeate was below or close to the CMC up to 24 h-----	78
<b>Fig. 3.5.</b> Linear Free Energy Relationship indicating the correlation ( $r^2 = 0.53$ ) between $\text{Log } K_B$ and $\text{Log } K_{OW}$ for sulfonamide antibiotics binding to CTABr-----	84
<b>Fig. 3.6.</b> Linear Free Energy Relationship depicting the correlation ( $r^2 = 0.78$ ) between $\text{Log } K_{OW}$ and $\text{p}K_{a2}$ for sulfonamide antibiotics binding to CTABr-----	84
<b>Fig. 3.7.</b> Protonation/deprotonation equilibria of sulfonamides showing positive, neutral and negative forms-----	85
<b>Fig. 3.8.</b> Modified $\text{Log } K_B$ plotted against $\text{Log } K_{OW}$ for the sulfonamides -----	86
<b>Fig. 4.1.</b> Conductivity of CTABr solutions in $\text{D}_2\text{O}$ . The discontinuity between two linear ranges indicates the CMC value of CTABr-----	95
<b>Fig. 4.2.</b> NMR spectrum of sulfamethazine in $\text{D}_2\text{O}$ with and without 10 mM CTABr-----	96
<b>Fig. 4.3.</b> Change in relative chemical shift of hydrogens as a function of CTABr concentration. Relative chemical shift values are shown where the chemical shift for each proton in the absence of CTABr was subtracted from each measured chemical shift-----	99
<b>Fig. 4.4.</b> Proposed locus and orientation of sulfonamide molecules in CTABr micelles-----	101
<b>Fig. 5.1.</b> (a) Semi-equilibrium dialysis cell and (b) illustration of separation behaviour across the dialysis membrane after addition of CTABr micelle/PAHs mixture-----	112
<b>Fig. 5.2.</b> Determination of critical micelle concentration (CMC) of CTABr in 1.25% ethanol by identifying the concentration where discontinuity of the two conductivity plot between lower and higher concentration range calibration curve was observed-----	114
<b>Fig. 5.3.</b> Equilibrium experiment of CTABr in SED-----	115
<b>Fig. 5.4.</b> Binding correlation of PAHs with $\text{Log } K_{OW}$ -----	122
<b>Fig. 6.1.</b> Chemical structure of (a) Sodium dodecyl Sulphate (SDS); and (b) Sodium Laurate (SOL)-----	130

**Fig. 6.2.** (a) Semi-equilibrium dialysis cell and (b) illustration of separation behaviour across the dialysis membrane after addition of SDS micelle/PAH mixture or SOL micelle/PAH mixture-----132

**Fig. 6.3.** Determination of critical micelle concentration (CMC) of SDS and SOL in 1.25% ethanol by identifying the concentration where discontinuity of the two conductivity plot between lower and higher concentration range calibration curve was observed-----134

**Fig. 6.4.** (a) Conductivity measurement over time showing diffusion of SOL surfactant in the SED cell from the retentate to the permeate. (b) Concentration of pyrene on permeate side of SED cell to confirm equilibration of free pyrene by 24 h-----135

**Fig. 6.5. (a)** Binding correlation of PAHs in SDS with the Log  $K_{OW}$  **(b)** binding correlation of PAHs in SOL with Log  $K_{OW}$ -----140

## List of Tables

<b>Table 1.1.</b> Examples of different organic compounds in wastewater-----	4
<b>Table 2.1.</b> Classification of surfactants-----	38
<b>Table 3.1.</b> Concentration of sulfonamides and surfactant (CTABr) in the retentate side (R) and permeate side (P) after 24 h equilibration in the SED experiment-----	79
<b>Table 3.2.</b> Binding constant ( $K_B$ ) between sulfonamides and CTABr determined by SED analysis-----	81
<b>Table 4.1.</b> Sample preparation of sulfonamides in D <sub>2</sub> O-----	94
<b>Table 4.2.</b> Log $K_B$ values as determined by NMR spectroscopy shown with corresponding values determined by semi-equilibrium dialysis-----	105
<b>Table 5.1.</b> (a) Lower range and (b) higher range Calibration data of PAHs-----	113
<b>Table 5.2.</b> (a) Analysis of (a) fluorene ----- (b) Pyrene (c) Naphthalene (d) Phenanthrene by spectrofluorometry and CTABr using conductivity in SED experiments at 24 h-----	116 117
<b>Table 5.3.</b> Method detection limit-----	118
<b>Table 5.4.</b> Binding constant between PAHs and CTABr determined by SED-----	121
<b>Table 5.5.</b> Variances of the binding constant with 9 replicates-----	124
<b>Table 5.6.</b> Variances of the binding constant with 3 replicates and compare variances between 9 and 3 replicates through F test-----	125
<b>Table 6.1. (a)</b> Analysis of PAH by spectrofluorometry and SDS using conductivity in SED experiments at 24 h----- (b) Analysis of PAH by spectrofluorometry and SOL using conductivity in SED experiments at 12 h-----	136 137
<b>Table 6.2.</b> Binding constant of PAHs in SOL and SDS-----	139

## List of Abbreviations

ACE	Affinity capillary electrophoresis
AOPs	Advanced oxidation processes
BOD	Biological oxygen demand
CMC	Critical micelle concentration
CE	Capillary electrophoresis
CPC	Cetyl pyridinium chloride
CECs	Contaminants of emerging concern
C <sub>12</sub> TABr	Dodecyltrimethylammonium bromide
C <sub>18</sub> TABr	Octadecyltrimethylammonium bromide
C <sub>14</sub> TABr	Tetradecyltrimethylammonium bromide
CTABr	Cetyltrimethylammonium bromide (Hexadecyltrimethylammonium bromide)
DNA	Deoxyribonucleic acid
Da	Dalton
DOC	Dissolved organic carbon
DEHP	Di-(2-ethylhexyl) phthalate
EOR	Enhanced oil recovery
EDTA	Ethylene diamine tetraacetic acid
FIG	Flow injection gradient
GAC	Granular activated carbon
HDO	Hydrogen-deuterium oxide
HPLC	High Performance Liquid Chromatography
<i>K</i> <sub>ow</sub>	Octanol-water partition co-efficient
LAS	Linear alkylbenzene sulfonate
MPLC	Micellar phase liquid chromatography
MEKC	Micellar electrokinetic chromatography
MEUF	Micellar enhanced ultrafiltration
MWCO	Molecular weight cutoff
MW	Molecular weight
NMR	Nuclear Magnetic Resonance

NF	Nano filtration
NAs	Naphthenic acids
NPEOs	4-Nonylphenoethoxylates
NPECs	4-Nonylphenoethoxycarboxylates
OTABr	Octadecyl trimethyl ammonium bromide
OSPW	Oil sands produced waters
OTABr	Octadecyl trimethyl ammonium bromide
OSPW	Oil sands produced waters
OTABr	Octadecyl trimethyl ammonium bromide
ppb	Parts per billion
ppm	Parts per million
PhACs	Pharmaceutically active compounds
PAHs	Polycyclic aromatic hydrocarbons
RNA	Ribonucleic acid
RO	Reverse osmosis
SDS	Sodium dodecyl sulphate
SOL	Sodium laurate
SED	Semi equilibrium dialysis
TDS	Total dissolved solids
THM	Tri halo methane
TOC	Total organic carbon
USEPA	United States Environmental Protection Agency
UF	Ultrafiltration
UNICEF	United Nations International Children's Emergency Fund
UNESCO	United Nations Educational, Scientific and Cultural Organization
WHO	World Health Organization
WWTP	Wastewater treatment plants



# Chapter 1

## Introduction

### 1.1 General Introduction

Water is recognized as one of the most essential natural resources.<sup>1</sup> The continued exponential growth in human population has created a corresponding demand for fresh water supply.<sup>2</sup> But, there are potential concerns for adverse human and ecological health effects due to water contamination. About 2.3 billion people are suffering from water-borne diseases worldwide (UNESCO, 2003). In developing countries, over 2.2 million people die every year because of unclean water and inadequate sanitation (WHO and UNICEF, 2000). Water-related infectious and parasitic diseases account for approximately 60% of infant mortality across the world.<sup>3</sup> Therefore, it is very important to protect our natural water resources from contamination in order to meet the fresh water demand world wide. Disposal of chemicals from industry, agriculture, health care and domestic activities are the potential sources for water contamination. Water resources might be contaminated because of hydrological cycle, geochemical mobilization, volcanic eruption and other natural disasters. Contaminants from various sources can enter and persist in the aquatic system to a greater extent than previously thought. The ultimate effect of many organic contaminants, particularly hormonally active chemicals,<sup>2</sup> personal care products, and pharmaceuticals,<sup>4,5</sup> is little known. The major concerns for the presence of these compounds in the environment are abnormal physiological processes and reproductive impairment,<sup>6-11</sup> increased incidences of cancer,<sup>12</sup> the development of antibiotic-resistant bacteria,<sup>13-16</sup> and the potential increased toxicity of chemical mixtures.<sup>17</sup> Wastewater effluents are the largest source of pollution by volume to surface water in Canada.<sup>18</sup> Wastewater effluents may contain many

pollutants and substances of concern including grit, debris, suspended solids, disease-causing pathogens, decaying organic waste, nutrients and hundreds of chemicals.<sup>18</sup> An estimated 2 million tons of sewage and other effluents are discharged into water systems around the globe every day. In developing countries the situation is more serious, where more than 90% of raw sewage and 70% of untreated industrial wastes are dumped into surface water.<sup>3</sup> It is not commonly practiced to investigate the removal of pharmaceuticals, personal care products or surfactants from wastewater as there are a few or no regulations on their release into water.<sup>19</sup>

Numerous studies have reported that trace organic compounds are found in the treated wastewater effluent.<sup>20</sup> The type of organic compounds present in the wastewater depends on their sources and degradation. Wastewater treatment plants (WWTP) are designed to remove bulk constituents such as biochemical oxygen demand, suspended solids, and nutrients rather than individual organic chemicals.<sup>21</sup> Therefore, trace organic contaminants and their degradation products are often not completely removed during treatment and are discharged to the natural environment.<sup>2,22,23</sup> Contaminants of emerging concern (CECs), including some personal care products, pharmaceuticals, and steroid hormones are known to be discharged in the effluents of wastewater treatment plants into receiving waters in Canada.<sup>24-30</sup> Studies conducted in Canada have also reported CECs of wastewater origin in drinking water.<sup>31-34</sup> The conventional water treatment processes including coagulation, sedimentation, and filtration is often adequate to remove excess turbidity and suspended solids but it cannot remove small dissolved molecules such as sulfonamides and polycyclic aromatic hydrocarbons (PAHs).

Pressure-driven membrane processes such as microfiltration, ultrafiltration, nanofiltration, and reverse osmosis are powerful tools for separation of a wide range of components from aqueous matrices.<sup>35</sup> Fouling, however, is a problem for the pressure-driven membrane processes. This is

especially applicable for the wastewater treatment system, where the concentration of contaminants which cause fouling is much higher than in the filtration of ground or surface water.<sup>35</sup> In this research, semi equilibrium dialysis (SED) has been proposed as an effective method to develop a model for the removal of trace organic contaminants like sulfonamide antibiotics and polycyclic aromatic hydrocarbons from wastewater. SED operates similar to micellar enhanced ultrafiltration (MEUF), but it is a non-pressure driven membrane separation system that can be set up in the laboratory using a simple apparatus.

## **1.2 Organic contaminants in wastewater**

A wide range of industries manufacture, use and generate complex organic chemicals such as pesticides, pharmaceuticals, paints and dyes, petrochemicals, detergents, and plastics. Organic compounds from feedstock materials, washing and cleaning agents, solvents and value added products, such as plasticizers, can also contaminate wastewater. Benzene, naphthalene, anthracene, cyanide, ammonia, phenols, and cresols, together with a range of more complex organic compounds known as polycyclic aromatic hydrocarbons, are generated from the production of iron.<sup>21</sup> Effluents of the pulp and paper industry contain suspended solids and biological oxygen demand (BOD). The nuclear and radiochemicals industry produce radioactive waste materials. Large-scale industries such as oil refineries, petrochemical plants, chemical plants, and natural gas processing plants commonly release large amounts of oil and suspended solids.<sup>36</sup>

Different organic compounds from the effluent of these industries can be directly or indirectly discharged to water environment. Various studies reported that trace organic contaminants such as surfactant metabolites, metal-chelating agents, antimicrobials, stimulants and deodorizers are

found in wastewater treatment plants (WWTP).<sup>20,21</sup> Several contaminants have been identified in wastewaters, such as alkylphenols, phthalates, phenols, anilines, polycyclic aromatic hydrocarbons, and flame retardants, among others.<sup>37</sup> Trace organic compounds can be classified into different classes as shown in table 1.1.

**Table 1.1.** Examples of different organic compounds in wastewater<sup>38</sup>

<b>Class</b>	<b>Example of compounds</b>
Antimicrobials	Triclosan, triclocarban
Flame-retardants	Tri (2-chloroethyl) phosphate, tributyl phosphate
Fragrances	Menthol, indole
Hormones	17- $\beta$ -estradiol, 17- $\alpha$ -ethynylestradiol, estrone
Metal-chelating agents	Ethylenediaminetetraacetic acid (EDTA), nitrilotriacetic acid
Pharmaceuticals	Acetaminophen, carbamazepime, sulfamethoxazole
Plasticizers	Di-(2-ethylhexyl) phthalate (DEHP)
Surfactant metabolites	4-Nonylphenol, 4-nonylphenolethoxylates (NPEOs) 4-Nonylphenolethoxycarboxylates (NPECs)

### 1.2.1 Sulfonamides

Sulfonamides are the organic compounds which are a class of antimicrobial pharmaceuticals. In recent years, the occurrence and fate of pharmaceutically active compounds (PhACs) in the aquatic environment has been considered as one of the emerging environmental issues.<sup>38-41</sup> Since different PhACs have different physiological and chemical behaviour, their persistence and distribution in the aquatic environment are also different. There are different pathways for the distribution of PhACs in the natural environment.

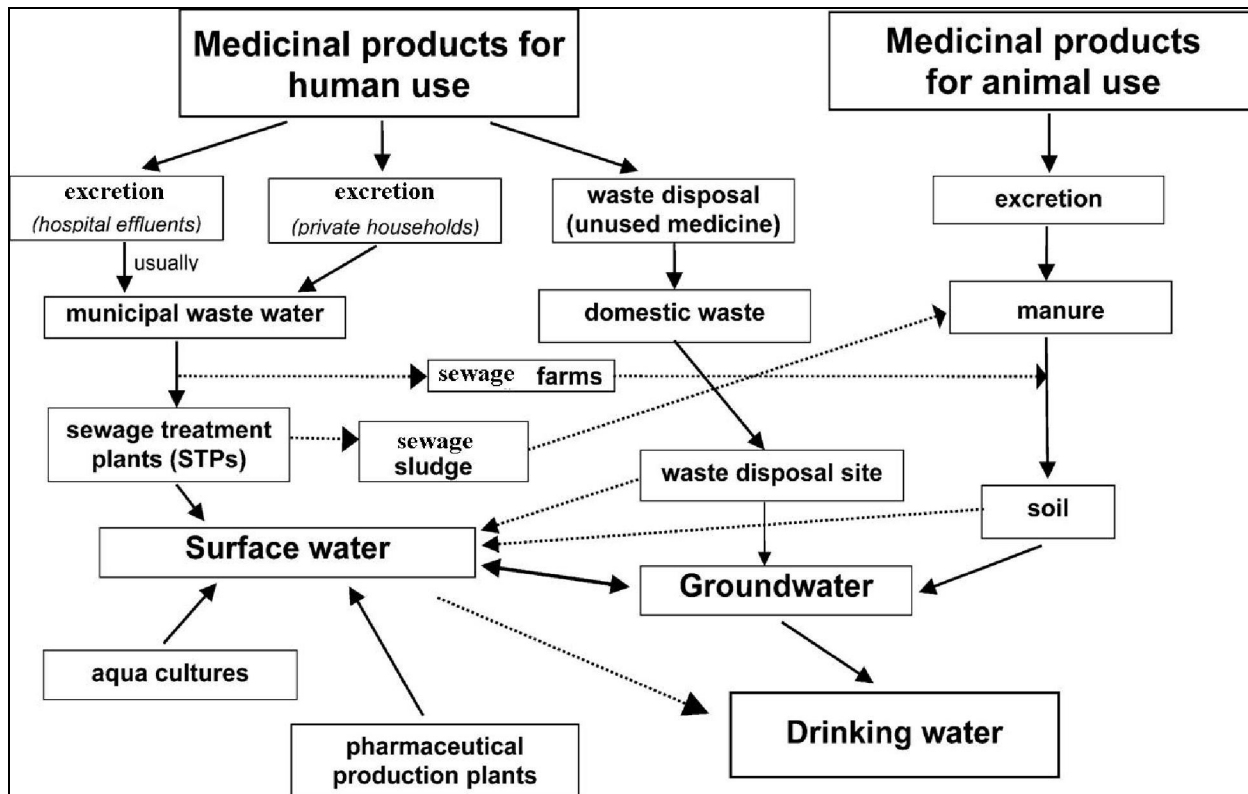


Fig. 1.1. Various pathways of pharmaceutical residues in the aquatic environment (modified).<sup>20</sup>

A major source of PhACs released into the aquatic environment is effluents from municipal sewage treatment plants. Almost all pharmaceuticals administered to humans are excreted in varying degrees and discharged directly into the sewer system. They can be excreted unchanged or partially transformed, mostly conjugated to polar molecules (e.g. glucuronides).<sup>20</sup> Manufacturing residues and landfill leachates are also potential sources for contributing PhACs in aquatic environment.<sup>40, 42</sup> The occurrence of pharmaceutical residues in the environment may also be caused by agriculture using large amounts of veterinary drugs and feed additives in livestock.<sup>20</sup> Several investigations have shown that the wastewater treatment process cannot completely eliminate pharmaceutical active compounds from wastewater, and therefore PhACs are released into the aquatic system after treatment.<sup>4, 43</sup>

### 1.2.2 Polycyclic Aromatic Hydrocarbons (PAHs)

Polycyclic aromatic hydrocarbons are organic compounds which are comprised of fused benzene rings. Pure PAHs are usually white crystalline solids at ambient temperature.<sup>44</sup> The physical properties of PAHs are different with the different PAHs. Their behavior in the environment has been investigated for more than 20 years.<sup>45</sup> PAHs have potential environmental concerns because of their toxicity, environmental persistence and prevalence. Low molecular wt. PAHs can be lost by evaporation.<sup>32</sup> Most do not break down easily in water.<sup>32</sup> Except for naphthalene, PAHs have low solubility (<1 ppm) in water. Octanol-water partition co-efficients ( $K_{OW}$ ) of PAHs are relatively high, indicating a relatively high potential for bioconcentration in organisms.<sup>46</sup> Several PAHs have been reported as carcinogenic and having acute toxicity. PAHs require metabolic conversion and activation in order to exhibit their latent carcinogenic properties. Therefore, studies of PAHs are focused on their metabolic transformation by aquatic and terrestrial organisms into mutagenic, carcinogenic and teratogenic (birth defect) agents such as dihydrodiol epoxides. These metabolites bind and disrupt DNA and RNA which are the basic foundation for tumour formation. PAHs are considered as priority pollutants by the United States Environmental Protection Agency (USEPA) and the European Community. The most potent carcinogens of the PAH are the benzofluoranthenes, benzo[a]pyrene, benz[a]anthracene, dibenzo[a,h]anthracene and indeno[1,2,3-cd]pyrene.<sup>45</sup> Some PAHs are listed individually on EPA's Priority Chemical list. These are acenaphthene, acenaphthylene, anthracene, benzo(g,h,i)perylene, fluorene, phenanthrene, and pyrene.<sup>44</sup> The presence of PAHs in the aquatic system near urban areas is very common due to the prolific use of fossil fuels by human civilization. PAHs found in water near urban areas normally come from the discharge of petroleum products like petroleum fuels and lubricants, the discharge of urban stormwater runoff containing PAHs from asphalt and car exhaust particles<sup>47-49</sup> and household wastes, which can account for 50–60 % of the total sewer

load for pyrene and phenanthrene.<sup>50</sup> PAHs could be discharged in the effluent of wastewater treatment plants to natural aquatic environments in dissolved form or adsorbed to particles.<sup>51</sup> Oil sands processing and related petrochemical processing activities also generate PAHs in waters and wastewater. In the case of industrial wastewater input to sewers, the permissible PAH concentration is 0.2 mg/L, according to legislation in Poland.<sup>52</sup> There are very few studies of the concentration of PAHs in contaminated wastewater. Concentrations of PAHs in urban wastewater depend on the wastewater treatment system, weather conditions, and the composition and the amount of wastewater. Polycyclic aromatic hydrocarbons are one of the most common classes of chemical species found in nature and the environment. It is very difficult to analyze them in the aquatic environment. In the last two decades, extensive research has been done for determining PAHs in varieties of matrices. Molecular fluorescence methods have been found to be very effective for the analysis of PAHs.<sup>53</sup>

### **1.3 Conventional wastewater treatment options**

Wastewater from urban areas is commonly treated by large centralized wastewater treatment plants (WWTP). Primary sources of municipal wastewater are from sanitary sewage which is generated from homes, businesses, institutions and industries. The secondary source is from storm water which is generated from rain or melting snow that drains off rooftops, lawns, parking lots, roads and other urban surfaces. There are two types of wastewater collection systems (a) combined sewer and (b) separate sewer systems.<sup>18</sup> In the combined sewer systems, sanitary sewage and storm water are collected together. In this system, if there is heavy precipitation, overflows will happen due to overloading the combined sewer collection system, and result in a direct discharge of raw sewage into surface waters. In the separate sewer system, the sanitary sewage collection and storm water collection are separated.<sup>54</sup> Below is a simplified schematic

diagram showing how pollutants enter the wastewater collection system from various sources before release to the environment.

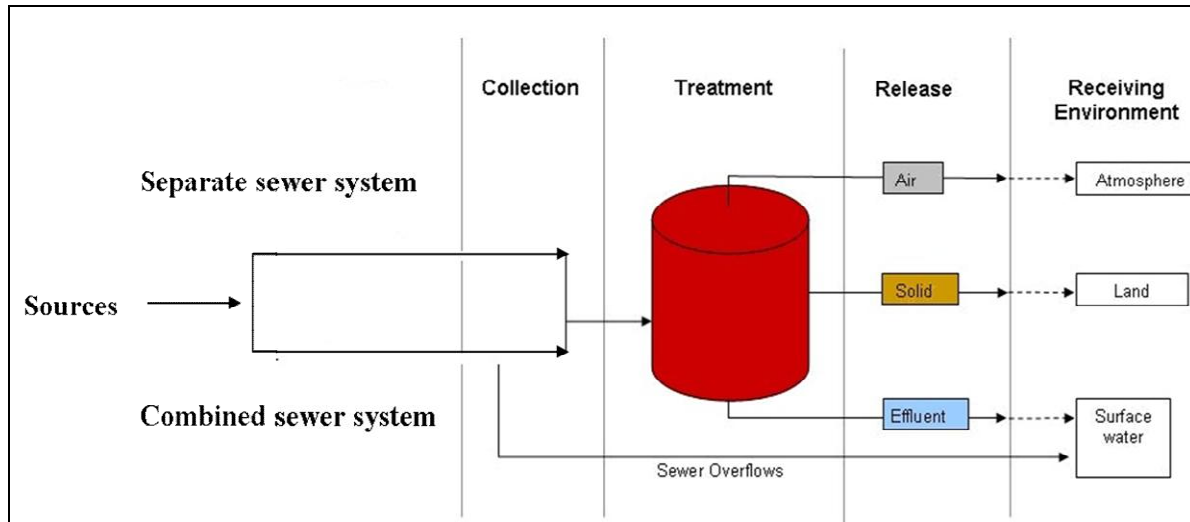


**Fig. 1.2.** Generic wastewater collection and treatment system (adapted).<sup>18</sup>

Wastewaters released from industries are merged in larger pipelines to finally be treated in Wastewater Treatment Plants. Some industrial facilities generate ordinary domestic sewage that can be treated by municipal wastewater plant. Other industries that generate wastewater with high concentrations of conventional pollutants (e.g. oil and grease), toxic pollutants (e.g. heavy metals, and volatile organic compounds) or other non-conventional pollutants such as ammonia require specialized treatment systems. Some of these facilities install a pre-treatment system to remove the toxic components, and then send the partially treated wastewater to the municipal treatment system. Other industries redesign their manufacturing processes and operate their own complete on-site treatment systems to reduce or eliminate pollutants.<sup>55</sup>



Different treatment strategies are required for the removal of different types of contamination from industrial wastewater.<sup>56,57</sup> Extension and refinement of water and wastewater treatment technologies have been intensified in the past decade, and more approaches have been applied for the design and operation of wastewater treatment.<sup>58</sup>

Many industries such as agro-food, petroleum and leather generate highly saline wastewater. The discharge of such saline wastewater to the environment adversely affects the aquatic life, water potability and agriculture. Solar evaporation is commonly applied for the concentration of salt of saline wastewater.<sup>59</sup> Ion exchange is also used to treat saline wastewater.<sup>56</sup> But, ion exchangers require costly regenerant and produce troublesome waste streams.<sup>59</sup> Reverse Osmosis (RO) is the most efficient and most commonly used membrane process in desalination. In this process, water is separated from dissolved salts in solutions by filtering through a semipermeable membrane at a pressure greater than the osmotic pressure caused by the dissolved salts in the wastewater.<sup>56</sup>

Biodegradable organic materials from plants or animals are usually treated by using extended conventional sewage treatment processes such as activated sludge or trickling filter.<sup>56,57</sup> Activated sludge is a biochemical process for treating sewage and industrial wastewater using oxygen and microorganisms to oxidize organic pollutants, producing a waste sludge (or floc) containing the oxidized material. In this process, air is injected in the aeration tank and thoroughly mixed with wastewater followed by settling down the waste sludge in the settling tank (also called a clarifier). On the other hand, a trickling filter consists of a bed of rocks, gravel, slag, peat moss, or plastic media over which wastewater flows downward and interacts with a layer (or biofilm) of microbial slime covering the bed media in presence of air. Aerobic conditions are maintained by

forced air flowing through the bed. The process involves biochemical oxidation through adsorption of organic compounds in the microbial slime layer.

Oils can be removed from water surfaces by skimming devices. Organic materials such as solvents, paints, pharmaceuticals, pesticides, coking products can be very difficult to treat. Tertiary treatment methods are often very specific to individual contaminants. Some of the methods are chemical oxidation, distillation, and adsorption. Chemical oxidation is a very useful treatment process for the selective transformation of the undesirable substances into less harmful species. During chemical oxidation, electrons are removed from a substance to increase its oxidation state. Even though chemical oxidation is thermodynamically favourable in wastewater treatment systems, it occurs at very slow rates of reaction; therefore, it is generally impractical to get complete oxidation from an engineering or economic point of view. Oxidation processes are considered as energy intensive, and therefore costly, which causes limited application in the wastewater treatment process.<sup>60</sup> However, appropriate integration of oxidation processes with other treatment processes can decrease the cost and enhance the overall organic removal efficiency. An example of this is found in the coupling of chemical oxidation and biological treatment, whereby biologically resistant compounds can, by partial transformation, be rendered more amenable to subsequent biodegradation. Ozone, permanganate, and chlorine are some of the oxidizing agents used in wastewater treatment. Ozone can be used in various steps of the treatment process to enhance biological processes and micro flocculation, iron, and manganese removal, degradation of pesticides and other micro pollutants, and taste and odor removal.<sup>61</sup> Ozone is particularly beneficial for the disinfection of potable water because it is effective against both bacteria and viruses and can also disinfect cysts and eggs.<sup>62-64</sup> Selected organic compounds such as phenols, aldehydes, aromatic amines, certain organosulfur compounds (thioalcohols,

thioethers), alcohols, alkyl-substituted aromatics, nitro-substituted aromatics, unsaturated alkenes, carbohydrates, aliphatic ketones, acids, esters, amines, halogenated hydrocarbons, saturated aliphatic compounds, and benzene are treated by chemical oxidation processes.<sup>65</sup>

The carbon adsorption process is also widely used for industrial wastewater treatment for the reduction of overall organic content, specific compound removal, byproduct recovery, and toxicity reduction.<sup>66-69</sup> Adsorption technology has been found to be very effective for groundwater cleanup operations that include treatment of drinking and process waters, treatment of waters for artificial recharge, and treatment of water from purge wells.<sup>70,71</sup> Adsorption is a partitioning process where contaminants are transferred from the aqueous phase to the surface of a solid phase where they accumulate. Activated carbon (e.g. anthracite) is the most common adsorbent used in wastewater treatment. Activated carbon is used in the water industry for taste and odor control for the removal of specific organic compounds. It is also used for removal of chloroorganic compounds, aliphatic and aromatic hydrocarbons, total organic carbon (TOC), trihalomethane (THM) precursors such as humic substances. It is a support medium for attached growth for biologically aided removal of organics, and is used for dechlorination.<sup>72</sup> Many water treatment plants replace or supplement sand or other filter media with granular activated carbon (GAC).

Liquefied gases such as propane, butane and carbon dioxide can be used as extractants for the removal of contaminants from wastewater. Liquefied gas extraction is potentially suitable for environmental clean up. It is reported that the butane extraction process is an effective method for removing of toxic organic contaminants from wastewater.<sup>75</sup> There are very few references available for detailed information of the systematic approach of this technique. Moreover,

liquefied petroleum gases have the potential for explosion and fire hazard due to their flammability properties. Therefore, it is not suitable method for wastewater treatment system.

### **1.3.1 Primary Treatment (mechanical treatment)**

Conventional wastewater treatment systems are typically divided into primary, secondary and tertiary treatment processes. When wastewater enters into the treatment facility, it typically flows through a step called preliminary screening, where a screen is used to remove large floating objects that may clog pumps and pipes further in the treatment process.<sup>54</sup> After the preliminary screening, wastewater is allowed to pass slowly through the large tanks called primary clarifiers or primary sedimentation tanks. Sludge will settle down in the tank and floating material such as grease and oils can be removed from the surface. Primary treatment involves several operations such as equalization (storing excess during peak flow times and later release during slow flow times), neutralization, sedimentation, oil separation, and flotation.<sup>76</sup> Primary clarifiers are usually equipped with mechanically driven scrapers that continually drive the collected sludge towards a hopper in the base of the tank from where it can be pumped to further sludge treatment stages. The clarified water flows on to the next step of treatment.<sup>76</sup>

### **1.3.2 Secondary Treatment (biological treatment)**

Secondary treatment is used to remove the bulk of the suspended solids, organic materials (both hazardous and non-hazardous), and other soluble materials. Secondary treatment processes can remove up to 90 percent of the organic matter in wastewater by using biological treatment processes.<sup>54</sup> First step in the secondary treatment process is to send the waste to an aeration tank.

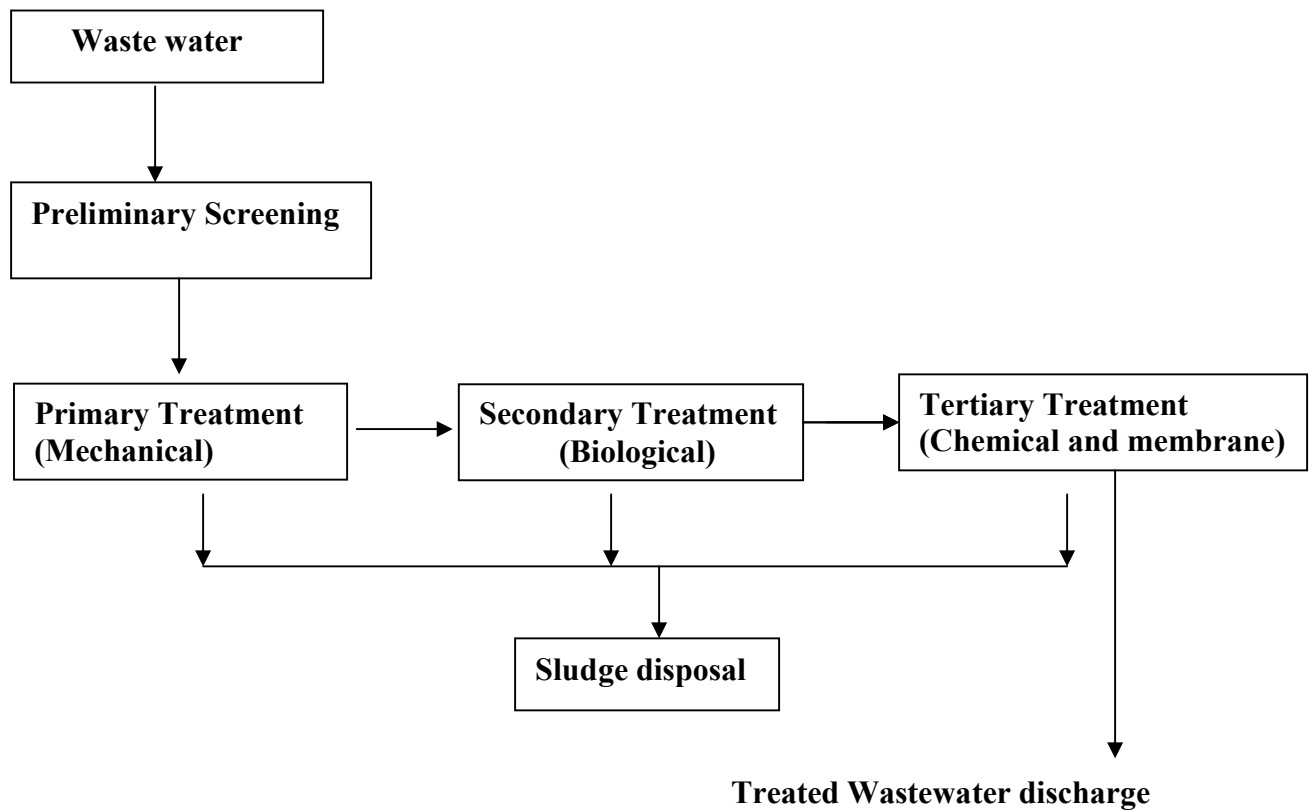


**Fig. 1.3.** Flow diagram of the conventional wastewater treatment system.

Oxygen-demanding substances like organic matter and ammonia are contributed by domestic sewage, and agricultural and industrial wastes from both plant and animal origin, such as those from livestock, food processing, paper mills, tanning, and other manufacturing processes. These substances are usually mineralized or converted to other compounds by bacteria if there is sufficient oxygen present in the water.<sup>54</sup> Bacteria are single celled organisms, which have basic requirements for their existence and reproduction. Many types of bacteria have been utilized in wastewater processing. If certain bacterium is supplied with an environment in which the proper pH, temperature, micro and macronutrients, and oxygen levels are present, it can quickly and effectively break pollutants present in wastewater down into less harmful components.

### **1.3.3 Tertiary treatment (Chemical treatment)**

Tertiary treatment is the final stage of treatment for removing contaminants from wastewater. It is used on some wastewater treatment systems, but not all. Most municipal WWTP in Canada do not have tertiary treatment, or only add chlorine disinfectant as a tertiary step. Tertiary treatment can involve a variety of methods such as sand filtration, coagulation, reverse osmosis, adsorption, and electro dialysis in order to remove any residual contaminants not eliminated during the previous treatment processes.<sup>76</sup> Ultrafiltration (UF), if used, may also be a tertiary treatment process. Small dissolved molecules as well as nutrients like phosphorus and nitrogen may remain in the effluent after secondary biological treatment. Conventional secondary biological treatment processes cannot remove all of the phosphorus, nitrogen and other small molecules. Therefore, tertiary treatment is required if additional small molecules or phosphorus and nitrogen must be removed from wastewater.

### **1.3.4 Limitations for sulfonamides and PAHs**

Pharmaceutically active compounds (PhACs) can be removed to some extent from sewage during the primary treatment process based on their chemical and physical properties including aqueous solubility, volatility and lipophilicity. In the biologically oxidative environment of secondary sewage treatment, removal of organic compounds is widely varied based on their susceptibility to microbial degradation. Therefore, some compounds will degrade while others will persist.<sup>78</sup> Low concentrations (<1 ppb) of sulfonamide antibiotics have been detected in surface waters as well as in the influent and effluent of wastewater treatment plants.<sup>2,79-83</sup> These compounds are only partially removed by conventional wastewater treatment systems. Advanced treatment processes, such as ozonation, show better removal, but have serious limitations due to cost and the possible formation of harmful by-products.<sup>83,84</sup>

For the removal of polycyclic aromatic hydrocarbons (PAHs) from wastewater, biological, physicochemical or combined methods can be used. In the physical process, PAHs can be removed from wastewater by using UF. However, in the course of UF separation, permeate flux will decrease over time due to deposition of substances on the membrane surface.<sup>52</sup>

#### **1.4 Oil sands produced water (OSPW)**

The oil sands in northern Alberta, Canada, are one of the largest oil deposits in the world, with proven reserves of 174 billion barrels of bitumen.<sup>85</sup> Oil sands mining consumes large volumes of water. On average 3 barrels of river water is required for every barrel of oil production.<sup>86</sup> Most of the water is used for hot water extraction. Hot water extraction is a process that separates bitumen from sand and clay. The resulting process water is alkaline, slightly brackish, and acutely toxic to aquatic biota due to the high concentrations of organic acids that are also leached from the bitumen during extraction.<sup>87</sup> Untreated oil sands produced waters (OSPW), including the water in tailings ponds, is a major environmental concern. Organic compounds found in tailings pond water include naphthenic acids (NAs), asphaltenes, benzene, creosols, humic and fulvic acids, phenols, phthalates, PAHs, and toluene.<sup>86</sup> Under a zero discharge policy, oil sands are required to store produced water in designated on site tailings ponds.<sup>88</sup> Recycling of tailings pond water has decreased fresh water withdrawals, but has increased scaling and corrosion of extraction facilities and causes the long term decrease in water quality.<sup>86</sup> Tailings comprised of water, dissolved salts, organics, minerals, and bitumen are pumped from separation vessels. The composition of tailings varies with ore quality, source, extraction processes, and age. Generally, it contains 70-80 wt% water, 20-30 wt% solids (i.e. sand, silt, and clays) and 1-3 wt% bitumen.<sup>89</sup>

### **1.4.1 Conventional OSPW contaminants and treatment**

Solid-liquid separation was the primary focus of the early stage research for water treatment in the oil sands. As reviewed by Kasperski (1992),<sup>89</sup> the treatment processes tested on tailings throughout the 1970s and 1980s included adsorption (fly ash, activated carbon, and bentonite), coagulation and flocculation, pre-coat filtration, membranes, electrophoresis-assisted gravity settling, pH adjustment, and freeze-thawing, among others.<sup>90</sup> Ion exchange was first proposed as a method of reducing water consumption in the hot water process by removing divalent and trivalent ions from process water immediately following tailings extraction.<sup>91</sup> Acidification increases rapid settling, and removes a large fraction of the dissolved organic carbon (DOC), resulting in lower toxicity in process water.<sup>92,93</sup> Activated carbon also significantly reduces DOC concentrations,<sup>92</sup> although recent studies have demonstrated that acidification is required for activated carbon to effectively adsorb naphthenic acids and reduce toxicity of process water.<sup>95</sup> Other treatments such as aeration, sand filtration, and centrifugation have negligible effects on dissolved substances and toxicity.<sup>93</sup> Spray freezing is identified as a winter treatment option for tailings pond water. Gao et al. (2004)<sup>94</sup> reported that spray freezing the tailings pond water at -10 °C can significantly separate total organic carbon (TOC), conductivity, chloride, and sulphate from the resulting ice.

There are various advanced treatment process used for the treatment of OSPW. A wide variety of associated pollutants, most notably soluble organic carbon compounds, oil and grease and heavy metals are removed by using adsorbents.<sup>90</sup> Activated carbon, natural organic matter, Zeolites, clays, and synthetic polymers are commonly used as adsorbents. Electrodialysis is considered an emerging technology in the oil industry with several successful bench and pilot-scale demonstrations.<sup>95,96</sup> In electrodialysis, feedwater is passed through an electrolytic cell divided by



alternating anion and cation permeable membranes. Electrodialysis is an energy and cost efficient solution to brine volume reduction with lower feedwater quality requirements, longer membrane life, and higher water recovery than reverse osmosis.<sup>90</sup>

#### **1.4.2 Limitations for OSPW treatment**

OSPW is a mixture of complex organic and inorganic species. Conventional wastewater treatment processes such as filtration, sedimentation, and flocculation cannot remove low molecular weight dissolved compounds in the produced water. Water treatment technologies are rapidly developing to meet the water management needs of oil industry, but the effectiveness of the treatment of these technologies in the oil sands operations remains unclear. Prevention of scaling, fouling, and corrosion are major concerns for oil sands operators, especially at in situ operations where produced water is recycled for steam generation.<sup>97</sup> Scale formation and fouling problems are reported at the extraction facilities of mining operations. Common components of scale formation from produced water are carbonate, silica, sulphate, phosphate, and iron oxides.<sup>86</sup> In terms of corrosion, chemicals of concern with respect to process water include TDS, sulphate, chloride, bicarbonate, ammonia, NAs, copper, and dissolved oxygen.<sup>86</sup> Over the last two decades, synthetic polymers and ceramic membranes have been studied by the oil industry for the removal of oil, suspended solids, and other pollutants from produced water.<sup>90</sup> Membrane filtration processes have been tested on OSPW, although earlier research focused on the treatment of produced water from in situ operations, rather than from surface mining streams.<sup>98</sup> Treatment of *in situ* produced water with ultra filtration and reverse osmosis has been shown effective for removing toxicity, but fouling from fine clay particles resulted in permeate flux declines.<sup>90</sup> More recently, nanofiltration membranes were tested on various effluents associated with surface mined oil sands and achieved >95% reduction of NAs concentration, and varying

reductions of chloride (15-39%), sulphate (93-98%), sodium (54%-65%), calcium (92%-95%), magnesium (90%-95%), and bicarbonate concentrations (58%-79%).<sup>90</sup> However, nanofiltration is not yet widely used and reverse osmosis remains at the development stage in the oil and gas industry due to concerns over fouling from oil and biofouling promoted by dissolved organic compounds.<sup>99</sup> Campos et al. (2002) reported that 92% of oil and grease were removed from produced water by treating with microfiltration, but fouling of the membranes necessitated cleaning every 20 h (based on small batch tests).<sup>100</sup> Fouling decreases permeate flux, increases trans-membrane pressure, and ultimately increases operating costs. Permeate flux of oily wastewater will decrease when a layer of oil coats the pores and active surface layer of a membrane, rendering it hydrophobic and reducing its permeability to water.<sup>101</sup>

With regards to the commercial application of microfiltration membranes for de-oiling of produced waters, Zaidi et al. (1992) reported that low flux rates, flux decline, and membrane durability remained major technological concerns.<sup>102</sup> Oilfield brine filtration requires membranes with high porosity (0.1 to 0.5  $\mu\text{m}$ ), surface hydrophilicity, adequate heat and pressure tolerance, and compatibility with cleaning agents and oilfield chemicals. Even though several counter measures have been adopted with back pulsing, aeration, surface chemistry modification and cleaning agent in order to minimize fouling problems, viable, economic and effective treatment technology is still needed in the oil sands processing industry.<sup>90</sup>

### **1.5 Advanced wastewater treatment by filtration**

Pressure driven membrane filtration is widely recognized as an advanced filtration process. Membrane filtration can be defined as a separation process that uses semi permeable membrane to divide the feed stream into a retentate (or concentrate) and a permeate fraction.<sup>103</sup> Pressure-

driven membrane processes use the pressure difference between the feed and permeate side as the driving force to transport the solvent (usually water) through the membrane.<sup>111</sup> Membrane filtration can be classified in terms of the size range of permeating species, the mechanisms of rejection, the driving forces employed, the chemical structure and composition of membranes, and the geometry of construction.<sup>104</sup> This classification distinguishes membrane filtration as microfiltration (MF), ultrafiltration (UF), nanofiltration (NF), and reverse osmosis (RO). Microfiltration and ultrafiltration membranes have a porous structure that retains components by a sieving mechanism. Separation depends on the pore size of the membrane and the size of the components to be retained. In microfiltration, the pore size of the membrane is indicated by the manufacturers and serves as a reference for the size of the retained particles. For ultrafiltration, the molecular weight cut-off (MWCO) concept is often used.<sup>111</sup> Microfiltration (MF) membranes have the largest pores, ranging from  $\sim 0.1 \mu\text{m}$  to  $1 \mu\text{m}$ , and the highest permeability, so that a sufficient water flux is obtained at a low pressure. MF is suitable for the removal of suspended solids, including larger micro organisms like protozoa and bacteria.<sup>105</sup>

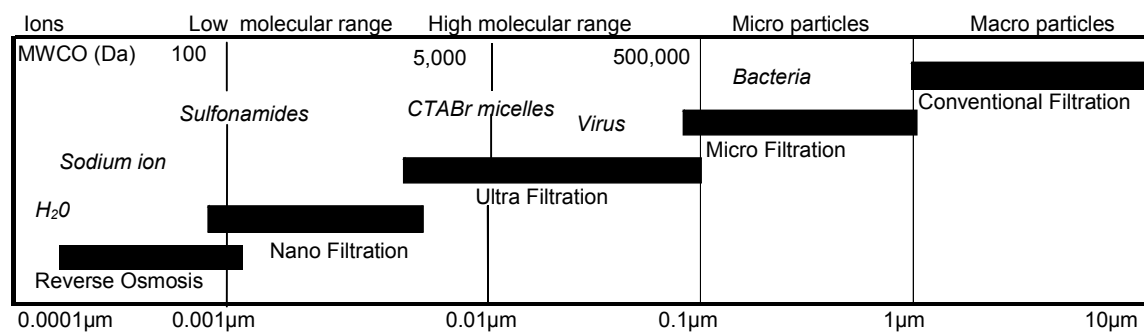


**Fig. 1.4.** Effective size ranges of different filtration systems.<sup>106</sup>

Ultrafiltration is a relatively inexpensive, versatile, expedient, simple, non-destructive, and reagent-free technique for separating macromolecules.<sup>107,108</sup> Ultra filtration (UF) membranes

typically have a molecular weight cut-off below 100,000 Daltons,<sup>109</sup> and can remove 99.9% of viruses. Molecules ranging in size from 3 kDa to 500 kDa (see Fig.1.4) are retained by certain ultra filtration membranes, while low molecular wt. molecules and ions, including sulfonamides (~0.17 kDa to 0.32 kDa), salts and water will pass through. UF can be used for the removal of viruses and organic macromolecules down to a diameter of around 20 nm.<sup>105</sup>

Ultrafiltration and microfiltration are increasingly used in water and wastewater treatment for producing disinfected water suitable for various applications. However, fouling of microfiltration or ultrafiltration membranes is the main limitation.<sup>110</sup> For nanofiltration (NF), the pore sizes are smaller than in UF, typically between 0.001  $\mu\text{m}$  to 0.01 $\mu\text{m}$ , which corresponds to dissolved compounds with a molecular weight of about 500-4000 Da. This makes NF suitable for the removal of relatively small organic molecules, multivalent ions<sup>92</sup> and organic dye molecules from surface water or groundwater, and degradation products from the effluent of biologically-treated wastewater.<sup>101</sup> Nanofiltration is situated between RO and UF. In comparison with RO, lower pressures are used to obtain comparable fluxes, which is an important energetic advantage over reverse osmosis.<sup>111</sup>

RO has the smallest pore size ( $< 0.001\mu\text{m}$ ) and requires high pressure to operate. RO can virtually separate all the ions while operating under a very high pressure difference and at a relatively low permeate flux. It is commonly used for desalting brackish water and seawater.<sup>104</sup>

### **1.5.1 Limitation of membrane filtration**

Fouling is a common problem for the applications of pressure-driven membrane processes. Fouling in RO and NF is mainly caused by adsorption of organic material on the membrane surface and/or pore blocking, and by scaling due to the precipitation of such materials as  $\text{CaCO}_3$

and  $\text{CaSO}_4$ .<sup>104</sup> Moreover, RO membranes are dense membranes without predefined pores.<sup>111</sup> As a result, permeation is slower and rejection is not a result of sieving, but of a solution-diffusion mechanism. The low permeability of reverse osmosis membranes requires high pressures and, consequently, relatively high energy consumption. This effect is even more pronounced in the presence of an osmotic pressure due to high concentrations of dissolved components that counteract the effect of the exerted pressure.<sup>111</sup>

### **1.5.2 Micellar Enhanced Ultra filtration (MEUF)**

MEUF is a modified form of ultrafiltration,<sup>112</sup> involving a combination of surfactant and UF for the separation of ions and small organic molecules which otherwise can only be separated using NF or RO.<sup>114</sup> In MEUF, contaminants first partition into surfactant aggregates called micelles prior to removal by UF, where the contaminants are below the molecular weight cut-off of the UF membrane but the micelles are above the cut-off. For some contaminants, MEUF combines the high removal efficiency of reverse osmosis with the high flux of ultrafiltration.<sup>113,114</sup> The advantages of MEUF are relatively low energy requirement and low pressure. Anisotropic membranes ranging in nominal pore size from about 1 to 10 nm (500 to 50,000 MWCO) can be used to reject surfactant micelles.<sup>127</sup> Furthermore, the performance for solute rejection for MEUF of solute with low molecular weight (MW) is quite similar to RO and NF. Therefore, MEUF may be an alternative to overcome the inherent limitations of the RO process.<sup>112</sup>

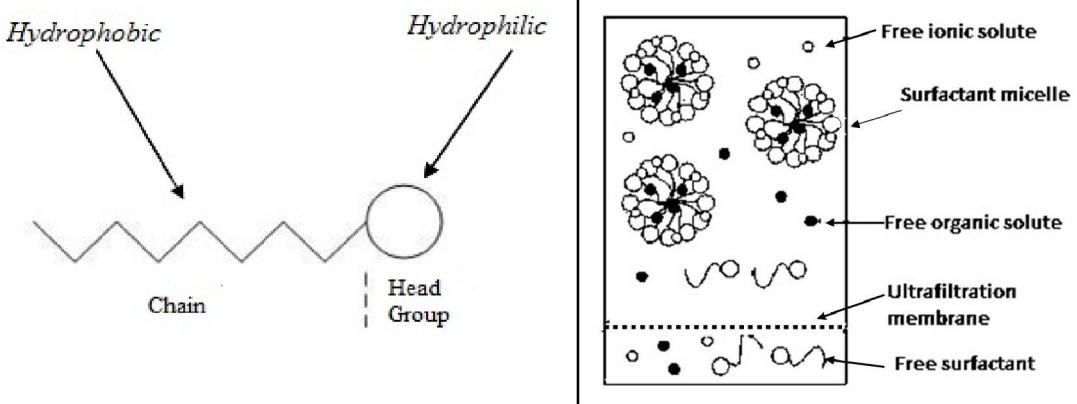


**Fig. 1.5. (a) Structure of a Surfactant. (b) Micellar enhanced ultra filtration (modified).<sup>128</sup>**

MEUF has been found to be an effective removal technique for a variety of trace contaminants in wastewater,<sup>129-133</sup> including heavy metals (e.g. lead, cadmium, zinc), toxic organic materials (e.g. phenols, di-butyl phosphate, tri-butyl phosphate, trihalomethanes) and lower molecular weight contaminants including Reactive Black 5 and Orange 16, Eosin dye, Direct Blue 71 and Methylene Blue.<sup>132-141</sup>

A recent report by Exall et al. demonstrated the removal of some sulfonamide antibiotics from wastewater on a pilot scale.<sup>142</sup>

### 1.6 Objective of the research

Due to variations from one contaminant to another, no single technology is capable of providing treatment for the whole spectrum of wastewater. Therefore, it is important to develop effective treatment technologies as well as to develop a predictive model for understanding removal efficiency for various contaminants. This will allow the efficient selection of MEUF parameters, including specific surfactants and membranes, for removal of contaminants of interest in a particular application. A major challenge for MEUF method development is characterizing model

or prototype systems to help optimize parameters of the treatment system, including matching micelle composition to the contaminants to be removed. The objective of this research was to develop a semi-equilibrium dialysis (SED) method to characterize contaminants binding to various micelles. Characterization included determining the binding constant of the organic micro contaminants, and developing a correlation of these binding constants with octanol water partition coefficients. The micelles studied include cationic (CTABr), anionic (SDS), and switchable surfactants (sodium laurate) in order to develop a predictive model for other compounds of interest. In this context, binding constants were determined for selected sulfonamides and polycyclic aromatic hydrocarbons (PAHs) in micelles. Binding was further characterized by determining structural orientation of the sulfonamides in micelles by  $^1\text{H}$  NMR spectroscopy.

### **1.7 Scope of the research**

Chapter 2 is a literature review of MEUF, including micelle formation, binding processes, binding characterization and different methodologies for determining binding constants, including SED and NMR spectroscopy.

Chapter 3 describes the determination of binding constants of the selected sulfonamides with CTABr micelles using the SED method. Binding characterization is explained by developing linear co-relationships with other constants.

Chapter 4 describes the binding constants of the selected sulfonamides determined by  $^1\text{H}$  NMR spectroscopy. Nonlinear binding curves from the chemical shift of selected protons and locus and orientation of the sulfonamide molecules within the micelle are discussed. The relationship between proton chemical shift and micelle binding is examined.

Chapter 5 describes the binding constant of the selected PAHs with CTABr micelles using the SED method, followed by discussing of the correlation with octanol-water partition constants.

Chapter 6 describes the binding constant of the selected PAHs with SDS and SOL micelles using the SED method, followed by discussing the correlation with octanol-water partition constants.

Finally, the conclusions and future work are discussed in Chapter 7

## 1.8 References

1. Vörösmarty, C. J.; McIntyre, P. B.; Gessner, M. O.; Dudgeon, D.; Prusevich, A.; Green, P.; Glidden, S.; Bunn, S. E.; Sullivan, C. A.; Liermann, C. R.; Davies, P. M. *Nature*, **2010**, *467*, 555–561.
2. Kolpin, D. W.; D.; Furlong, E. T.; Meyer, M. T.; Thurman, E. M.; Zaugg, S. D.; Barber, L. A.; Buxton, H. T. *Environ. Sci. Technol.* **2002**, *36*, 1202-1211.
3. Azizullah, A.; Khattak, M. N. K.; Richter, P.; Häder, D. P. *Environment International*, **2011**, *37*, 479–497.
4. Daughton, C. G.; Ternes, T. A. *Environ. Health Perspect.* **1999**, *107*, 907-938.
5. Jorgensen, S. E.; Halling-Sorensen, B. *Chemosphere*, **2000**, *40*, 691-699.
6. Purdom, C. E.; Hardiman, P. A.; Bye, V. V. J.; Eno, N. C.; Tyler, C. R.; Sumpter, J. P. *Chem. Ecol.* **1994**, *8*, 275-285.
7. White, R.; Jobling, S.; Hoare, S. A.; Sumpter, J. P.; Parker, M. G. *Endocrinology*, **1994**, *135*, 175-182.
8. Sharpe, R. M.; Skakkebaek, N. E. *Lancet*, **1993**, *341*, 1392-1395.
9. Panter, G. H.; Thompson, R. S.; Sumpter, J. P. *Environ. Sci. Technol.* **2000**, *34*, 2756-2760.
10. Harrison, P. T. C.; Holmes, P.; Humfrey, C. D. N. *Sci. Total Environ.* **1997**, *205*, 97-106.
11. Jobling, S.; Nolan, M.; Tyler, C. R.; Brighty, G.; Sumpter, J. P. *Environ. Sci. Technol.* **1998**, *32*, 2498-2506.
12. Davis, D. L.; Bradlow, H. L. *Sci. Am.* **1995**, *273*, 166-172.
13. DuPont, H. L.; Steele, J. H. *Rev. Infect. Dis.* **1987**, *9*, 447-460.



14. Gilliver, M. A.; Bennett, M.; Begon, M.; Hazel, S. M.; Hart, C. A. *Nature*, **1999**, *401*, 233-234.
15. Khachatourians, G. G. *Can. Med. Assoc. J.* **1998**, *159*, 1129-1136.
16. Smith, K. E.; Besser, J. M.; Hedberg, C. W.; Leano, F. T.; Bender, J. B.; Wicklund, J. H.; Johnson, B. P.; Moore, K. A.; Osterholm, M. T. N. *New Engl. J. Med.* **1999**, *340*, 1525-1532.
17. Sumpter, J. P.; Jobling, S. *Environ. Health Perspect.* **1995**, *103*, 174-178.
18. "Wastewater management" Environment and climate change Canada. <https://www.ec.gc.ca/eu-ww/> (accessed 03/2015).
19. Pasquini, L.; Munoz, J. F.; Rimlinger, N.; Dauchy, X.; France, X.; Pons, M. N.; Gorner, T. *Chemical Papers*, **2013**, *67* (6), 601–612.
20. Heberer, T. *Toxicology Letters.* **2002**, *131*, 5-17.
21. Conn, K. E. ; Siegrist, R. L. *Occurrence and Fate of Trace Organic Contaminants in Onsite Wastewater Treatment Systems and Implications for Water Quality Management*, Colorado water Institute, USA; Technical report, **2009**. Available on line; <http://www.cwi.colostate.edu/publications/cr/210.pdf> (accesses 06/2015)
22. Barber, L. B.; Murphy, S. F.; Verplanck, P. L.; Sandstrom, M. W.; Taylor, H. E.; Furlong, E. T. *Environ. Sci. Technol.* **2006**, *40*, 475-486.
23. Glassmeyer, S. T.; Furlong, E. T.; Kolpin, D. W.; Cahill, J. D.; Zaugg, S. D.; Werner, S. L.; Meyer, M. T.; Kryak, D. D. *Environ. Sci. Technol.* **2005**, *39*, 5157-5169.
24. Metcalfe, C. D.; Koenig, B. G.; Bennie, D. T.; Servos, M.; Ternes, T. A.; Hirsch, R. *Environ. Toxicol. Chem.* **2003**, *22*, 2872-2880.
25. Lishman, L.; Smyth, S. A.; Sarafin, K.; Kleywegt, S.; Toito, J.; Peart, T.; Lee, B.; Servos, M.; Beland, M.; Seto, P. *Sci. Total Environ.* **2006**, *367*, 554-558.
26. Chen, M.; Ohman, K.; Metcalfe, C.; Ikonomou, M.G.; Amatya, P. L.; Wilson, J. J. *Water Qual. Res. J. Can.* **2006**, *41*(4), 351-364.
27. Yang, J. J.; Metcalfe, C.D. *Sci. Total Environ.* **2006**, *363*, 149-165.
28. Lajeunesse, A.; Gagnon, C.; Sauvé, S. *Anal Chem*, **2008**, *80*, 5325-5355.
29. Schuerer, M.; Ramil, M.; Metcalfe, C. D.; Groh, S.; Ternes, T.A. *Anal. Bioanal. Chem.* **2010**, *396*, 845-856.
30. Metcalfe, C. D.; Chu, S.; Judt, C.; Li, H.; Oakes, K. D.; Servos, M. R.; Andrews, D. M.; *Environ. Toxicol. Chem.* **2010**, *29*,79-89.

31. Servos, M. R.; Smith, M.; McInnis, R.; Burnison, K.; Lee, B. H.; Seto, P.; Backus, S. *Water Qual. Res. J. Can.* **2007**, *42*(2), 130-137.
32. Garcia-Ac, A.; Segura, P. A.; Viglino, L.; Furtos, A.; Gagnon, C.; Prevost, M.; Sauve, S. *J Chromatography*, **2009**, *1216*, 8518-8527.
33. Kleywegt, S.; Pileggi, V.; Yang, P.; Hao, C.; Zhao, X.; Rocks, C.; Thach, S.; Cheung, P.; Whitehead, B. *Sci. Total Environ.* **2011**, *409*, 1481-1488.
34. Metcalfe C. D. ; Hoque, M. E.; Sultana, T.; Murray, C.; Helm, P.; Kleywegt, S. *Environ. Sci: Processes and Impacts*, **2014**, *16*, 473-481.
35. DerBruggen, B. V.; Vandecasteele, C.; Gestel, T. V.; Doyen, W.; Leysen, R. *Environ. Prog.* **2003**, *22*(1), 46-56.
36. Beychok, M. R. *Aqueous Wastes from Petroleum and Petrochemical Plants (1st ed.)*. John Wiley & Sons. 1967, LCCN 67019834.
37. Avila, J. S.; Bonet, J.; Velasco, G.; Lacorte, S. *Sci. Total Environ.* **2009**, *407*, 4157–4167.
38. Stan, H. J.; Heberer, T. *Analisis*, **1997**, *25*(7), 20–23.
39. Halling-Sørensen, B.; Nielsen, S. N.; Lansky, P. F.; Ingerslev, F.; Hansen, L.; Lützhøft, H. H.; Jørgensen, S. E. *Chemosphere*, **1998**, *36*, 357–394.
40. Daughton, C. G., Jones-Lepp, T. (Eds.), *Pharmaceuticals and Personal Care Products in the Environment: Scientific and Regulatory Issues*. Symposium Series 791, American Chemical Society, Washington DC, 2001.
41. Kummerer, K. *Chemosphere*, **2001**, *45*, 957–969.
42. Holm, J. V.; Ruge, K.; Bjerg, P. L.; Christensen, T. H. *Environ. Sci. Technol.* **1995**, *29*, 1415–1420.
43. Zwiener, C.; Frimmel, F. H. *Water Research*, **2000**, *34*, 1881–1885.
44. Polycyclic Aromatic Hydrocarbons (PAHs), USEPA. *Office of Solid Waste*, Washington, DC 20460, Jan 2008. Available on line; <http://archive.epa.gov/epawaste/hazard/wastemin/web/pdf/pahs.pdf> (accesses 01/2016).
45. Wild, S. R.; Jones, K. C. *Environ. Pollut.* **1995**, *88*, 91-108.
46. "Polycyclic aromatic hydrocarbon" Health Canada. <http://www.hc-sc.gc.ca/> (accessed 06/2013).
47. Tanaka, H.; Onda, T.; Ogura, N. *Environ. Sci. Technol.* **1990**, *24*, 1179–1186.

48. Wang, W. T.; Simonich, S.; Giri, B.; Xue, M.; Zhao, J.; Chen, S.; Shen, H.; Shen, G.; Wang, R.; Cao, J.; Tao, S. *Environ. Pollut.* **2011**, *159*(1), 287–293.
49. Wang, W. T.; Simonich, S.; Giri, B.; Chang, Y.; Zhang, Y.; Jia, Y.; Tao, S.; Wang, R.; Wang, B.; Li, W.; Cao, J. *Sci. Total Environ.* **2011**, *409*(15), 2942-2950.
50. Mattsson, J.; Avergård, I.; Robinson, P. *Vatten*, **1991**, *47*,204–211.
51. Qi, W.; Liu, H.; Pernet-Coudrier, B.; Qu, J. *Environ. Sci. Pollut. Res.* **2013**, *20*, 4254–4260.
52. Smol, M.; Wlodarczyk-makula, M. *Arch. of Environ. Protect.* **2012**, *38*(2), 49-58.
53. Patra, D. *Applied Spectroscopy Reviews*, **2003**, *38*(2), 155-185.
54. *Primer for Municipal Wastewater Treatment Systems*; Office of Wastewater Management, Environmental Protection Agency: Washington, DC, USA, 2004; Available online: <http://www.epa.gov/npdes/pubs/primer.pdf> (accessed on 8 October 2015).
55. Wang, L. K.; Hung, Y. T.; Lo, H. H.; Yapijakis, C. *Handbook of Industrial and Hazardous Wastes Treatment*. CRC Press, 2004.
56. Metcalf and Eddy, Inc. *Wastewater Engineering: Treatment, Disposal, Reuse, 4th ed. Inc.*, McGraw-Hill, New York, 2003.
57. Beychok, M. R. *Aqueous Wastes from Petroleum and Petrochemical Plants (1st ed.)*, John Wiley & Sons, 1967.
58. Weber, W. J.; Smith, E. H. *Environ. Sci. Technol.* **1996**, *20* (10), 970-979.
59. Lefebvre, O.; Moletta, R. *Water Research*, **2006**, *40*, 3671-3682.
60. Glaze, W. H. In *Control of Organic Substances in Water and Wastewater*. EPA-600/8-83-011; Berger, B.B., Ed.; EPA: Washington. D.C. 1983, pp. 148-74.
61. Paraskeva, P.; Graham, N. J. D. *Water Environ. Res.* **2002**, *74* (6), 569-581.
62. Anderson, R. In *Proceedings of the Role of Ozone in Wastewater Treatment*; Imperial College in conjunction with Ozotech: London, United Kingdom; 1997, pp 9-26.
63. Langlais, B.; Reckhow, D.; Brink, D. *Ozone in Water Treatment-Application and Engineering*; Lewis Publishers: Chelsea, Michigan; 1991, pp 224-229.
64. Rice, R. G.; Netzer, A. *Handbook of Ozone Technology and Applications; Ozone for Drinking Water Treatment*. Lewis Publishers: Chelsea, Michigan; Vol. II, 1984.
65. Weber, W. J.; Smith, E. H. *Environ. Sci. Technol.* **1986**, *20* (10), 970-979.

66. Weber, W. J., Jr. In *Proceedings. Application of Adsorption to Wastewater Treatment*; Eckenfelder, W. W., Jr., Ed.; Enviro Press: Nashville, Tenn., 1981; pp. 5-27.
67. O'Brien, R. P.; Rizzo, J. L.; Schuliger, W. G. In *Control of Organic Substances in Water and Wastewater*, EPA-600/8-83-001; Berger, B. B., Ed.; EPA. Washington, D.C., 1983; pp. 337-62.
68. DeJohn, P. B.; Edwards, R. W. In *Proceedings. Application of Adsorption to Wastewater Treatment*; Eckenfelder, W. W., Jr., Ed.; Enviro Press: Nashville, Tenn., 1981; pp. 109-27.
69. Shelley, M. L.; Randall, C. W.; King, P.H. *J. Water Pollut. Control Fed.* **1976**, *48*, 753-761.
70. O'Brien, R. P.; Fisher, J. L. *Water Eng. Manag.* **1983**, *130*, 30-36.
71. Schalekamp, M. J. *Am. Water Works Assoc.* **1984**, *76*, 78-83.
72. Sontheimer, H. J. *Am. Water Works Assoc.* **1979**, *71*, 612-22.
73. Titus, D. *Chem Eng.* **1993**, *6*, 29.
74. USEPA, *CF system organics extraction process in New Bedford Harbor, MA(R)*. EPA/540/S5-90/002. Washington, USA, 1990.
75. Chun, Y.; Khay-chun, T.; Yan-rong, X. *J. Environ. Sci.* **2002**, *14(1)*, 1-6.
76. Armenante, P. M. *Biotreatment of industrial and hazardous waste*, Chapter 4: Bioreactors. In: Levin, M.A and Gealt, M.A (eds.); McGraw-Hill, Inc. New York; 1993; pp. 66.
77. Srivastava, S. "Bioremediation Technology," A Greener and Sustainable Approach for Restoration of Environmental Pollution," In *Applied Environmental Biotechnology: Present Scenario and Future Trends*, Springer India, **2015**; pp 1-18.
78. Khan, S. J.; Ongerth, J. E. *Chemosphere*, **2004**, *54*, 355-367.
79. Monteiro, S. C.; Boxall A. B. A. *Rev. Environ. Contam. Toxicol.* **2010**, *202*, 53-154.
80. Watkinson, A. J.; Murby, E. J.; Kolpin, D. W.; Costanzo, S. D. *Sci. Total Environ.* **2009**, *407(8)*, 2711-2723.
81. Kümmerer, K. *Chemosphere*, **2009**, *75*, 417-435.
82. Miao, X. S.; Bishay, F.; Chen, M.; Metcalfe C.D. *Environ. Sci. Technol.* **2004**, *38*, 3533-3541.
83. Zhang, T.; Li, B. *Crit. Rev. Env. Sci. Tech.* **2011**, *41(11)*, 951-998.
84. Lin, A. Y. C.; Lin, C. F.; Chiou, J. M.; Hong, P. K. A; *J Hazard Mater.* **2009**, *171*, 452.

85. Alberta Energy and Utilities Board. *Alberta's reserves 2004 and supply/demand outlook 2005-2014*. Report no. ST98-2005; 2005. <https://www.aer.ca/documents/sts/ST98/ST98-2005.pdf> (accessed on 04/2015).
86. Allen, E.W. *J. Environ. Eng. Sci.* **2008**, 7, 123-138.
87. MacKinnon, M. D.; Sethi, A. In *Proceedings of Our Petroleum Future Conference*, Alberta Oil Sands Technology and Research Authority (AOSTRA), Edmonton, AB; 1993.
88. Dominski, M. "Surface mined oil sand: tailing practices, performance, and projections, Alberta Energy and Utilities Board". In *Proceedings of the 3rd International Heavy Oil Conference*, Calgary, AB, March 5-7, 2007.
89. Kasperski, K.L. A review of properties and treatment of oil sands tailings. *AOSTRA J. Res.* **1992**, 8, 11-53.
90. Allen, E. W. *J. Environ. Eng. Sci.* **2008**, 7, 499-524.
91. Camp, F. W. *Utilizing ion exchange to reduce water requirement of hot water process*. United States Patent 3,496,093; 1970.
92. Hall, E. S., Tollefson, E. L. "Hydrocarbon removal from and upgrading of aqueous waste from oil sands recovery operations." *Report prepared for Alberta Environmental Research Trust*, Alberta Environment, Edmonton, AB, 1979.
93. MacKinnon, M. D.; Retallack, J. T. "Preliminary characterization and detoxification of tailings pond water at the Syncrude Canada Ltd. Oil Sands Plant," In *Land and Water Issues Related to Energy Development*. Ann Arbor Science, MI. 1981, pp. 185-210.
94. Gao, W.; Smith, D. W.; Segó, D. C. *Water Research*, **2004**, 38, 579-584.
95. Miller, J. A.; Lawrence, A.W.; Hickey, R. F.; Hayes, T. *Desalination*, **1997**, 108, 247-253.
96. Sirivedhin, T.; Mccue, J.; Dallbauman, L. *Ecol. Eng.* **2004**, 19, 1-11.
97. Zalewski, W.; Bulkowski, P. *J. Can. Petrol. Technol.* **1998**, 37, 51-55.
98. Banerjee, A. *Treatment of oil sands industry waste water using reverse osmosis membranes*. M.Sc. Thesis, University of Calgary, 1984.
99. Hayes, T.; Arthur, D. "Overview of emerging produced water treatment technologies," In *Proceedings of the 11 th Annual International Petroleum Environmental Conference*, 12-15 October, 2004.
100. Campos, J. C.; Borges, R. M. H.; Oliveira Filho, A. M.; Nobrega, R.; Sant' Anna, J. *Water Research*, **2002**, 36, 95-104.

101. Mueller, J.; Cen, Y.; Davis, R. H. *J. Membr. Sci.* **1997**, *129*, 221-235.
102. Zaidi, A.; Simms, K.; Kok, S. *Water Sci. Technol.* **1992**, *25*, 163-176.
103. Mallevialle, J.; Odendall, P. E.; Wiesner, M. R. *Water Treatment Membrane Processes*. McGraw-Hill, New York, 1996.
104. Zhou, H.; Smith, D. W. *J. Environ. Eng. Sci.* **2002**, *1*, 247-264.
105. Wintgens, T.; Melin, T.; Schafer, A.; Khan, S.; Muston, M.; Bixio, D.; Thoeve, C. *Desalination*, **2005**, *178*, 1-11.
106. Varbanets, M. P.; Zurbrugg, C.; Swartz, C.; Pronk, W. *Water Research*, **2009**, *43*, 245-265.
107. Buffle, J.; Deladoey, P.; Haerdi, W. *Anal. Chim. Acta*, **1978**, *101*, 339-357.
108. Logan, B. E.; Jiang, Q. *J. Environ. Eng.* **1990**, *116*, 1046-1062.
109. Bechtel, M. K.; Bagdasarian, A.; Olson, W. P.; Estep, T. N. *Biomaterials, Artificial Cells and Artificial Organs*. **1988**, *16(3)*, 123-128.
110. Abdessemed, D.; Nezzal, G.; Aim, R. B. *Desalination*, **2000**, *131*, 307-314.
111. Van der Bruggen, B.; Schaep, J.; Wilms, D.; Vandecasteele, C. *J. of Membrane Sci.* **1999**, *156*, 29-41.
112. Purkait, M. K.; DasGupta, S.; De, S. *J. Hazard. Mater.* **2006**, *136 (3)*, 972-977.
113. Zaghbani, N.; Hafiane, A.; Dhahbi, M. *J. Hazard. Mater.* **2009**, *168(2)*, 1417-1421.
114. Baek, K.; Yang, T. W. *Desalination*, **2004**, *167*, 101-110.
115. Zeng, G. M.; Xu, K.; Huang, J. H.; Li, X.; Fang, Y. Y.; Qu, Y. H. *J Membrane Sci.* **2008**, *310 (1-2)*, 149-160.
116. Purkait, M. K.; DasGupta, S.; De, S. *Sep. Purif. Technol.* **2004**, *37 (1)*, 81-92.
117. Dunn, R. O.; Scamehorn, J. F.; Christian, S. D. *Sep. Sci. Technol.* **1985**, *20 (4)*, 257-284.
118. Yenphan, P.; Chanachai, A.; Jiratananon, R. *Desalination*, **2010**, *253(1)*, 30-37.
119. Zeng, G. M.; Li, X.; Huang, J. H.; Zhang, C.; Zhou, C. F.; Niu, J.; Shi, L. J.; He, S. B.; Li, F. *J. Hazard. Mater.* **2011**, *185(2)*, 1304-1310.
120. Landaburu-Aguirre, J.; García, V.; Pongrácz, E.; Keiski, R. L. *Desalination*, **2009**, *240(1)*, 262-269.

121. Luo, F.; Zeng, G. M.; Huang, J. H.; Zhang, C.; Fang, Y. Y.; Qu, Y. H.; Li, X.; Lin, D.; Zhou, C. F. *J. Hazard. Mater.* **2010**, *173(1)*, 455-461.
122. Xu, K.; Ren, H. Q.; Zeng, G. M.; Ding, L. L.; Huang, J. H. *Colloids and Surfaces A: Physicochemical and Engineering Aspects*, **2010**, *356(1)*, 150-155.
123. Misra, S. K.; Mahatele, A. K.; Tripathi, S. C.; Dakshinamoorthy, A. *Hydrometallurgy*, **2009**, *96(1)*, 47-51.
124. Chung, Y. S.; Yoo, S. H.; Kim, C. K. *J. Membra. Sci.* **2009**, *326(2)*, 714-720.
125. Ahmad, A. L.; Puasa, S. W.; Zulkali, M. M. D. *Desalination*, **2006**, *191(1)*, 153-161.
126. Zaghbani, N.; Hafiane, A.; Dhahbi, M. *Desalination Water Treat.* **2009**, *6(1-3)*, 204-210.
127. Fillipi, B. R., Brant, L. W., Scamehorn, J. F. and Christian, S. D. *J. of Colloid Interface Sci.* **1999**, *213(1)*, 68-80.
128. Ahmad, A. L.; Puasa, S. W. *Chemical Engineering Journal*, **2007**, *132*, 257-265.
129. Armstrong, D. W.; *Sep. Purif. Methods*, **1985**, *14*, 213.
130. Hinze, W. L.; Armstrong, D. W. In *Ordered Media in Chemical Separations*, ACS Symposium Series, 342, 1987.
131. Dorsey, J. G. In *Advances in Chromatography*; J. Calvin Giddings, E. Grushka, P. R. Brown, eds., Marcel Dekker, 1987, Chapter 5, pp. 167-214.
132. Berthod, A.; Girard, L.; Gonnet, C. In *Ordered Media in Chemical Separations*, ACS Symposium Series, 342, 1987.
133. Berthod, A.; Girard, L.; Gonnet, C. *Anal. Chem.* **1986**, *58*, 1362.
134. Lissi, E.; Abuin, E.; Rocha, A. M. *J. Phys. Chem.* **1980**, *84*, 2406-2408.
135. Hamdiyyah, M. A. *J. Phys. Chem.* **1986**, *90*, 1345.
136. Reekmans, S.; Luo, H.; Auweraer, M. V.; De Schryver, F. C. *Langmuir*, **1990**, *6*, 628.
137. Armstrong, D. W.; Nome, E. *Anal. Chem.* **1981**, *53*, 1662.
138. Garcia, M. A.; Marina, M. L.; Diez-Masa, J. C. *Journal of Chromatography A*, **1996**, *732*, 345-359.
139. Arunyanarl, M.; Cline Love, L. Y. *Anal. Chem.* **1984**, *56*, 1557.
140. Garcia, M. A.; Vera, S.; Marina, M. L. *Chromatographia*, **1991**, *32*, No 3/4.

141. Terabe, S.; Otsuk, K.; Ichikawa, K.; Tsuchiya, A.; Ando, T. *Anal. Chem.* **1984**, *56*, 111.

142. Exall, K.; Balakrishnan, V. K. ; Toito, J.; McFadyen, R. *Sci. Total Environ.* **2013**, *461–462*, 371–376.



## Chapter 2

### Literature review

#### 2.1 Surfactant and micelle formation

A surfactant is a surface active agent that is comprised of a polar head group and a non-polar tail group. The dual nature of the surfactant causes self aggregation.<sup>1</sup> Normally, surfactants behave as a dissolved substance in aqueous solution at low concentrations. Adsorption of surfactant is observed at the air-water interface leading to decreased surface tension due to reduction of surface free energy.<sup>2</sup> With increasing concentrations of surfactant, the adsorption also increases (see Fig. 2.1). As there will be a balance between adsorption and desorption (due to thermal motion), the interfacial condition requires some time to be established. The surface activity of surfactants should therefore be considered a dynamic phenomenon. This can be determined by measuring surface or interfacial tension versus time for a freshly formed surface. The polar or ionic head groups of the surfactant usually interacts strongly with an aqueous phase via dipole-dipole or ion-dipole interactions when it is solvated.<sup>3</sup>

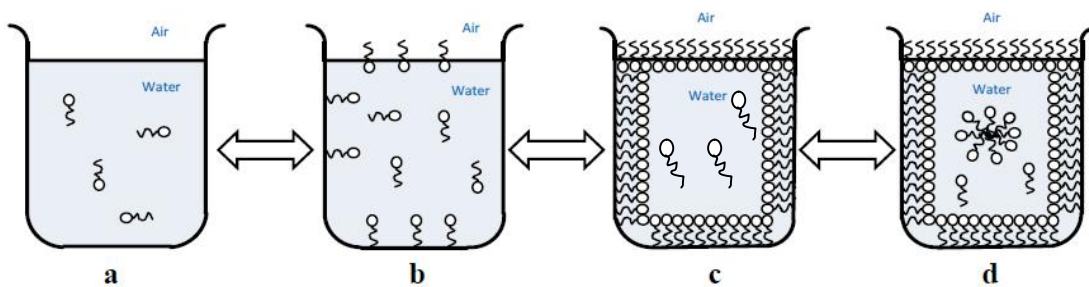


**Fig. 2.1.** Micelle formation process: a) A surfactant as dissolved substance b) Adsorption of surfactant at the air-water interface c) a monolayer of surfactants is formed at the interfaces d) formation of micelles (adapted).<sup>2</sup>

At a certain concentration, all interfaces become saturated with surfactant monomers and surfactant molecules start aggregating to form micelles. A typical micelle size is 5 nm and it is made of about 100 surfactant molecules.<sup>4</sup> The concentration where aggregation of surfactant molecules occurs is called the critical micelle concentration (CMC). If the surfactant concentration is higher than CMC, excess surfactant molecules form micelles and the monomer concentration remains constant. The CMC can be affected by various factors, such as increasing the size of the "head" (polar or hydrophilic group) or decreasing size of the "tail" (non-polar or hydrophobic group), which will result in an increased CMC. However, the CMC will decrease with decreasing charge density of the polar head groups by the addition of counter ions or electrolyte to the ionic surfactant. Besides these factors, temperature and pH can also influence the CMC. The CMC of a surfactant is an important parameter as it is specific for each surfactant and influences the control of solubilisation and emulsification.<sup>5</sup> For surfactants with a very high CMC, few or no micelles will be formed, resulting in little binding with contaminants. On the contrary, for surfactants with a lower CMC, more micelles will be formed and more contaminants will bind with micelles.

From a thermodynamic perspective, the process of micelle formation will include both electrostatic and hydrophobic contributions to the overall Gibbs energy of the system. Since the hydrocarbon (i.e., hydrocarbon chain) part of the surfactant is hydrophobic and not miscible in water, the self-assembly of these hydrophobic parts into a phase separate from the water can be attributed to the hydrophobic effect. The hydrophobic Gibbs energy (or the transfer Gibbs energy) can be defined as the Gibbs energy for the process of transferring the hydrocarbon chains from water to the micelle.<sup>3</sup> In considering enthalpy and entropy contributions to the Gibbs free energy of transfer for the hydrophobic effect, the entropy dominates. The transfer of the

hydrocarbon solute from the water into the hydrocarbon solvent (micelle phase) is accompanied by a decrease in the Gibbs transfer energy.<sup>6</sup> The presence of the hydrophobic hydrocarbon chains in the water increases the ordering of water molecules in the vicinity of the chains. The increase in entropy caused by restoring the normal hydrogen-bonded structure of water, accompanied by the disappearance of more highly ordered water, often termed icebergs, around the hydrocarbon chain. The overall process has the tendency to bring the hydrocarbon molecules together to form micelles through hydrophobic interactions.<sup>3</sup> Another way to describe the formation of micelles is to consider a cavity forming in the water phase that is filled in with surfactant chains, with surfactant head-groups aligned at the cavity/water interface.

The Gibb's free energy ( $\Delta G$ ) for micelle formation can be estimated by considering a series of three steps.<sup>7</sup> (Fig. 2.2).

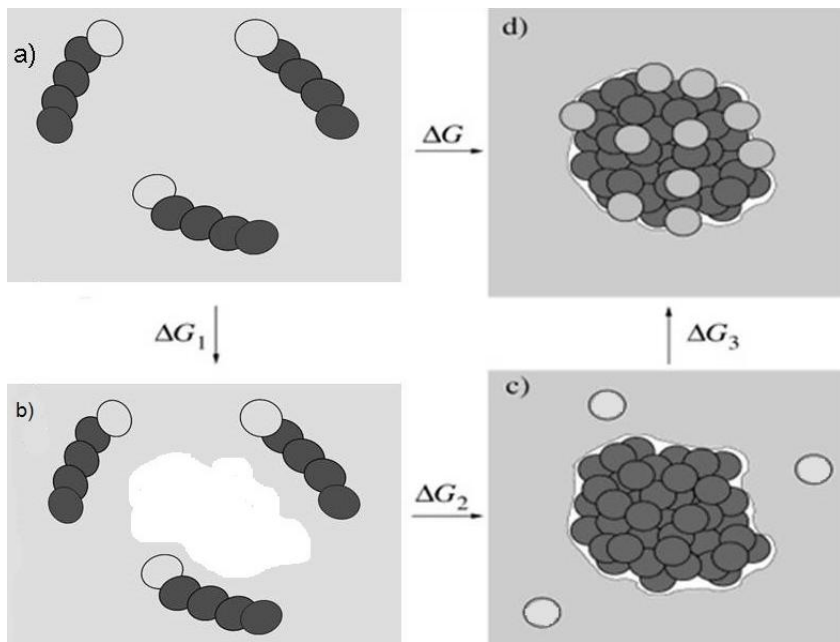


**Fig. 2.2.** Thermodynamic cycle of micelle formation. The process of assembling  $n$  separated amphiphiles (a) to a micelle (d) can be treated as though it occurs in three steps: (1) Creating a cavity in the solvent (light gray) (b); (2) Transferring the hydrophobic chains (dark gray) from the aqueous solution into the cavity (c); (3) Distributing the polar headgroups (gray) over the surface of the cavity and reconnecting them to the hydrophobic chains (d) (adapted).<sup>7</sup>

In the first step, free energy is required to form a cavity in the water phase. Assuming a spherical cavity with a surface area of at least  $1 \text{ nm}^2$ , the free energy for the formation of the cavity can be expressed as  $\Delta G_1 = \gamma A$ , where  $A$  denotes the surface area of the cavity and  $\gamma$  is the water-vapor surface tension. In general, there is also pressure-volume work for forming a cavity in a liquid. For water at standard conditions, the pressure is sufficiently small that this contribution is negligible for cavities with diameters less than 5 nm.

The second step is the formation of the hydrophobic micelle core by the hydrophobic tails of surfactants. This can be considered as disconnecting the tails from the headgroups and then moving the hydrophobic tails from water into the tail-filled cavity. One part of the free energy to fill the cavity is  $-n\Delta\mu$ , where  $-\Delta\mu$  is the free energy change in transferring the hydrophobic tail (i.e., the alkane chain) into the oily hydrophobic core from water. Another part is an interfacial contribution due to the presence of van der Waals attractions between oil (tails) and water. As discussed in Huang et al.,<sup>8</sup> these attractions cause the oil-water surface tension,  $\gamma_{ow}$ , to be lower than the water-vapor surface tension,  $\gamma$ . Thus, the free energy for filling the cavity is:

$$\Delta G_2 = -n \Delta\mu - \Delta\gamma A \quad (2.1)$$

$$\text{where } \Delta\gamma = \gamma - \gamma_{ow}. \quad (2.2)$$

In this case,  $\Delta\mu$  is close to the transfer free energy for moving the associated alkane chain from oil into water, because the densely packed interior of a micelle is much like a hydrocarbon liquid.<sup>9</sup>

The third step is the placing of the hydrophilic headgroups on the micelle surface. In this step, the hydrophilic headgroups are reconnected to the hydrophobic tails, placing them at the water-oil interface in order to maintain a favorable solvation energy.<sup>7</sup> This positioning needs to be done

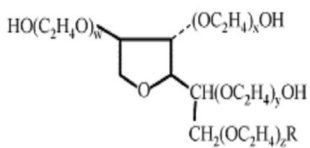
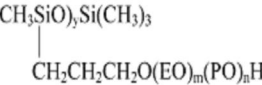
simultaneously with enforcing the connectivity between heads and tails and maintaining the densely packed interior. These conditions result in an entropic cost that increases extensively with aggregation size. The driving force of the third step can be conveniently estimated from the electrostatic factors of positioning the polar headgroups, subject to the constraints associated with attaching them to the hydrocarbon chains.<sup>10,11</sup> Different factors including temperature, pressure, and the presence and nature of additives can affect micellization which is opposed by thermal and electrostatic forces.<sup>12</sup>

### **2.1.2 Classification of surfactants**

The widespread importance of surfactants in practical applications, and the interest in their nature and properties, have produced a wealth of literature on this subject.<sup>3</sup> The surfactant industry is dominated by several types: alkylbenzene sulfonates, alcohol ethoxylates, sulfates and ethersulfates.<sup>13</sup> These are the major ingredients of laundry detergents, household, and personal care products. Growing interest in increasing performance in these areas has also led to research into mixed surfactant systems. Other commercial interests have also influenced the development of new surfactants. For example, during the oil crisis in the 1970s, enhanced oil recovery methods, such as microemulsions, were heavily investigated.<sup>3</sup> Scientific curiosity has also driven surfactant research into areas such as organization of surfactant molecules into interesting shapes, structures, and unique properties.<sup>14</sup> Surfactants are also the subject of investigation into the origins of life, meteorites containing lipid-like compounds have been found to assemble into boundary membranes and may be an interstellar prebiotic earth source of cell-membrane material.<sup>15</sup> Surfactants are used in micellar enhanced ultrafiltration (MEUF) for the removal of various organic and/or inorganic pollutant from wastewater.<sup>16</sup> Over the past ten years, new surfactant molecules have been developed; however, additional surfactant molecules are in

demand for specific applications such as nanoparticle synthesis, and more diverse and environmentally friendly consumer products.<sup>3</sup> Surfactants have been classified based on their polar head group. Several examples are listed in Table 2.1.

**Table 2.1. Classification of surfactants<sup>3</sup>**

Class	Examples	Structures
Anionic	Na stearate	$\text{CH}_3(\text{CH}_2)_{16}\text{COO}^- \text{Na}^+$
	Na dodecyl sulfate	$\text{CH}_3(\text{CH}_2)_{11}\text{SO}_4^- \text{Na}^+$
	Na dodecyl benzene sulfonate	$\text{CH}_3(\text{CH}_2)_{11}\text{C}_6\text{H}_4\text{SO}_3^- \text{Na}^+$
Cationic	Laurylamine hydrochloride	$\text{CH}_3(\text{CH}_2)_{11}\text{NH}_3^+ \text{Cl}^-$
	Trimethyl dodecylammonium chloride	$\text{C}_{12}\text{H}_{25}\text{N}^+(\text{CH}_3)_3 \text{Cl}^-$
	Cetyl trimethylammonium bromide	$\text{CH}_3(\text{CH}_2)_{15}\text{N}^+(\text{CH}_3)_3 \text{Br}^-$
Non-ionic	Polyoxyethylene alcohol	$\text{C}_n\text{H}_{2n+1}(\text{OCH}_2\text{CH}_2)_m\text{OH}$
	Alkylphenol ethoxylate	$\text{C}_9\text{H}_{19}-\text{C}_6\text{H}_4-(\text{OCH}_2\text{CH}_2)_n\text{OH}$
	Polysorbate 80 $w + x + y + z = 20$ $\text{R} = (\text{C}_{17}\text{H}_{33})\text{COO}$	
	Propylene oxide-modified polymethylsiloxane (EO = ethyleneoxy, PO = propyleneoxy)	$(\text{CH}_3)_3\text{SiO}((\text{CH}_3)_2\text{SiO})_x(\text{CH}_3\text{SiO})_y\text{Si}(\text{CH}_3)_3$ 
Zwitterionic	Dodecyl betaine	$\text{C}_{12}\text{H}_{25}\text{N}^+(\text{CH}_3)_2\text{CH}_2\text{COO}^-$
	Lauramidopropyl betaine	$\text{C}_{11}\text{H}_{23}\text{CONH}(\text{CH}_2)_3\text{N}^+(\text{CH}_3)_2\text{CH}_2\text{COO}^-$
	Cocoamido-2-hydroxypropyl sulfobetaine	$\text{C}_n\text{H}_{2n+1}\text{CONH}(\text{CH}_2)_3\text{N}^+(\text{CH}_3)_2\text{CH}_2\text{CH}(\text{OH})\text{CH}_2\text{SO}_3^-$

### 2.1.2.1 MEUF using cationic surfactants

The hydrophilic head of cationic surfactants bears a positive charge which makes it possible to attract anionic contaminants.<sup>17,18</sup> Cationic surfactants, used in fabric softeners, corrosion inhibitors and antimicrobial agents,<sup>19</sup> are very useful in wastewater treatment by MEUF. Cetylpyridinium chloride (CPC) is identified as one of the potential cationic surfactants that can be used to remove anionic contaminants from wastewater. The potential of CPC has been tested for the removal of organic materials from wastewater. Purkait et al.<sup>20</sup> showed that 74% of an

eosin dye was removed by MEUF using CPC. Ahmad et al.<sup>17, 21</sup> found that reactive dyes such as Reactive Black 5 and Reactive Orange 16 can be removed 99% through MEUF by using CPC. Hexadecyltrimethylammonium bromide (CTABr) is a cationic surfactant shown to have an 85.9% removal efficiency for phenol as reported by Luo et al.<sup>22</sup> These researchers also reported that for surfactants with the same hydrophilic headgroups (CTABr and octadecyl trimethyl ammonium bromide (OTABr)), the hydrocarbon chain length (hydrophobic tail) affected the solubilization (transfer) of phenol into micelles.<sup>22</sup> They also found that increasing the hydrocarbon chain length of the surfactant resulted in decreasing the CMC, hence enhancing the solubilization of phenol into micelles. Another study conducted by Zaghbani et al.<sup>23</sup> on the effect of hydrophobic alkyl chain length on the removal of Eriochrome Blue Black R dye using n-alkyltrimethylammonium bromide surfactants, dodecyltrimethylammonium bromide (C<sub>12</sub>TABr), tetradecyltrimethylammonium bromide (C<sub>14</sub>TABr), CTABr and octadecyltrimethylammonium bromide (C<sub>18</sub>TABr) showed that the dye retention increased as the hydrophobic alkyl chain length increased (C<sub>12</sub>TABr (34.6%) < C<sub>14</sub>TABr (51.1%) < CTABr (99.6%) < C<sub>18</sub>TABr (99.9%)) due to hydrophobic interaction which increased solubilization of dyes by the micelles.

In this PhD research, for the removal of sulfonamides from the wastewater, CTABr has been considered as an effective surfactant candidate for MEUF due to the charge-charge interaction. This is because many sulfonamides are stable anions at neutral pH in wastewater. These negative sulfonamides will presumably give better binding with the cationic CTABr surfactant. CTABr is also considered for the removal of neutral compounds (PAHs) where the charge of the headgroup will not affect binding but the micelle interaction will occur due to hydrophobic effects.

### **2.1.2.2 MEUF using anionic surfactants**

The hydrophilic head of an anionic surfactant has a negative charge<sup>18</sup> which interacts with the cationic charge of contaminants such as metal ions.<sup>24</sup> Anionic surfactants are widely used in detergent powders since they are known to be more effective than other surfactants in soil removal, especially for natural fabrics.<sup>19</sup> MEUF using anionic surfactants have been found to be effective for the removal of both inorganic and organic contaminants from wastewater.<sup>25, 26</sup> The anionic surfactant sodium dodecyl sulphate (SDS) has been widely used for the removal of heavy metal ions from wastewater. Yenphan et al.<sup>27</sup> and Samper et al.<sup>24</sup> proved 90% to 100% removal of  $Pb^{2+}$  was achieved using SDS. Samper et al.<sup>24</sup> also studied the removal of other metal ions ( $Cd^{2+}$ ,  $Cu^{2+}$ ,  $Ni^{2+}$ ,  $Zn^{2+}$ ) using SDS and linear alkylbenzene sulfonate (LAS) as the surfactant via MEUF. Misra et al.<sup>28</sup> also found that SDS was very effective for the removal of uranyl ions ( $UO_2^{2+}$ ) as well as di-butyl phosphate and tri-butyl phosphate from aqueous solutions.

In this PhD research, the anionic surfactant SDS was considered for the removal of neutral compounds (PAHs) where, as was the case for cationic surfactant, the charge of the headgroup is not important but micelle interaction will occur due to hydrophobic effects.

### **2.1.2.3 MEUF using switchable surfactants**

A switchable surfactant can be defined as a surfactant which can be changed from one form to another by activation of a trigger, and as a consequence the surfactant activity can be completely reversed.<sup>29</sup> The trigger is usually addition of a chemical reagent such as  $CO_2$ <sup>29-31</sup> or air, or a chemical process such as oxidation/reduction cycles<sup>32</sup> or photochemistry.<sup>12</sup> There are various applications of switchable surfactants. They are beneficial in emulsion polymerization, in the oil industry, in pharmaceutical manufacturing, and in other commercial chemical processes.<sup>29,33</sup> During drilling in the oil industry, water is pumped into an underground oil reservoir to increase



the extraction of oil. Surfactants can be added to the water to promote the formation of a stable oil-water emulsion to increase the efficiency of the oil extraction. If a switchable surfactant is used, it can be switched off and the emulsion can be broken and separated into distinct layers, increasing the efficiency of the enhanced oil recovery (EOR) process.<sup>29</sup> Switchable surfactants can also be used to control CO<sub>2</sub> hydrate formation in oil and petroleum transport applications as well as in demulsification and deoiling applications.

There are not yet any reports regarding the treatment of wastewater using switchable surfactants in the MEUF system. Sodium laurate (SOL) is a commercially available switchable surfactant, which has been used in this PhD research to examine its potential for the treatment of wastewater in MEUF. SOL has been used only to study the removal efficiency of PAHs and binding characterization of PAHs in the "on" form rather than switching "on and off", which might be a topic for future research.

## **2.2 Binding of contaminants to micelles**

Contaminants can exist in different forms in wastewater, including cationic, anionic, neutral or zwitterionic. Micelles formed by ionic surfactants have an inner hydrocarbon zone, an outer ionic layer called the Stern layer and an intermediate region termed the palisade layer.<sup>34</sup> Depending on their chemical properties, contaminants can be dissolved in the hydrocarbon core, adsorbed on the Stern layer or sandwiched in the palisade layer.<sup>34</sup> Charge-charge interactions are presumably dominant for the binding of ionic contaminants to micelles, with the contaminants adsorbed on the outer Stern layer.<sup>35</sup> On the other hand for neutral contaminants like PAHs, hydrophobic interactions would be the primary force for binding to micelles. The hydrocarbon-like interior of the micelles determines their capacity to bind non-polar hydrophobic compounds. For most

non-polar hydrophobic compounds, the locus of solubilization is probably the hydrocarbon core of the micelle.

### **2.2.1 Separation of bound contaminants using MEUF**

MEUF is a microheterogeneous system that can solubilize and compartmentalize both ionic and neutral organic compounds into different regions of a micelle aggregate structure.

In MEUF, the surfactant is added above its critical micelle concentration (CMC) into an aqueous solution containing contaminants (e.g metal ions, organic materials, inorganic ions).<sup>22</sup> When the surfactant concentration exceeds the CMC value, the surfactant monomers can assemble<sup>36, 37</sup> and aggregate to form micelles<sup>22</sup> having a hydrodynamic diameter significantly larger than the pore diameter of an ultrafiltration membrane.<sup>36, 27, 28,38</sup>

The contaminants or solute will be entrapped in micelles if they are strongly attracted by the micelle surface and/or can be solubilized in the micelle interior.<sup>39</sup> Micelles with a larger diameter than the membrane pore size containing solubilized contaminants will be retained behind the membrane during ultrafiltration, leaving only water, unsolubilized contaminants and surfactant monomers to cross to the permeate side.<sup>28,39</sup> MEUF enhances the performance of ultrafiltration by retaining smaller contaminants that would normally pass through conventional ultrafiltration membranes. Contaminant partitioning occurs to the micellar phase, followed by ultrafiltration of the solution to remove the micelles and bound contaminants.<sup>37,,40,41,42</sup> Low molecular weight sulfonamides (~170-320 Da) and PAHs (~128-300 Da) can easily pass through a typical ultra filtration membrane (100,000 Da),<sup>43</sup> but the same sulfonamides or PAHs bound to micelles will remain in the retentate side.

## 2.3 Measurement of binding constants

Measurement of binding constants gives quantitative information about the interaction between acid-base, metal-ligand, enzyme-substrate, and various organic and inorganic species with micellar system which is very important in analytical chemistry, industrial process chemistry, etc. Techniques such as spectrophotometry, fluorometry, NMR, and HPLC, have been used to measure binding constants.<sup>44</sup> The flow injection gradient (FIG) technique has been successfully used for accurate and automated determination of formation constants of various chemical systems<sup>45-47</sup> and for the characterization of a variety of chemical systems including acidity constants<sup>51</sup> and proton-ligand equilibria.<sup>44</sup> Electrospray ionization mass spectrometry has been used in monitoring the intensities of both unbound and bound guest or host during a titrimetric experiment.<sup>49-53</sup> This method has been used to examine dissociation constants for oligonucleotide-serum albumin complexes,<sup>51</sup> the binding constants of vancomycin-peptide complexes and ristocetin peptide complexes,<sup>50</sup> the dissociation constants for proteinphosphopeptide complexes,<sup>49</sup> and the dissociation constants for aminoglycoside-RNA models.<sup>52</sup>

Capillary electrophoresis (CE) is a very powerful tool for understanding the nature and strength of biological interactions.<sup>54-57</sup> With the continuing development of CE, there has been increasing interest in determining binding constants of the solute-ligand complexes. This has given rise to a new method known as affinity capillary electrophoresis (ACE).<sup>58,59</sup> ACE has already been used to measure binding constants in a number of systems, including the interactions of lectins with sugars,<sup>60-62</sup> albumin with drugs,<sup>63,64</sup> vancomycin with peptides,<sup>56-68</sup> enantiomers with cyclodextrins, carbonic anhydrase with drugs or cations and antibodies with antigens.<sup>69</sup>

When a ligand forms a complex with a macromolecule, the concentration of free ligand in the equilibrium mixture can be monitored by the rate of dialysis across a suitable membrane.<sup>70</sup> By using radioactive ligands, the rate can be monitored quickly, without changing the concentration of the ligand in the reaction mixture. This method was originally developed for rapid binding measurement of sugars and nucleotides to yeast hexokinases.<sup>71,72</sup> This method was later successfully used for binding measurements of nucleotides,<sup>70,73</sup> pyrophosphate,<sup>74</sup> calcium ions,<sup>75</sup> and amino acids.<sup>76</sup> The rate of dialysis can be monitored conveniently by use of the simple device illustrated in Fig.2.5. The apparatus is comprised of a dialysis cell with an upper chamber containing macromolecules and the labelled ligand, separated by a membrane from the lower chamber. Buffer is continuously pumped into the lower chamber at constant rate and from which sample is collected for radioactivity measurements.<sup>70</sup>

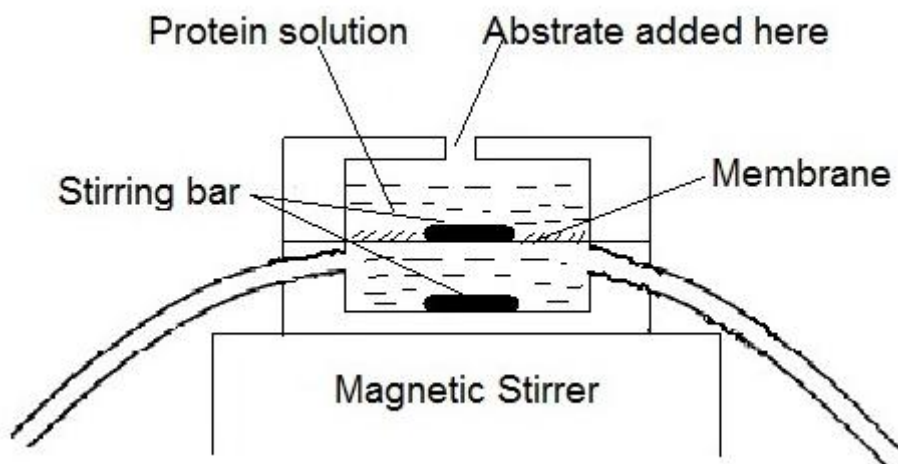


**Fig. 2.3.** Diagram of the apparatus of measuring substrate binding by rate of dialysis (adapted).<sup>72</sup>

The interaction between organic molecules and micelles is of increasing analytical interest and good results have been obtained when determinations of some organic compounds are carried out in micellar media, by several techniques<sup>77-79</sup> Binding constants have been determined for various

organic and inorganic species with micellar systems using *in situ* techniques such as fluorescence,<sup>80</sup> enthalpy of association,<sup>81</sup> and NMR.<sup>82,83</sup> *Ex situ* techniques, involving separation of micelles and bound species from unbound molecules, have also been employed, such as micellar liquid chromatography<sup>84</sup> and semi-equilibrium dialysis (SED).<sup>41,85</sup> Binding constant measurements for chemical species and micelles using absorbance measurements<sup>86-89</sup> have been reported by Sepulveda.<sup>90</sup> A high performance liquid chromatography<sup>91,92</sup> model has been developed by Armstrong and Nome,<sup>93</sup> and the dissociation constants method<sup>94-97</sup> has been studied by Berezin<sup>98</sup> for determining binding between chemical species and micelles. Other methods are ultrafiltration,<sup>99,100</sup> isopiestic,<sup>101</sup> and solubility<sup>102-104</sup> based on absorbance measurements and using the model developed by Sepulveda<sup>90</sup> and Bunton and colleagues.<sup>105</sup> Selected binding measurement techniques are discussed below.

### 2.3.1 Binding constant by Fluorometer

A fluorometric method has been adapted to determine the binding constants (K) between different systems and micelles.<sup>106</sup> This method is based on the variation of the fluorescence of the system in the presence of increasing amounts of a surfactant. Fluorescence measurements have been used to determine binding constants using selective quenchers.<sup>107-109</sup> This method permits the determination of binding constants in strong acid or alkaline media. De La Guardia et al. used this method to determine binding constants of 1-naphthol and 2-(4-alkylamino-2 hydroxyphenyl) benzo-X azoles (X being an O or an S atom, PAS-O and PAS-S) with cationic, anionic, and nonionic surfactants.<sup>106</sup> In this study, fluorescence was reported to be higher in the presence of different cationic, anionic, and nonionic surfactants than in aqueous media, and a fluorescence enhancement was found at concentrations above the CMC.<sup>106</sup>

Binding constants between fluorescent molecules and surfactants have been determined from the following equation

$$\frac{1}{[(I/I_o)-1]} = \frac{1}{[(I_M/I_o)-1]} \times [1 + 1/(\gamma KC_s)] \quad (2.3)$$

where,  $C_s$  is concentration of surfactant,  $I_M$  is the maximum fluorescence obtained and  $K$  is the binding constant.

Since fluorescence enhancement takes place at concentrations higher than the CMC,  $C_s$  values must be replaced by  $C_M$ , the concentration of surfactant in micellar form according to:

$$C_M = (C_s - CMC) \quad (2.4)$$

Therefore, substitution of Eq. (2.4) into Eq. (2.3) gives an expression which relates the fluorescence enhancement to the concentration of micellized surfactant:

$$\frac{1}{[(I/I_o)-1]} = \frac{1}{[(I_M/I_o)-1]} \times [1 + 1/\gamma K(C_M + CMC)] \quad (2.5)$$

When extinction coefficient does not vary in the micellar media, then  $\gamma = 1$ . If micelles do not modify the extinction coefficient at the excitation wavelength, then the regression between

$1/[(I/I_o)-1]$  and  $1/C_M$  gives a straight line and the value of the binding constant between the system and the micelles can be obtained from the quotient of the intercept and the slope of this line.<sup>106</sup>

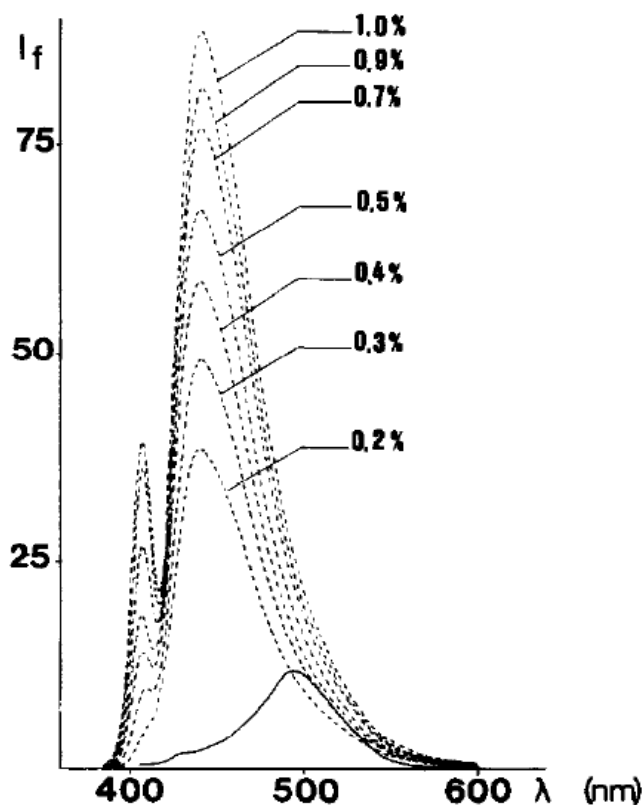


**Fig. 2.4.** Effect of Triton X-100 concentration on the fluorescence emission of PAS-S at an excitation wavelength of 412 nm and in 1 M HCl medium. Solid line is the fluorescence spectrum without surfactant. Dashed lines are the fluorescence emission spectra in the presence of different concentrations (% w/v) of Triton X-100.<sup>106</sup>

### 2.3.2 Binding constant by micellar High Performance Liquid Chromatography

Micelles are well known for their ability to solubilize hydrophobic compounds in aqueous solution.<sup>4</sup> Micelles provide a hydrophobic site for partition of solutes from the mobile phase and can replace traditional modifiers in reversed phase HPLC (RP-HPLC).<sup>110-114</sup> Micelle-solute association constants for some benzene and naphthalene derivatives with sodium dodecyl sulphate (SDS) and hexadecyltrimethylammonium bromide (CTABr) in the presence of n-butanol and sodium chloride have been determined by HPLC using micellar mobile phases. In micellar phase liquid chromatography (MPLC), only those solutes that interact with the micelle

through electrostatic interaction or hydrophobic effects, are affected by a change in micelle concentration in the mobile phase. The parameters that characterize the micellar systems (CMC, aggregation number and charge of the micelle) are modified by the addition of salts or alcohols to the solution.<sup>115-118</sup> These additives can also modify the solute-micelle distribution equilibrium. There are three equilibria involved in the MPLC process. The first equilibrium is the distribution of the solute between the micelle and bulk water, defined as the water-micelle partition coefficient ( $P_{MW}$ ). The second is the partitioning of the solute between the stationary phase and the micelle, defined as the stationary phase-micelle partition coefficient ( $P_{SM}$ ). The third is the distribution of the solute between the stationary phase and water, defined as the stationary phase-water partition coefficient ( $P_{SW}$ ). Using these equilibrium expressions, Armstrong and Nome<sup>119</sup> have reported the correlation between retention and micelle concentration as follows:

$$\frac{V_s}{(V_e - V_m)} = \frac{v(P_{MW} - 1)C_m}{P_{SW}} + \frac{1}{P_{SW}} \quad (2.6)$$

where,  $V_s$ ,  $V_e$  and  $V_m$  are the stationary phase volume, elution volume of the solute and the void volume of the column respectively;  $v$  is the molar volume of the surfactant and  $C_m$  is the micellized surfactant concentration in the mobile phase,  $C_m = C_t - CMC$ ;  $C_t$  is the total surfactant concentration in solution. A plot of  $\frac{V_s}{V_e - V_m}$  vs  $C_m$  is linear and the solute-micelle constant per surfactant monomer,  $K_2 = v(P_{MW} - 1)$ ,<sup>120</sup> can be calculated by measuring the slope: intercept ratio.

If the surfactant molar volume  $v$  is known, the partition coefficient of solute between bulk water and micelle,  $P_{MW}$ , can also be calculated. Arunyanart and Cline Love<sup>121</sup> have derived a similar equation which has a correlation with the capacity factor  $k'$  and micellized surfactant concentration  $C_m$ . This equation is,



$$1/k' = \frac{K_2 C_m}{\phi[L_S]K_1} + \frac{1}{\phi[L_S]K_1} \quad (2.7)$$

where  $K_2$  is the binding constant,  $\phi$  (phase ratio) =  $V_s / V_m$ ;  $[L_S]$  is the stationary phase concentration, and  $K_1$  is the binding constant for the solute between the bulk solvent and the stationary phase. A plot of  $1/k'$  vs  $C_m$  would produce a straight line and the value of the solute-micelle binding constant  $K_2$ , can be obtained from the slope: intercept ratio.

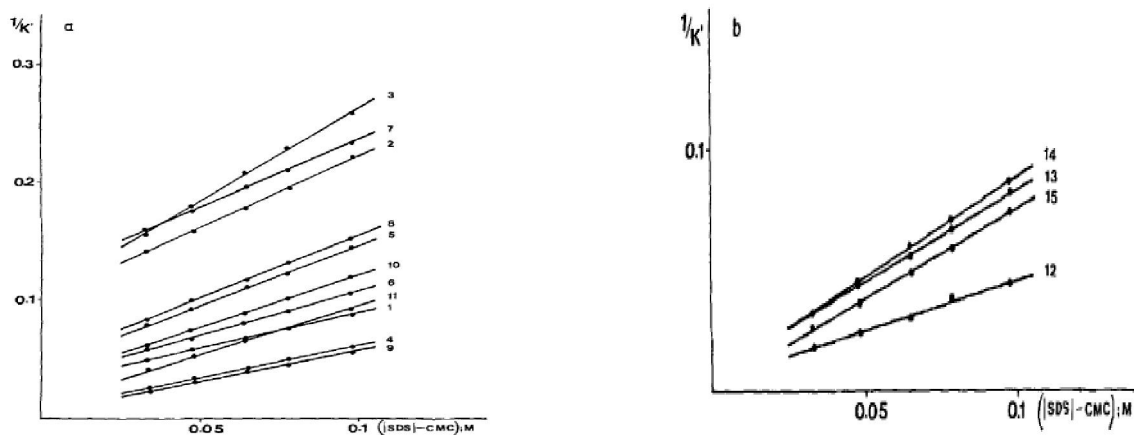


**Fig. 2.5.** Variation of  $1/k'$  vs micellized SDS concentration in solution. Mobile phase: 0.1 M NaCl/SDS (a) benzene derivatives (b) naphthalene derivatives.<sup>122</sup>

### 2.3.3 Binding constant by micellar electrokinetic chromatography

Micellar electrokinetic chromatography (MEKC) is a capillary electrophoresis method (CE)<sup>123-125</sup> which is well established for measuring solute-micelle association constants, even though its potential has largely remained unexplored.<sup>126</sup> Solutes (ionized and non-ionized) are distributed between the micelle and the surrounding non-micellar phase according to their solute-micelle association. In MEKC, micelles are formed mostly from anionic surfactants; therefore, their migration in an electric field is retarded with respect to the electroosmotic flow. Micellar electrokinetic chromatography was studied to determine solute-micelle association constants for a

group of benzene derivatives and polycyclic aromatic hydrocarbons using sodium dodecyl sulphate (SDS) as a surfactant. Among the different buffer studies, only those of  $\text{pH} \geq 9$  [2-(N-cyclohexylamino) ethanesulphonic acid and ammonium acetate] gave an electroosmotic flow high enough to allow the elution of all of the compounds studied.

If the micellar concentration in the buffer is low, the solute capacity factor ( $k'$ ) in MEKC can be related to the total surfactant concentration in the buffer as follows:<sup>110, 113</sup>

$$k' = (K_2 + v) (C - CMC) \quad (2.7)$$

where  $K_2$  is the solute-micelle association constant per surfactant monomer,  $v$  is the molar volume of the micelle and  $C$  is the total surfactant concentration in the buffer. In MEKC,  $k'$  is

$$\text{defined as } k' = \frac{(t_r - t_o)}{t_o [1 - (t_r / t_m)]} \quad (2.8)$$

where,  $t_o$  is the migration time of the electroosmotic flow marker.  $t_r$  is the migration time of the solute and ,  $t_m$ , is the migration time of the micelle. From Eq. 2.7, solute micelle-association constants can be calculated from the slope of the straight line obtained from the plot of the variation of the capacity factor of the solute with the total surfactant concentration in the separation buffer. However, this method is not appropriate for compounds that are strongly associated with the micelles, for which the term  $[1 - (t_r / t_m)]$  in Eq. 2.8 can be close to zero.

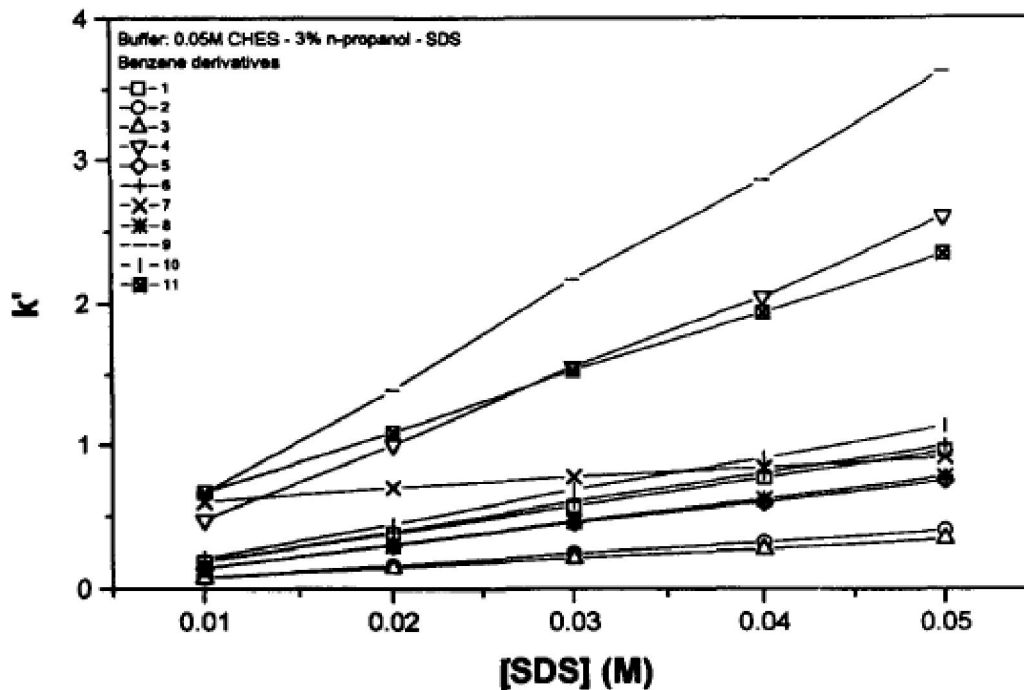


**Fig. 2.6.** Variation of the capacity factor ( $k'$ ) for benzene derivatives as a function in 0.05 M CHES buffer modified with 3% n-propanol.<sup>120</sup>

From the slope of this straight line, the solute-micelle association constant can be obtained if the molar volume of the surfactant is known. Fig. 2.8 shows the linear variation of the capacity factor as a function of the SDS concentration. However, variation of the capacity factor of the most hydrophobic compounds does not show a straight line; instead a larger scatter of the points is observed. The non-linear variation of the capacity factor as a function of the surfactant concentration for the most hydrophobic compounds may be due to the large error in the determination of the capacity factor as a result of the solute migration times, which were similar to the micelle migration time.<sup>120</sup>

#### 2.3.4 Binding constant by SED

Semi-equilibrium dialysis (SED) is a passive method of Micellar-enhanced ultrafiltration (MEUF). In this method, aqueous surfactant micelles, at concentrations greater than the critical micelle concentration (CMC), can bind or solubilize target solutes and prevent them from passing through ultrafiltration membranes having molecular weight cutoff values in the range 1000-50000.<sup>127</sup> Semi-equilibrium dialysis (SED), can be used to determine the binding of ions and organic solutes to surfactant micelles.<sup>128-131</sup> Equilibrium dialysis has been used for many decades for the study of binding of low molecular weight solutes to macromolecules.<sup>132-134</sup> But, the use of equilibrium dialysis method in studying the solubilization of organic solutes by aqueous surfactant micelles is complicated because of gradual transfer of surfactant from the retentate into the permeate compartment, resulting in the formation of micelle in the permeate side due to solubilization of significant quantities of the organic solute in micelles.<sup>135-139</sup> Presence of micelles in the permeate side can lead to a quite large errors in inferred values of partition constants for transfer of solutes from the “bulk aqueous solution” into the micelle.<sup>140</sup>

The binding or solubilization potential (the ability of surfactant micelles to increase the total hydrocarbon concentration in solution beyond the aqueous solubility component) can be quantified by the micelle-water partition coefficient,  $K$ , partitioning of hydrocarbons between the micellar and the aqueous pseudo-phases.<sup>141</sup> Depending on the properties of the contaminants, partitioning will occur into the different zones of the micelle. In the interior zone, the micelle can solubilize less polar molecules. In the layer on the surface of a charged micelle, oppositely charged ions or molecules can be strongly adsorbed by charge-charge interactions.

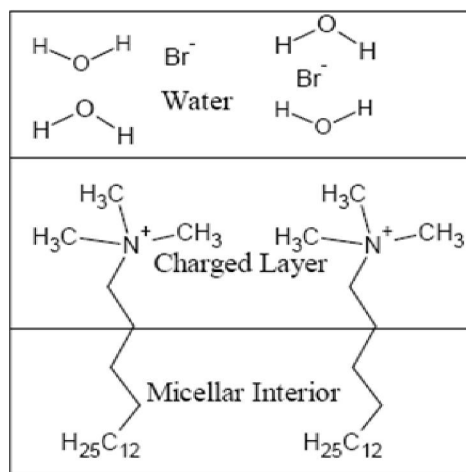


**Fig. 2.7.** Cross-sectional representation of a CTABr micelle.

To determine solubilization potentials for aqueous hydrocarbon concentrations below the solubility limit, semiequilibrium dialysis (SED) cells have been utilized.<sup>85</sup>

Christian et al. have reported that the dialysis method is quite convenient for studying solubilization equilibria.<sup>130</sup> In a SED experiment, the surfactant cannot reach equilibrium in any reasonable period of time, and in fact true equilibrium would be a state in which there is no difference between the concentrations of either the surfactant or the organic solute in the two compartments of the dialysis cell.<sup>140</sup> They termed the method “semi-equilibrium dialysis”, because equilibrium can be reached with respect to the dissolved organic compound, but the surfactant will continue to diffuse through the membrane as long as there is a difference in total concentration between the two chambers of the cell. They reported the solubilization constant of phenol in aqueous n-hexadecylpyridinium chloride (CPC) solutions at 25 °C.<sup>141</sup> SED uses a separation cell to retain micelles and bound contaminants on one side of the dialysis membrane, and then separately examines the “retentate” and “permeate” sides of the cell. In SED, it is assumed that unbound species and free surfactant molecules come to near-equilibrium conditions on both sides of the membrane.<sup>142</sup> This means a measured concentration of a contaminant on the

permeate side of the cell can be assumed to be equal to the concentration of free contaminants on the retentate side. The total contaminant measured on the retentate side will be the sum of the free and micelle-bound forms of the contaminant. SED is a process in which two chambers are separated by a dialysis membrane acting as an ultrafilter. The molecular weight cut off (MWCO) of the membrane is chosen in such a way that the receptor component of the sample (the micelle, in this case) will remain in the retentate side.<sup>143</sup>

I use the term “Semi-equilibrium” in this thesis as it is assumed that free molecules and free surfactant molecules are at equilibrium across the membrane, but there will not be any micelles on the permeate side. “Complete equilibrium” would have equal concentrations of molecules and micelles on both sides, and might take several days to be achieved. Our onsite prepared SED cell is very simple (Fig. 2.10).

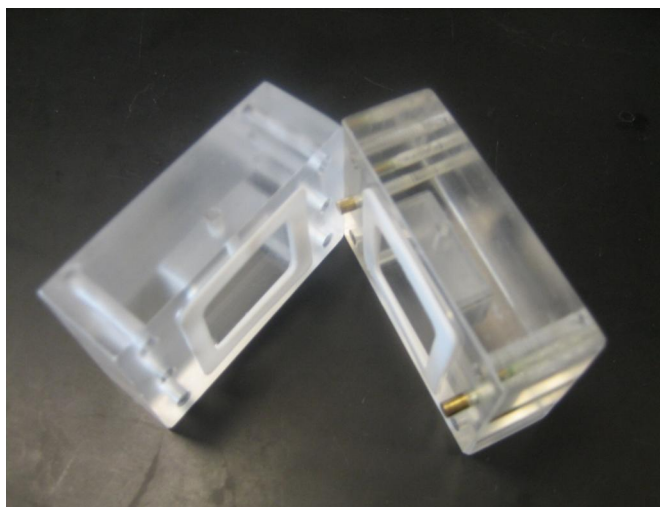


**Fig. 2.8.** In house prepared SED cell

In this study, solution of contaminant and surfactant are placed into the retentate side and de-ionized water is placed in the permeate side of the SED cell. Contaminants and surfactant will start to diffuse and contaminants will start to bind with micelles at the same time.

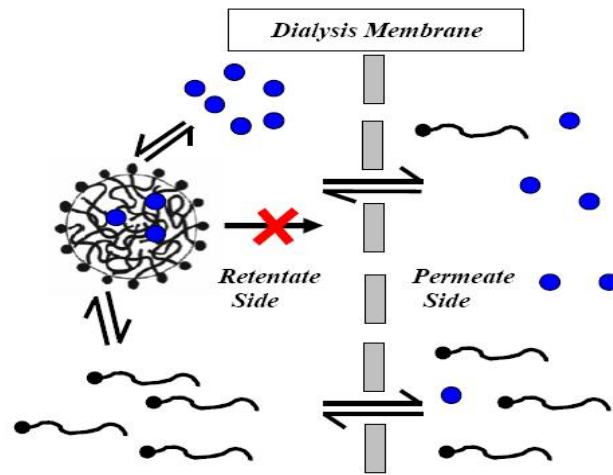


**Fig. 2.9.** Schematic diagram of the semi-equilibrium Dialysis (SED) process.

After 24 h, the total concentration of the contaminants and surfactants in the retentate side and free concentrations of the contaminants and surfactants in the permeate side were determined. We calculated the partition coefficient also called binding constant of the banded contaminants and free contaminants using the following equations:

$$K_B = \frac{[Contaminants]_M}{[Contaminants]_A} \quad (2.9)$$

where,  $K_B$  is the binding constant

$[Contaminants]_M$  = Concentration of contaminants in the micelle

$[Contaminants]_A$  = Concentration of free contaminants in aqueous solution

### 2.3.5 Binding constant by <sup>1</sup>H NMR spectroscopy

NMR spectroscopy is probably the most informative technique for determining binding constants, as it has high specificity and can provide structural information on the nature of the complex.<sup>144</sup> Chemical shift, spin coupling, and relaxation times are all sensitive to the short-range interactions encountered in molecular complexes.<sup>145</sup> Applications of NMR spectroscopy to the study of molecular complexes generally, and to cyclodextrin inclusion complexes specifically, have been reviewed.<sup>146</sup> Many studies have been conducted on the binding of cyclodextrins to a wide assortment of compounds, some utilizing NMR.<sup>145</sup> The binding constant of cyclodextrins with alprostadil has been reviewed by several authors.<sup>145, 147-149</sup> However, very little research has been done for determining micellar binding constants by NMR.<sup>150,151</sup> NMR chemical shifts have become by far the most important method for determining the binding constant between two molecules in solution. This method utilizes the difference between the chemical shifts of a molecular species in the free and bound states.<sup>152, 153</sup> Protons of the free and bound ligand will experience different chemical environments in the solution and therefore they will have different chemical shifts.<sup>154</sup>

In terms of the micellar binding complex, chemical shift changes towards higher field or lower field will give very important information of the locus and orientation of the molecule in the micelle. From chemical shift changes, binding constants have been determined for various host-guest systems.<sup>43</sup> An external or internal standard is used to provide a reference signal to measure chemical shift.<sup>40-42</sup> The external standard method has the advantage of inertness to the system to be measured, but this method requires susceptibility corrections. The reference signal from an internal standard must be sharp and well separated from other signals in the NMR spectrum, but will have the advantage that no bulk-susceptibility corrections are required. Corrected data using



external standards gave the same binding constants as those determined using internal standards,<sup>44,45</sup> however, such corrections are tedious, particularly for multicomponent systems. Therefore, the use of internal standards is preferred for determining binding constants so that there would be minimum error in chemical shift measurements. Such standards in aqueous systems include methanol, tetramethylammonium ion, sodium methyl sulfate, sodium methanesulfonate, and HDO.<sup>155</sup>

For the 1:1 stoichiometry in which, binding or equilibrium constant is given by:

$$K = \frac{[SL]}{[S][L]} \quad (2.10)$$

where, [S] is the concentration of free substrate, [L] is the concentration of free ligand, and [SL] is the concentration of the complex. Instead of measuring separate concentrations, determining molecular complexation constants is a common approach for generating a binding curve.<sup>145</sup> A binding curve can be created from the chemical shift differences of the proton of the free ligand and the substrate ligand complex. Using non-linear regression analysis a binding constant can be determined.

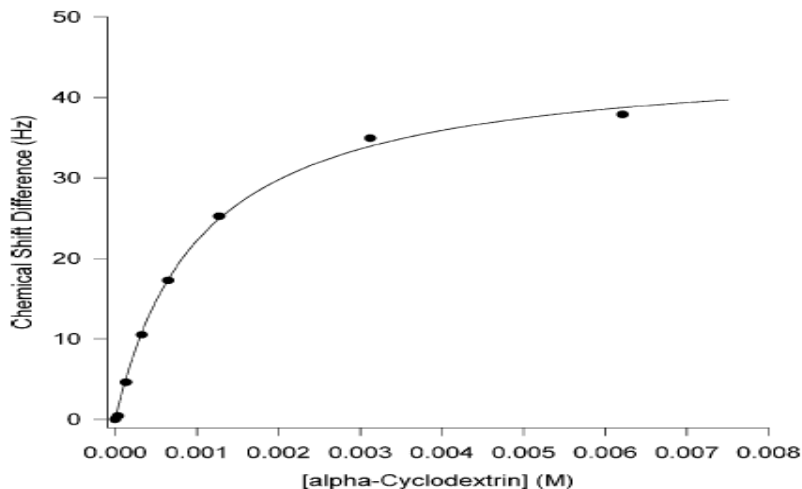


**Fig. 2.10.** Binding curve of  $\alpha$ -cyclodextrin with alprostadil complex. The filled circles correspond to the experimental data points and the smooth curve is the best (spline-smoothed) fit of the data points.<sup>145</sup>

## 2.4 Characterization of the binding constant

To predict the removal efficiency of the MEUF method, it is important to understand the binding constant ( $K_B$ ).<sup>82</sup> The binding constant is also sometimes referred to as the partition coefficient or equilibrium partition. An octanol-water ( $K_{OW}$ ) partition coefficient (determined for n-octanol) is widely used to measure the hydrophobicity of a solute.  $K_{OW}$  is also a function of the Gibbs energy of transfer from water to octanol and describes the thermodynamic tendency for the compound to partition preferentially in different media.<sup>156</sup> Semi-equilibrium dialysis (SED) is an approach that has been introduced to characterize binding of contaminants with micelles. It is predicted that binding constants derived from SED will act as an acceptable model parameter for the removal efficiencies for the MEUF system. Contemplating this approach, it would also be useful to derive a predictive methodology for the estimation of binding constants from a series of measured parameters of the contaminants, such as  $K_{OW}$  or  $K_a$  in order to further characterize micellar

systems and the predicted performance of MEUF treatment.  $^1\text{H}$  NMR spectroscopy is an important additional tool that can be used to better characterize the binding process of the contaminants with the micelle.  $^1\text{H}$  NMR will provide structural information of the contaminants inside the micelle. This will suggest locus and orientation of the binding protons of the contaminants in the micelles. This will validate the theory of the binding tendency with the Octanol-water free energy relationship.

#### **2.4.1 Binding constant ( $\text{Log } K_B$ ) and its co-relation with Octanol-Water partition ( $\text{Log } K_{OW}$ )**

The binding constant as described here is, in reality, the partition coefficient of a target molecule between two phases. For neutral molecules, partition is usually between a hydrophobic (non-polar) phase and another phase that is hydrophilic (polar). In a MEUF system, neutral contaminants are partitioned between the interior hydrophobic part of a micelle and the water phase. In order to predict binding efficiency of various contaminants with micelles, it may be useful to compare with a standard partitioning parameter.  $K_{OW}$  is a standard parameter for representing hydrophobic/hydrophilic partitioning behaviour.  $K_{OW}$  is considered as a model parameter because (1) it is the parameter with the largest number of measured values, and it also contains the widest selection of solute functional groups, and (2) most of these values have been determined in a single laboratory and therefore they are more reliable and self-consistent, and (3) the usefulness of  $K_{OW}$  as a model parameter for describing the binding forces between small hydrophobic molecules and macromolecules has already been established.<sup>157,158</sup> During the last 30 years, determining  $K_{OW}$  values has proven to be a valuable tool in many areas of natural sciences that include chemistry, biochemistry, biology, pharmacology, and environmental sciences.<sup>150,156</sup> During that period many scientific papers have been published in which

correlations of octanol / water partition coefficients with many physical, chemical, or biological properties have been demonstrated for a large variety of organic chemicals.<sup>151,156</sup>

The broad success of this particular physicochemical property in quantitatively predicting a variety of *in vitro* and *in vivo* processes suggest that the octanol-water partition constant should be compared with micelle binding constants. The relationship between non-ionic micelle—water and octanol-water partition constants were first investigated by Collett and Koo<sup>159</sup> for a variety of para substituted benzoic acid derivatives in poly-sorbate 20 micelles. Subsequently, Azaz and Donbrow<sup>160</sup> showed that a correlation existed between octanol-water or heptane-water partition constants and micelle-water partition constants for a variety of phenolic compounds. Tomida et al.<sup>161</sup> investigated similar relationships for 34 benzoic acid derivatives in polyoxyethylene lauryl ether micelles. For polar compounds, it is very difficult to predict binding behavior because their interaction with the micelle depends on specific parameters unique to both the micelle and the solute such as charge and the water content of the micelle. On the other hand, for neutral non-polar hydrophobic compounds expected to be in the hydrophobic core of the micelle, the relationship between  $K_B$  and  $K_{OW}$  should be more predictable. There are numerous articles available in the literature relating to the micellar solubilization of nonpolar or slightly polar hydrophobic chemicals. The solubilization of low molecular weight hydrocarbon solutes in various types of micelles have been reported.<sup>162</sup> Partition constants of low molecular weight chloromethanes between water and micelles of two anionic and one cationic surfactants have been recently studied.<sup>163</sup>

### 2.4.2 Binding constant (Log $K_B$ ) and its co-relation with free energy

The binding constant has a direct relationship with Gibbs free energy (G). The Gibbs energy change ( $\Delta G$ ) indicates the degree of spontaneity of an adsorption process. The more negative value of  $\Delta G$  reflects more energetically favourable for adsorption.<sup>164</sup>  $\Delta G$  of adsorption can be expressed as;

$$\Delta G = -RT \ln K_a \quad (2.10)$$

where,  $K_a$  is the thermodynamic equilibrium constant without units,  $T$  is the absolute temperature and  $R$  is the gas constant. Gibbs free energy is derived from enthalpy (H) and entropy (S). Gibb's free energy is defined as the driving force for a system to reach a chemical equilibrium. The energy comes from the enthalpy and entropy of the reaction in the system.

$$\text{Therefore, } \Delta G \text{ can be expressed as : } \Delta G = \Delta H - T \Delta S \quad (2.11)$$

Substituting equation (2.10) into equation (2.11) gives

$$\ln K_a = -\Delta H/RT + \Delta S/R \quad (2.12)$$

The plot of  $\ln K_a$  against  $1/T$  theoretically yields a straight line that allows calculation of  $\Delta H$  and  $\Delta S$  from the respective slope and interception of equation (2.12). These thermodynamic estimates can offer insight into the type and mechanism of an adsorption process.<sup>164</sup>

It is easy to estimate the equilibrium constant for the partitioning of soluble components into micelles if the change in free energy of a partition process is known. This approach has been successfully reported<sup>40</sup> and expanded<sup>41, 82</sup> for the partitioning of various contaminants to cationic micelles. Therefore, it is possible to predict binding constant from a free-energy relationship, which has a correlation with equilibrium constants.<sup>165</sup> This type of analysis has also been used successfully to compare  $K_{OW}$  and  $K_B$  for phenols in anionic micellar systems.<sup>159</sup>

## 2.5 References

1. Clint, J. H. *Surfactant Aggregation*, Blackie & Son Ltd: Bishopbriggs, 1992, 1.
2. Tutar, S. Switchable Surfactants, M.Sc. Thesis, Chalmers University of Technology, Sweden, 2011.
3. Schramm, L. L.; Stasiuk, E. N.; Marangoni, D. G. *Annu. Rep. Prog. Chem., Sect. C*, **2003**, *99*, 3–48.
4. Goyal, P. S.; Aswal, V. K. *Current Science*, **2001**, *80*(8).
5. Rosen, M. J. *Surfactants and Interfacial Phenomena*, 3rd. ed., John Wiley & Sons, Hoboken, **2004**, 105.
6. Hartley, G. S. *Aqueous solutions of paraffin-chain salts: a study in micelle formation*. Hermann & Cie; 1936.
7. Maibaum, L.; Dinner, A. R.; Chandler, D. *J. Phys. Chem. B* **2004**, *108*, 6778-6781.
8. Huang, D. M.; Chandler, D. *J. Phys. Chem. B* **2002**, *106*, 2047-2053.
9. Tanford, C. *The Hydrophobic Effect: Formation of Micelles & Biological Membranes*; Wiley Publishing: New York, 1980.
10. de Gennes, P. G. *J. Phys. Lett. (Paris)* **1979**, *40*, L69-L72.
11. Stillinger, F. H. *J. Chem. Phys.* **1983**, *78*, 4654-4661.
12. Sakai, H.; Matsumura, A.; Yokoyama, S.; Saji, T.; Abe, M. *J. Phys. Chem. B* **1999**, *103*, 10737.
13. Karsa, D. R.; Bailey, R. M.; Shelmerdine, B.; McCann, S. A., in *Industrial Applications of Surfactants IV*, ed. D. R. Karsa, Royal Society of Chemistry, Cambridge, UK, 1999, p. 1.
14. Hoffman, H.; *Ber. Bunsenges. Phys. Chem.* **1994**, *98*, 1433.
15. Deamer, D. W.; Pashley, R. M. *Origins Life Evol. Biosphere*, **1989**, *19*, 21.
16. Bade, R.; Lee, S. H. *J. Water Sustain.* **2011**, *1*, 85-102.
17. Ahmad, A. L.; Puasa, S. W.; Zulkali, M. M. D. *Desalination*, **2006**, *191*(1), 153-161.
18. Myers, D. *Surfactant Science and Technology*, Third Edition ed. New Jersey: John Wiley & Sons. Inc, 2006.
19. Schmitt, T. M. *Analysis of Surfactants*. New York: Marcel Dekker, Inc., 1992.

20. Purkait, M. K.; DasGupta, S.; De, S. *J. Hazard. Mater.* **2006**, *136*(3), 972-977.
21. Ahmad, A. L.; Puasa, S. W. *Chem. Eng. J.* **2007**, *132*, 257-265.
22. Luo, F.; Zeng, G. M.; Huang, J. H.; Zhang, C.; Fang, Y. Y.; Qu, Y. H.; Li, X.; Lin, D.; Zhou, C. F. *Journal of hazardous materials*, **2010**, *173*(1), 455-461.
23. Zaghbani, N.; Hafiane, A.; Dhahbi, M. *J. Hazard. Mater.* **2009**, *168*, 1417-1421.
24. Samper, E., Rodríguez, M., De la Rubia, M. A. and Prats, D. *Separation and Purification Technology*, **2009**, *65*(3), 337-342.
25. Landaburu-Aguirre, J., García, V., Pongrácz, E. and Keiski, R. L. *Desalination*, **2009**, *240*(1), 262-269.
26. Danis, U.; Aydiner, C. *J. Hazard. Mater.* **2009**, *162*, 577-587.
27. Yenphan, P.; Chanachai, A.; Jiraratananon, R. *Desalination*, **2010**, *253*(1), 30-37.
28. Misra, S. K.; Mahatele, A. K.; Tripathi, S. C.; Dakshinamoorthy, A. *Hydrometallurgy*, **2009**, *96*(1), 47-51.
29. Liu, Y.; Jessop, P. G.; Cunningham, M.; Eckert, C. A.; Liotta, C. L. *Science*, **2006**, *313*, 958-960.
30. D. J. Heldebrant, P. G. Jessop, C. A. Thomas, C. A. Eckert, C. L. Liotta, *J. Org. Chem.* **2005**, *70*, 5335.
31. Jessop, P. G. "Reversibly Switchable Surfactants and Methods of Use Thereof, " *PCT Int. Appl.* **2007**, WO 2007/056859 A1.
32. T. Saji, K. Hoshino, S. Aoyagui, *J. Am. Chem. Soc.* **1985**, *107*, 865.
33. Su, X.; Robert, T.; Mercer, S. M.; Humphries, C.; Cunningham, M. F.; Jessop, P. G. (2013). *Chemistry—A European Journal*, **2013**, *19*(18), 5595-5601.
35. Rosen, M. J. *Surfactants and Interfacial Phenomena*; John Wiley & Sons, Inc.: New York, 1989; Chapter 4.
34. Valsaraj, K. T.; Thibobeaux, L. J. *Water Research*, **1989**, *23*( 2), 183-189.
36. Chung, Y. S.; Yoo, S. H.; Kim, C. K. *Journal of Membrane Science*, **2009**, *326*(2), 714-720.
37. Zeng, G. M.; Xu, K.; Huang, J. H.; Li, X.; Fang, Y. Y.; Qu, Y. H. *J. Membrane Sci.* **2008**, *310*(1), 149-160.

38. Huang, J. H.; Zeng, G. M.; Fang, Y. Y.; Qu, Y. H.; Li, X. *Journal of Membrane Science*, **2009**, 326(2), 303-309.
39. Zaghbani, N.; Hafiane, A.; Dhahbi, M. *Desalination and Water Treatment*, **2009**, 6, 204-210.
40. Purkait, M. K.; DasGupta, S.; De, S. *Sep. Purif. Technol.* **2004**, 37 (1), 81-92.
41. Dunn, R. O.; Scamehorn, J. F.; Christian, S. D. *Sep. Sci. Technol.* **1985**, 20 (4), 257-284.
42. Baek, K.; Yang, J. *Chemosphere*, **2004**, 57 (9), 1091-1097.
43. Bechtel, M. K., Bagdasarian, A., Olson, W.P.; Estep, T. N. *Biomaterials, Artificial Cells, and Artificial Organs* **1988**, 16(3), 123-128.
44. Tran, C. D.; Baptista, M. S.; Tomooka, T. *Langmuir*, **1998**, 14, 6886-6892.
45. Betteridge, D.; Fields, B. *Anal. Chim. Acta*, **1981**, 132, 139.
46. Turner, D. R.; Santos, M. C.; Coutinho, P.; Goncaves, M. L.; Knox, S. *Anal. Chim. Acta*, **1992**, 258, 259.
47. Ruzicka, J.; Hansen, E. H. *Flow Injection Analysis*, 2nd ed.; Wiley: New York, **1988**.
48. Vacarcel, M.; Luque de Castro, M. D. *Flow-Injection Analysis, Principals and Applications*; Ellis Horwood Limited: Chichester, U.K., **1987**.
49. Loo, J. A.; Hu, P.; McConnell; Mueller, M. T.; Sawyer, T. K.; Thanabal, V. *J. Am. Soc. Mass Spectrom.* **1997**, 8, 234-243.
50. Lim, H. K.; Hsieh, Y. L.; Ganem, B.; Henion, J. *J. Mass Spectrom.* **1995**, 30, 708-714.
51. Greig, M. J.; Gaus, H. Cummins, L. L.; Sasmor, H.; Griffey, R. H. *J. Am. Chem. Soc.* **1995**, 117, 10765-10766.
52. Griffey, R. H.; Hofstadler, S. A.; Sannes-Lowery, K. A.; Ecker, D. J.; Crooke, S. T. *Proc. Natl. Acad. Sci. U.S.A.* **1999**, 96, 10129-10133.
53. Prieto, M. C.; Whittal, R.; Balwin, M.; Burlingame, A. L.; Balhorn, R. In *Proceedings 47th ASMS Conference on Mass Spectrometry and Allied Topics*, Dallas, TX, June 13-17, 1999; pp 614-615.
54. Cann, J. R. *Anal. Biochem.* **1996**, 237, 1.
55. Horejsi, V.; Tichfi, M. *J. Chromatogr.* **1986**, 376, 49.
56. Ek, K.; Righetti, P. G. *Electrophoresis*, **1980**, 1, 137.



57. Ek, K.; Gianazza, E.; Righetti, P. G. *Biochim. Biophys. Acta*, **1980**, 626, 356.
58. Chu, Y. H.; Avila, L. Z.; Gao, J.; Whitesides, G. M. *Acc. Chem. Res.* **1995**, 28, 461.
59. Goodal, D. M. *Biochem. Soc. Trans.* **1993**, 21, 125.
60. Honda, S.; Taga, A.; Susuki, K.; Susuki, S.; Kakehi, K. *J. Chromatogr.* **1992**, 597, 377.
61. Kuhn, R.; Frei, R.; Christen, M. *Anal. Biochem.* **1994**, 218, 131.
62. Shimura, K.; Kasai, K. I. *Anal. Biochem.* **1995**, 227, 186.
63. Kraak, J. C.; Busch, S.; Poppe, H. *J. Chromatogr.* **1992**, 608, 257.
64. Barker, G. E.; Russo, P.; Hartwick, R. A. *Anal. Chem.* **1992**, 64, 3024.
65. Carpenter, J. L.; Camilleri, P.; Dhanak, D.; Goodall, D. *J. Chem. Soc., Chem. Commun.* **1992**, 804.
66. Chu, Y. H.; Whitesides, G. M. *J. Org. Chem.* **1992**, 57, 3524.
67. Chu, Y. H.; Avila, L. Z.; Biebuyck, H. A.; Whitesides, G. M. *J. Org. Chem.* **1993**, 58, 648.
68. Liu, J.; Volk, K. J.; Lee, M. S.; Pucci, M.; Handwerker, S. *Anal. Chem.* **1994**, 66, 2412.
69. Bose, S.; Yang, J.; Hage, D. S. *J. Chromatogr. B.* **1997**, 697, 77-88.
70. Colowick, S. P.; Womack, F. C. *J. Biol. Chem.* **1969**, 244, 774-777.
71. Scatchard, G.; *Ann. N. Y. Acad. Sci.* **1949**, 51, 660.
72. Womack, F. C.; Colowick, S. P. *Fed. Proc.* **1968**, 27, 454.
73. Hummel, J. P.; Dreyer, W. J. *Biochim. Biophys. Acta*, **1962**, 63, 530.
74. Gilbert, W.; Muller-Hill, B. *Proc. Nat. Acad. Sci. U. S. A.* **1966**, 56, 1891.
75. Anraku, Y. *J. Biol. Chem.* **1986**, 243, 3116.
76. Piperno, J. R.; Oxender, D. L. *J. Biol. Chem.* **1966**, 241, 5732.
77. Hinze, W. L. in *Solution Chemistry of Surfactants, Vol. I, Use of Surfactants and Micellar Systems in Analytical Chemistry* (K. L. Mittal, Ed.), Plenum, New York, 1979.
78. Pelizzetti, E.; Pramauro, E. *Anal. Chim. Acta* **1985**, 169, 1-29.
79. Cline Love, L. J.; Habarta, J. G.; Dorsey, J. G. *Anal. Chem.* **1984**, 56, 1133A-1148.

80. Dhar, S.; Rana, D. K.; Sarkar, A.; Mandal, Ghosh, T. K., S.; Battacharya, S. C. *Coll. Surf. A. Physicochemical and Engineering Aspects*, **2009**, 349 (1-3) 117-124.
81. Bunton, C. A.; Sepulveda, L. *J Phys Chem*. **1979**, 83(6), 680-683.
82. Farias, T.; de Menorval, L. C.; Zajac, J.; Rivera, A. *Colloid Surface A*, **2009**, 345, 51-57.
83. Xu, K.; Ren, H. Q.; Zeng, G. M.; Ding, L. L.; Huang, J. H. *Colloid Surface A*, **2010**, 356, 150-155.
84. Waters, L. J.; Kasprzyk-Hordern, B. *J. Therm. Anal. Calori.* **2010**, 102(1), 343-347.
85. Rouse, J. D.; Sabatini, D. A.; Deeds, N. E.; Brown, R. E. *Environ. Sci. Technology*. **1995**, 29, 2484-2489.
86. Pramauro, E.; Saini, G.; Pelizzetti, E. *Anal. Chim. Acta*, **1984**, 166, 233-241.
87. Pelizzetti, E.; Pramauro, E. *J. Phys. Chem.* **1984**, 88, 990-999.
88. Frank, H. S.; Oswald, R. L. *J. Am. Chem. Soc.* **1947**, 69, 1321-1325.
89. Bunton, C. A.; Romsted, L. S.; Sepulveda, L. *J. Phys. Chem.* **1980**, 84, 2611-2618.
90. Sepulveda, L. *J. Colloid Interface Sci.* **1974**, 46, 372-379.
91. Pramauro, E.; Pelizzetti, E. *Anal. Chim. Acta*, **1983**, 154, 153-158.
92. Yarmchuk, P.; Weinberger, R.; Hirsch, R. F.; Cline Love, L. *J. Anal. Chem.* **1982**, 54, 2233-2238.
93. Armstrong, D. W.; Nome, F. *Anal. Chem.* **1981**, 53, 1662-1666.
94. Pramauro, E.; Minero, C.; Pelizzetti, E. In *Ordered Media in Chemical Separations (Hinze, W. L., and Armstrong, D. W., Eds.)*, A.C.S., Washington DC, **1987**.
95. Pramauro, E.; Pelizzetti, E. *Anal. Chim. Acta*, **1981**, 126, 253-257.
96. Pramauro, E.; Pelizzetti, E. *Ann. Chim. (Rome)*, **1982**, 72, 117-126.
97. Graglia, R.; Pramauro, E.; Pelizzetti, E. *Ann. Chim. (Rome)*, **1984**, 74, 41-51.
98. Yatsimirskii, A. K.; Martinek, K.; Berezin, I. V. *Tetrahedron*, **1971**, 27, 2855-2868.
99. Dougherty, S. J.; Berg, J. C. *J. Colloid Interface Sci.* **1974**, 48, 110-121.
100. Dougherty, S. J.; Berg, J. C. *J. Colloid Interface Sci.* **1974**, 49, 135-138.

101. Hirose, C.; Sepulveda, L. *J. Phys. Chem.* **1981**, *85*, 3689-3694.
102. Bunton, C. A.; Robinson, L. *J. Am. Chem. Soc.* **1968**, *90*, 5972-5979.
103. Bunton, C. A.; Robinson, L. *J. Org. Chem.* **1969**, *34*, 773-780.
104. Sepulveda, L.; Soto, R. *Makromol. Chem.* **1978**, *179*, 765-771.
105. Bunton, C. A.; Rivera, F.; Sepulveda, L. *J. Org. Chem.* **1978**, *43*, 1166-1173.
106. De La Guardia, M.; Cardells, E. P.; Sancenon, J.; Carrion, J. L. *Microchem. J.* **1991**, *4*, 193-200.
107. Quina, F. H.; Toscano, V. G. *J. Phys. Chem.* **1977**, *81*, 1750-1754.
108. Almgrem, M.; Grieser, F.; Thomas, J. K. *J. Am. Chem. Soc.* **1979**, *101*, 279-291.
109. Lissi, E.; Abuin, E.; Rocha, A. M. *J. Phys. Chem.* **1980**, *84*, 2406-2408.
110. Armstrong, D. W.; Henry, S. J. *J. Liq. Chromatogr.* **1980**, *3*, 657.
111. Armstrong, D. W.; Stine, G. Y. *Anal. Chem.* **1983**, *55*, 2317.
112. Armstrong, D. W.; *Sep. Purif. Methods*, **1985**, *14*, 213.
113. Hinze, W. L.; Armstrong, D. W. In *Ordered Media in Chemical Separations*, ACS Symposium Series, 342, 1987.
114. Dorsey, J. G. In *Advances in Chromatography*; J. Calvin Giddings, E. Grushka, P. R. Brown, eds., Marcel Dekker, 1987, Chapter 5, pp. 167-214.
115. Berthod, A.; Girard, L.; Gonnet, C. In *Ordered Media in Chemical Separations*, ACS Symposium Series, 342, 1987.
116. Berthod, A.; Girard, L.; Gonnet, C. *Anal. Chem.* **1986**, *58*, 1362.
117. Hamdiyyah, M. A. *J. Phys. Chem.* **1986**, *90*, 1345.
118. Reekmans, S.; Luo, H.; Auweraer, M. V.; De Schryver, F. C. *Langmuir*, **1990**, *6*, 628.
119. Armstrong, D. W.; Nome, E. *Anal. Chem.* **1981**, *53*, 1662.
120. Garcia, M. A.; Marina, M. L.; Diez-Masa, J. C. *J. Chromatogr. A*, **1996**, *732*, 345-359.
121. Arunyanarl, M.; Cline Love, L. Y. *Anal. Chem.* **1984**, *56*, 1557.
122. Garcia, M. A.; Vera, S.; Marina, M. L. *Chromatographia*, **1991**, *32*, No 3/4.

123. Terabe, S.; Otsuk, K.; Ichikawa, K.; Tsuchiya, A.; Ando, T. *Anal. Chem.* **1984**, *56*, 111.
124. Terabe, S.; Otsuk, K.; Ando, T. *Anal. Chem.* **1985**, *57*, 834.
125. Vindervogel, J.; Sandra, P. *Sort*, **1992**, *100*, 250.
126. Kord, A. S.; Strasters, J. K.; Khaledi, M. G. *Anal. Chim. Acta*, **1991**, *246*, 131.
127. Mahmoud, F. Z.; Christian, S. D.; Tucker, E. E.; Taha, A. A.; Scamehorn, J. F. *J. Phys. Chem.* **1989**, *93*, 5903-5906.
128. Gibbs, L. L.; Scamehorn, J. F.; Christian, S. D. *J. Membrane Sci.* **1987**, *30*, 67.
129. Smith, G. A.; Christian, S. D.; Tucker, E. E.; Scamehorn, J. F. In *Use of Ordered Media in Chemical Separations*; ACS Symposium Series 342, Washington, DC, 1987, p 184.
130. Christian S. D.; Smith, G. A.; Tucker, E. E.; Scamehorn, J. F. *Langmuir*, **1985**, *1*, 564.
131. Christian S. D.; Smith, G. A.; Tucker, E. E.; Scamehorn, J. F. *J. Solution Chem.* **1986**, *15*, 519.
132. Freifelder, D. In *Physical Biochemistry-Applications to Biochemistry and Molecular Biology*, 2nd ed.; W. H. Freeman and Co.: San Francisco, 1982; p 675.
133. Cantor, C. R.; Schimmel, P. R. In *Biophysical Chemistry*; W. H. Freeman and Co.: San Francisco, 1980; Part 111, pp 1328-1339.
134. Molyneux, P. In *Water-Soluble Synthetic Polymers: Properties and Behavior*; CRC Press: Boca Raton, FL, 1984; Vol. 11, pp 101-105.
135. Patel, N. K.; Kostenbauder, H. B. *J. Am. Pharm. Assoc., Sci. Ed.* **1958**, *47*, 289.
136. Kazmi, S. J. A.; Mitchell, A. G. *J. Pharm. Pharmacol.* **1971**, *23*, 482.
137. Mitchell, A. G.; Brown, K. F. *J. Pharm. Pharmacol.* **1966**, *18*, 115.
138. Patel, N. K.; Foss, N. E. *J. Pharm. Sci.* **1965**, *54*, 1495.
139. Patel, N. K.; Foss, N. E. *J. Pharm. Sci.* **1964**, *53*, 94.
140. Ucbiyama, H.; Christian, S. D.; Tucker, Scamehorn, J. F. *J. Phys. Chem.* **1993**, *97*, 10868-10871.
141. Christian, S. D.; Smith, G. A.; Tucker, E. E. *Langmuir*, **1985**, *1*, 564-567.
142. Cashin, P. J. M.Sc thesis, Queen's University, Kingston, ON, **2011**.

143. *Guide to Equilibrium Dialysis*, Harvard Bioscience Inc, **2002**, Distributed by the Nest Group, Southborough, MA 01772-1323. <http://www.nestgrp.com/pdf/Ap1/EqDialManual.pdf> (accessed 04/2015).
144. Schneider, H. J. ; Hacket, F.; Rudiger, V. *Chem. Rev.* **1998**, *98*, 1755-1785.
145. Ramstad, T.; Hadden, C. E.; Martin, G. E.; Speaker, S. M.; Teagarden, D. L.; Thamann, T. *J. International Journal of Pharmaceutics*, **2005**, *296*, 55–63.
146. Yamamoto, Y.; Inoue, Y. *J. Carbohydr. Chem.* **1989**, *8*, 29–46.
147. Thorsteinn, L.; Brewster, M. E. *J. Pharm. Sci.* **1996**, *85*, 1017–1025.
148. Connors, K. A. *Chem. Rev.* **1997**, *97*, 1325–1357.
149. Liu, Y.; Han, B.H.; Zhang, H. Y. *Curr. Org. Chem.* **2004**, *8*, 35–46.
150. Dearden, J. C. *Environ. Health Perspect.* **1986**, *61*, 203-228.
151. Hermens, J. L. M. In *Handbook of Environmental Chemistry*; Hutzinger, O., Ed.; Springer Verlag: Berlin, 1989; Vol. 2E, pp 111-162.
152. Schneider, H. J.; Yatsimirsky, A. K. In *Principles and Methods in Supramolecular Chemistry*; John Wiley and Sons: New York, **2000**; Chapter E4.
153. Fielding, L. *Tetrahedron*, **2000**, *56*, 6151.
154. Billo, J. E. Calculation of Binding constants, *Excel for Chemists: A Comprehensive Guide, second edition*, Department of Chemistry, Boston College, Chestnut Hill, Massachusetts, 2001.
155. Funasaki, N.; Nomura, M.; Ishikawa, S.; Neya, S. *J. Phys. Chem. B* **2001**, *105*, 7361-7365.
156. Sangster, J. *J. Phys. Chem. Ref. Data*, **1989**, *18*, 1111-1229.
157. Hanaoh, C. *Acc. Chem. Res.* **1969**, *2*, 232.
158. Leo; Hansch. *J. Org. Chem.* **1971**, *36*(11).
159. Collett, J. L.; Koo L. *J. Pharmac. Sci.* **1975**, *64*, 1253-1255.
160. Azaz, E.; Donbrow, M. *J. Colloid Interface Sci.* **1976**, *57*, 11-19.
161. Tomida, H.; Totsuyanagi, T.; Ikeda, K. *Chern. Pharmac. Bull.* **1978**, *26*, 2824--2831.
162. Valsaraj, K. T.; Thibodeaux, L. J. *Water Research*, **1989**, *23*(2), 183-189.

163. Valsaraj, K. T.; Gupta, A.; Thibodeaux, L. J.; Harrison, D. P. *Water Research*, **1988**, *22*, 1173-1183.

164. Liu, Y. *J. Chem. Eng. Data*, **2009**, *54*, 1981–1985.

165. IUPAC, *In Compendium of Chemical Terminology*; 2nd ed.; Blackwell Scientific Publications: **1997**.

## Chapter 3

# Determining binding of sulfonamide antibiotics to CTABr micelles using semi-equilibrium Dialysis

### 3.1 Introduction

A variety of pharmaceuticals have been detected in various surface waters, as well as in wastewater treatment plant influent and effluent.<sup>1-6</sup> Sulfonamide antibiotics have frequently been detected at low concentrations (<1 ppb) that cause concern in the aquatic environment.<sup>3-5</sup> The concern is related to direct effects on organisms in receiving water bodies and to the potential for promotion of antibiotic resistance.<sup>4</sup> These compounds are poorly removed by conventional municipal and industrial wastewater treatment systems.<sup>6</sup> While advanced treatment processes such as ozonation show promise,<sup>6,7</sup> the high cost and potential formation of harmful by-products are serious limitations.

Membrane filtration processes, such as ultrafiltration (UF), are increasingly employed in water and wastewater treatment. The UF membrane is characterized by relatively large pore sizes, which reduces fouling and allows use of lower pressures, but does not remove small dissolved molecules. To improve removal efficiency, the effective size of a low molecular weight contaminant can be increased by binding it to a larger entity. In this context, micellar enhanced ultrafiltration (MEUF) has been shown to be an effective removal technique for a variety of trace contaminants in wastewater, including dyes, metals and nutrients,<sup>8,9</sup> as well as for removal of sulfonamide antibiotics.<sup>10</sup> This technique, described in detail by Dunn et al.,<sup>11</sup> makes use of the tendency for surfactants in water to spontaneously aggregate to form micelles at concentrations above the critical micelle concentration (CMC). Formation of a micelle generates new zones (pseudo-phases) into which molecules may partition, depending on the polarity of the molecule.

The interior, low polarity (hydrophobic) region of the micelle can solubilize less polar molecules. In the case of an ionic surfactant, the outer polar or charged layer of the micelle can also interact strongly with oppositely charged ions or molecules with strong dipoles. In MEUF, contaminants partition into the micellar pseudo-phase, followed by ultrafiltration of the solution to remove the micelles and bound contaminants.<sup>11-14</sup>

To predict the removal efficiency of a method such as MEUF, it is important to understand the extent to which a species is able to bind to a particular micelle, usually expressed quantitatively as a partition or binding constant.<sup>8,9,15</sup> For example, Exall et al.<sup>10</sup> measured the empirical performance of MEUF for removal of three sulfonamides, but did not have the benefit of binding constant information to include in explaining the results obtained.

Partition constants, often referred to as binding constants or association constants, reflect the pseudo two-phase nature of the micelle-water system, have been determined for various organic and inorganic species with micellar systems using *in situ* techniques such as fluorescence,<sup>16</sup> enthalpy of association,<sup>17</sup> and NMR.<sup>15,18</sup> *Ex situ* techniques, involving a separation of micelles and bound species from unbound molecules, have also been employed, such as micellar liquid chromatography,<sup>19</sup> micellar electrokinetic chromatography,<sup>20-22</sup> and semi-equilibrium dialysis (SED).<sup>11,23</sup> In the SED method, membranes retain the micelles and bound species, while allowing free surfactant monomers and unbound species to come to near-equilibrium concentrations on both sides of the membrane. The difference between the total solubilize concentration in the permeate and retentate solutions reflects the amount that is bound to the micelles.<sup>11</sup> In this study, we determine micellar binding constants for a series of sulfonamide antibiotics using the SED method.



## **3.2 Materials and methods**

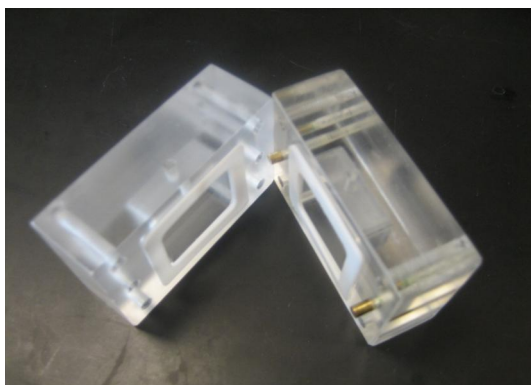
### ***3.2.1 Materials***

Cetyltrimethylammonium bromide (CTABr) and the sulfonamides sulfadoxine, sulfathiazole, sulfamethoxazole, sulfamerazine, sulfadiazine, sulfamethazine, sulfacetamide, sulfaguanidine, and sulfanilamide were purchased from Sigma-Aldrich Chemicals (Oakville, ON). Deionized water was obtained from a Milli-Q system (Millipore, Etobicoke, ON). Pierce brand snakeskin dialysis tubing was purchased from Fisher Scientific (Ottawa, ON) with a molecular weight cut-off (MWCO) of 7000 Da.

### ***3.2.2 Semi-equilibrium dialysis method***

Semi-equilibrium dialysis cells were produced in-house, consisting of two halves machined in methacrylate polymer, each with an internal volume of approximately 5 mL (See Fig. 3.1). The two halves were separated by a dialysis membrane held in place by a Teflon gasket on either side. The 7000 Da MWCO dialysis membrane is similar to the 6000 MWCO membrane previously used in SED.<sup>11</sup>

Samples were introduced into the dialysis cell and removed for analysis via a threaded hole located in the top of each half, which was kept sealed with a stainless steel screw during the experiment.



(a)

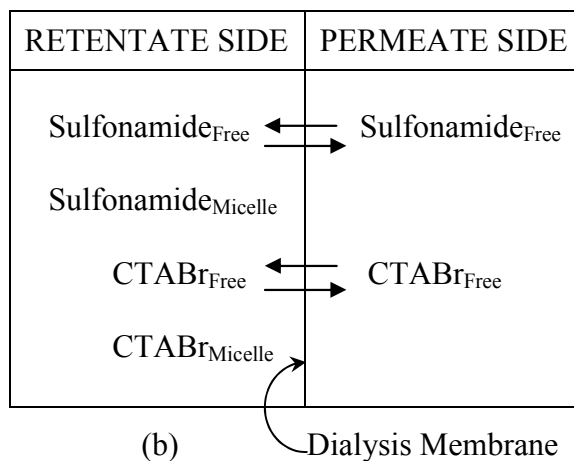


**Fig. 3.1.** a) Semi-equilibrium dialysis cell and b) illustration of separation behaviour across the dialysis membrane after addition of CTABr micelle/sulfonamide mixture to left hand side.

On the permeate side of the equilibrium dialysis cell, 4.0 mL of deionized water was added and on the retentate side, 2.0 mL of sulfonamide solution and 2.0 mL of CTABr solution were added, resulting in a total volume of 4.0 mL on each side of the dialysis membrane. The dialysis membrane was hydrated in Milli-Q water for two minutes prior to use. Cells were allowed to equilibrate for 24 h at room temperature ( $22 \pm 1$  °C), at which point sample aliquots were removed from each side and analyzed by HPLC and conductivity.

### 3.2.3 Sample preparation

Sulfonamide stock solutions were prepared in 100-mL volumetric flasks by adding known amounts and dissolving by 30 min. sonication (See appendix A1). The CTABr stock solution (20 mM) was prepared by adding 0.7289 g to a 100-mL volumetric flask followed by sonication.

### **3.2.4 Analysis procedure**

Sulfonamide concentrations were determined by a high-performance liquid chromatography (HPLC) method adapted from Sun et al.<sup>24</sup> This used a C18 column (5  $\mu$ m packing, 4.6x250 mm column), a Varian Prostar (PS)-210 pump set to 1.5 mL/min flow rate, and a PS-310 UV detector set to 254 nm (Varian-Agilent, Mississauga, ON). Varian Star software was used for instrument operation and data analysis. A gradient elution method was used, with phosphate buffer at pH 2.9 as aqueous solution (A) and HPLC grade CH<sub>3</sub>OH as organic solvent (B). Initial mobile phase was 90% A and 10% B for 4 min. Four min after injecting 10  $\mu$ L of sample, A was decreased to 50% over 3 min, then decreased to 10% over 2 min and held at that level for another 2 min. Before injecting the next sample, 90% A and 10% B mobile phase was for 5 min to re-equilibrate the column. The total run time was 16 min. Sample chromatograms are shown in appendix A 2.1 and A 2.2.

### **3.2.5 CMC determination**

The surfactant concentration was measured using a Jenway-470 Conductivity Meter (VWR International, Mississauga, ON). A plot of conductivity vs. concentration is shown in Fig. 3.2. The CMC was determined to be 0.92 mM by finding the intersection of the distinct linear ranges at high and low concentrations. This CMC value is in good agreement with the previously reported value of 0.93 mM.<sup>25</sup> To determine CTABr concentration in sample solutions, two separate calibration functions were used for concentrations below and above the CMC value. Other methods for CTABr concentration measurement, such as Br<sup>-</sup> analysis methods, could be used. However, the error in the overall  $K_B$  calculation would not be significantly reduced.

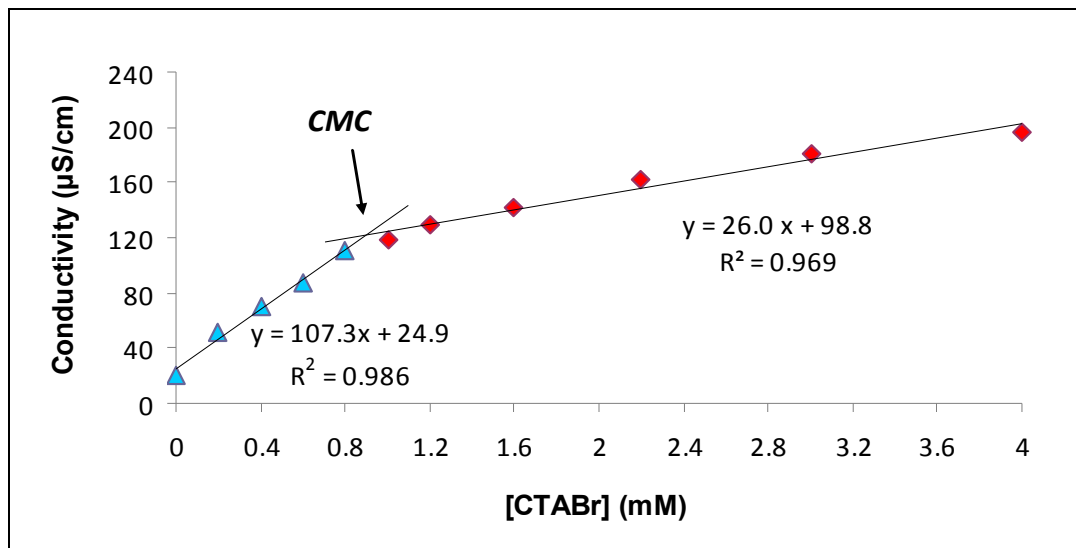


**Fig. 3.2.** Conductivity of CTABr solutions. The discontinuity between two linear ranges indicates the CMC value of CTABr (0.92 mM).

### 3.2.6 Characterizing the SED method

In separate experiments, equilibration of sulfonamide and CTABr across the SED membrane was monitored. The results for sulfadiazine are shown in Fig. 3.3. An initial concentration of 1 mM was placed on the retentate side, and small volumes (50-100 µL) removed from the permeate side at various times for analysis by HPLC. The same volume was withdrawn from the retentate side to keep the volumes equal. The results confirm that the free sulfadiazine concentration reached equilibrium by 24 h. Measurements beyond 24 h are not reported as the sulfonamide concentration increased further, likely a result of micelles appearing on the permeate side.

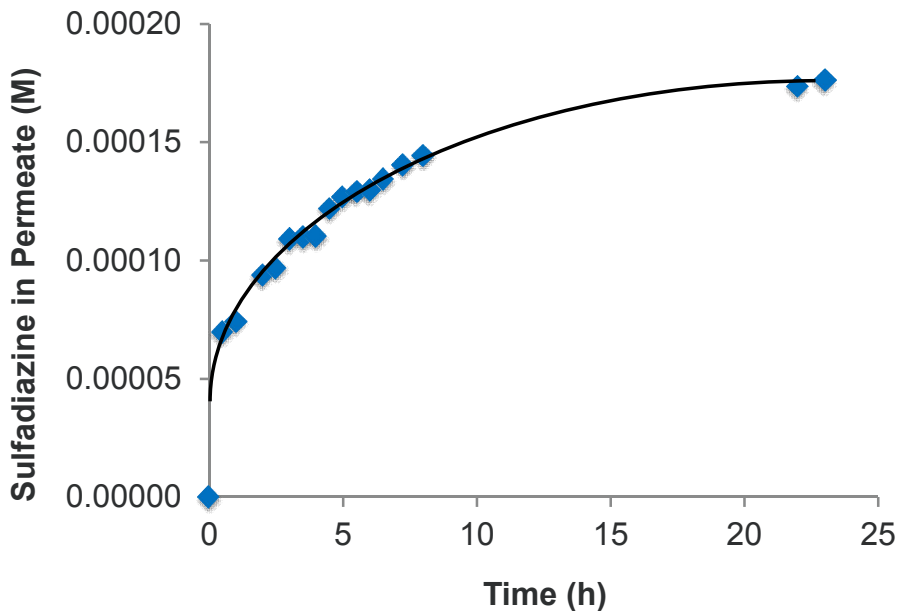


**Fig. 3.3.** Concentration of sulfadiazine on permeate side of SED cell to confirm equilibration of free sulfadiazine by 24 h. Sulfadiazine concentration was determined by HPLC with UV detection. The smooth curve is to guide the eye.

Samples were drawn at various times from both the permeate and retentate sides for conductivity testing to determine the surfactant concentration. These samples (1-2 mL) were withdrawn using a disposable needle (0.70 x 100 mm) on a plastic syringe, and then were replaced in the SED cell as the conductivity measurement does not disturb the sample. The results shown in Fig. 3.4 confirm that free surfactant was close to equilibrium in about 6 h, and the concentration remained close to the CMC level beyond 24 h. Minimal micelles would be expected on the permeate side at the 24 h mark. These results confirm that the conditions for semi-equilibrium were achieved in these experiments.

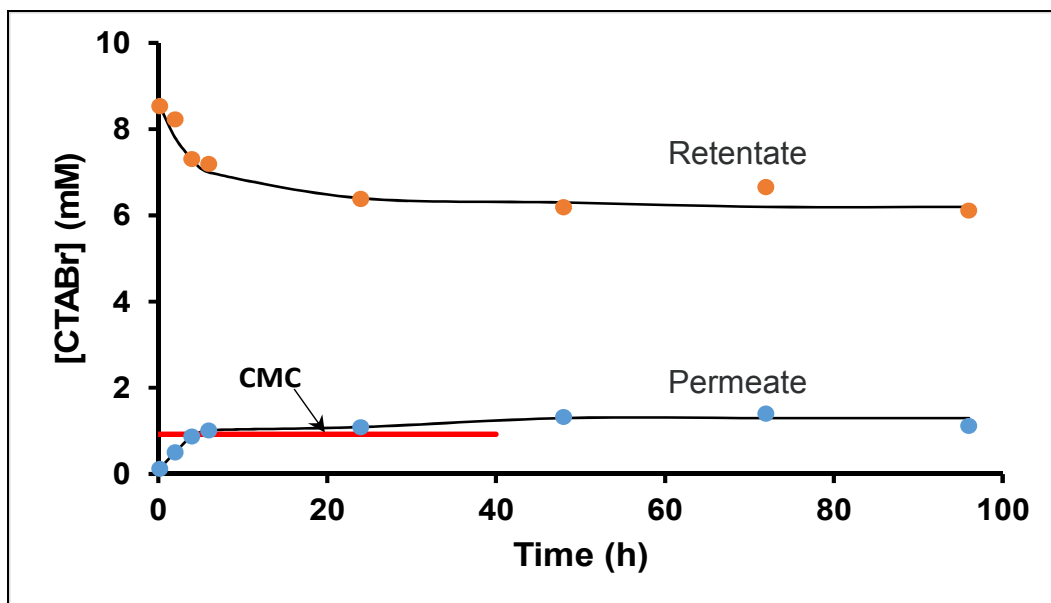


**Fig. 3.4.** Concentration measurement over time showing diffusion of CTABr surfactant in the SED cell from the retentate to the permeate. The surfactant concentration was measured by conductivity using the calibration functions in Fig. 3.2.

### 3.3 Results and discussion

#### 3.3.1 Determination of binding constants by SED

The concentrations of sulfonamide and CTABr measured after 24 h of the SED experiments are shown in Table 3.1. There was a significant concentration difference between the permeate and retentate sides for both the sulfonamides and CTABr, indicating that the micellar pseudo-phase was unable to pass through the membrane. The concentration of CTABr in the retentate was well above the CMC and was consistent between replicates for different sulfonamides. The concentration of CTABr in the permeate at 24 h was between 20-100% above the CMC of the surfactant, with some variation possibly due to the sulfonamide in solution affecting the conductivity measurement. It is also possible that the presence of sulfonamide will influence the CMC value. Exall et al. reported that CMC decreased by about 0.06 mM with the addition of sulfonamide in CTABr.<sup>10</sup>

**Table 3.1. Concentration of sulfonamides and surfactant (CTABr) in the retentate side(R) and permeate side (P) after 24 h equilibration in the SED experiment.**

Sulfonamide	HPLC analysis		Conductivity analysis	
	[Sulfonamide] <sub>R</sub> (M)	[Sulfonamide] <sub>P</sub> (M)	[CTABr] <sub>R</sub> (M)	[CTABr] <sub>P</sub> (M)
1. Sulfadoxine	4.06 x10 <sup>-5</sup>	7.00 x10 <sup>-7</sup>	0.0130	0.0012
2. Sulfathiazole	5.25 x 10 <sup>-5</sup>	1.40 x10 <sup>-6</sup>	0.0125	0.0015
3. Sulfamethoxazole	3.72 x10 <sup>-5</sup>	1.38 x10 <sup>-6</sup>	0.0144	0.0016
4. Sulfamerazine	5.83 x10 <sup>-5</sup>	2.50 x10 <sup>-6</sup>	0.0146	0.0018
5. Sulfamethazine	5.79 x10 <sup>-5</sup>	3.79 x10 <sup>-6</sup>	0.0139	0.0015
6. Sulfadiazine	4.10 x10 <sup>-5</sup>	5.61 x10 <sup>-6</sup>	0.0118	0.0039
7. Sulfacetamide	4.78 x10 <sup>-5</sup>	5.30 x10 <sup>-6</sup>	0.0128	0.0014
8. Sulfaguanidine	3.72 x10 <sup>-5</sup>	3.27 x10 <sup>-5</sup>	0.0126	0.0042
9. Sulfanilamide	3.61 x10 <sup>-5</sup>	3.18 x10 <sup>-5</sup>	0.0141	0.0017

An equation relating the results in Table 3.1 to  $K_B$  is derived according to:

$$K_B = \frac{[Sulfonamide]_M}{[Sulfonamide]_A} \quad (3.1)$$

where,  $K_B$  is the binding constant or equilibrium constant,  $[Sulfonamide]_A$  is the concentration of free sulfonamide in aqueous solution, and  $[Sulfonamide]_M$  is the concentration of sulfonamide within the volume of the micelles. This latter term can be further defined by:

$$[Sulfonamide]_M = \frac{n_{Sulfonamide,M}}{Vol_M} \quad (3.2)$$

where,  $n_{sulfonamide,M}$  is the number of sulfonamide molecules associated with micelles and  $Vol_M$  is the volume of the micelle phase. The volume of the micelle phase can be approximated by:

$$Vol_M = n_{CTABr,M} \times M_V \quad (3.3)$$

where,  $n_{CTABr,M}$  is the number of CTABr surfactant molecules that are in micelle form and  $M_V$  is the molar volume of CTABr, with a reported<sup>26</sup> value of  $3.64 \times 10^{-1} \text{ L/mol}$ . These can be substituted into the equation for  $K_B$ :

$$K_B = \frac{n_{Sulfonamide,M}}{[Sulfonamide]_A \times n_{CTABr,M} \times M_V} \quad (3.4)$$

Under the assumptions for SED,  $[Sulfonamide]_A$  is the same in the retentate and permeate solutions and is simply  $[Sulfonamide]_{Permeate}$ , which is measured directly. To get  $n_{sulfonamide,M}$ , it is assumed that the concentration of sulfonamide in the retentate ( $[Sulfonamide]_{Retentate}$ ) is the total of the aqueous and micelle-bound concentrations, so the micelle-bound concentration is  $[Sulfonamide]_{Retentate} - [Sulfonamide]_{Permeate}$  and:

$$n_{sulfonamide,M} = \{[Sulfonamide]_{Retentate} - [Sulfonamide]_{Permeate}\} \times V_{retentate} \quad (3.5)$$

For the value of  $n_{CTABr,M}$ , it is assumed that all CTABr above CMC on the retentate side is in micelle form, and therefore:

$$n_{CTABr,M} = \{[CTABr]_{Retentate} - CMC\} \times V_{Retentate} \quad (3.6)$$

Substituting 5 and 6 into 4 gives:

$$K_B = \frac{\{[Sulfonamide]_{Retentate} - [Sulfonamide]_{Permeate}\} \times V_{Retentate}}{[Sulfonamide]_{Permeate} \times \{[CTABr]_{Retentate} - CMC\} \times V_{Retentate} \times M_V} \quad (3.7)$$

Which simplifies to a final working equation for calculating  $K_B$ :

$$K_B = \frac{\{[Sulfonamide]_{Retentate} - [Sulfonamide]_{Permeate}\}}{[Sulfonamide]_{Permeate} \times \{[CTABr]_{Retentate} - CMC\} \times M_V} \quad (3.8)$$

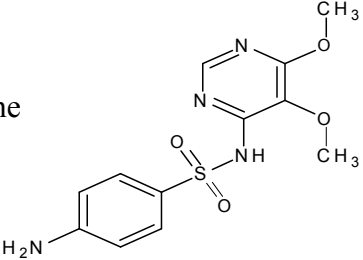
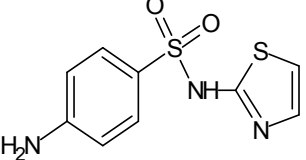
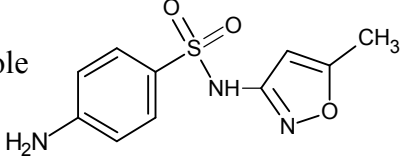
The results of the  $K_B$  calculation are given in Table 3.2. SED experiments were done in triplicate for sulfadoxine and sulfacetamide, and in duplicate for the other sulfonamides. Confidence intervals were calculated for the Log  $K_B$  values using the standard deviation of replicate  $K_B$  results. The errors for sulfadoxine and sulfacetamide were  $\pm 0.08$  and  $\pm 0.19$ , respectively, from the triplicate data. The errors for the other sulfonamides are estimates from duplicate data, but since they ranged from  $\pm 0.03$  to  $\pm 0.20$ , they are likely reasonable based on comparison with the triplicate values.

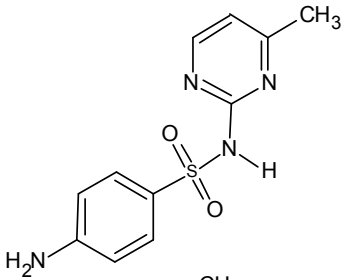
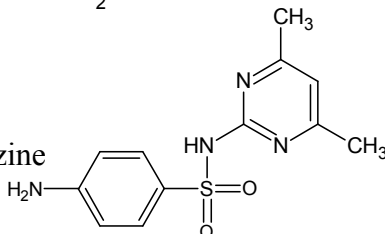
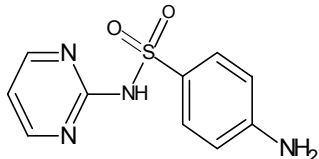
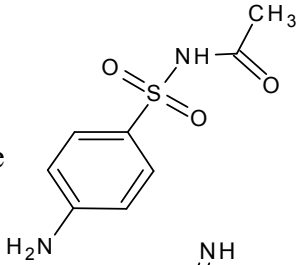
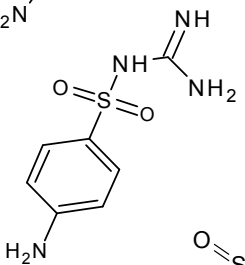
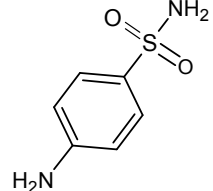
The retentate sulfonamide concentrations were all in the range of  $3 \times 10^{-5}$  M to  $6 \times 10^{-5}$  M. The permeate concentrations ranged from  $7 \times 10^{-7}$  M to  $3 \times 10^{-5}$  M, reflecting systems where micelle



binding was very strong (permeate concentration low) or weaker (permeate concentration approaches retentate concentration). The sums of the retentate and permeate concentrations were from 44% to 120% of the nominal concentration based on the amount of sulfonamide added. Some of this discrepancy was from error in the concentration measurements, but the general trend of mass balance below 100% suggested that some sulfonamide was lost from the solutions, such as by precipitation or adsorption. The CTABr concentrations measured on the retentate side were between 11 mM and 14 mM. Most of these were within error of the nominal concentration range (9-10 mM). It is possible that the presence of sulfonamide affected the solution conductivity measurement, providing a higher apparent CTABr concentration. Note that recalculating  $\text{Log } K_B$  values using nominal CTABr concentrations instead of measured CTABr concentrations (results not shown) resulted in changes of less than 0.2  $\text{Log } K_B$  units, which is within the error range of the  $\text{Log } K_B$  measurements.

**Table 3.2. Binding constant ( $K_B$ ) between sulfonamides and CTABr determined by SED analysis**

Compound	Structure	$pK_{a2}^a$	$\text{Log } K_{ow}^b$	$\text{Log } K_B$
1. Sulfadoxine		5.77	0.70	$4.14 \pm 0.08$
2. Sulfathiazole		7.20	0.05	$3.96 \pm 0.20$
3. Sulfamethoxazole		5.41	0.89	$3.75 \pm 0.06$

4. Sulfamerazine		6.71	0.14	3.67 ± 0.06
5. Sulfamethazine		7.59	0.89	3.50 ± 0.06
6. Sulfadiazine		6.36	-0.09	3.22 ± 0.10
7. Sulfacetamide		5.32	-0.96	3.29 ± 0.19
8. Sulfaguanidine		11.25	-1.22	1.53 ± 0.03
9. Sulfanilamide		10.58	-0.62	1.46 ± 0.05

<sup>a</sup>see references 27, 28, 29

<sup>b</sup>see reference 27

### 3.3.2 Physico-chemical applications of micellar binding constants

The  $\text{Log } K_B$  values determined in this work can be compared with other parameters to examine the physico-chemical interactions between sulfonamides and micelles. Quina and co-workers<sup>30</sup> proposed that  $\text{Log } K_B$  values are related to five linear solvation free energy parameters: solute hydrogen bond acidity, solute basicity, solute dipolarity, solute polarizability, and solute molar volume. These same parameters were also used in the construction of linear solvation free energy relationships for  $\text{Log } K_{OW}$  values of organic compounds.<sup>31</sup> Treiner and Mannebach<sup>32</sup> found that such correlations could be derived for a variety of halocarbon compounds, with  $\text{Log } K_B = 0.91 \cdot \text{Log } K_{OW} - 0.23$ . However, the correlation for halocarbons differed from that reported earlier by Treiner and Chattopadhyay<sup>33</sup> for alcohols, ketones, and nitriles, leading to the conclusion that the relationship between micellar uptake and  $\text{Log } K_{OW}$  could differ for each class of compound.<sup>34</sup>

The extent of the variation between classes of compounds largely depends on the relative contribution of each solvation free energy parameter to the binding process. The  $\text{Log } K_B$  values determined through SED were plotted against  $\text{Log } K_{OW}$  values for the sulfonamides.<sup>27</sup> The resulting plot (Fig 3.5) shows poor linearity ( $r^2 = 0.53$ ), suggesting that, for these compounds, hydrophobic interactions are not the dominant interaction accounting for binding with the micelles. The weak  $\text{Log } K_{OW}$  dependence is also illustrated by examining the three lowest  $\text{Log } K_{OW}$  compounds (sulfanilamide, sulfaguanidine and sulfacetamide).

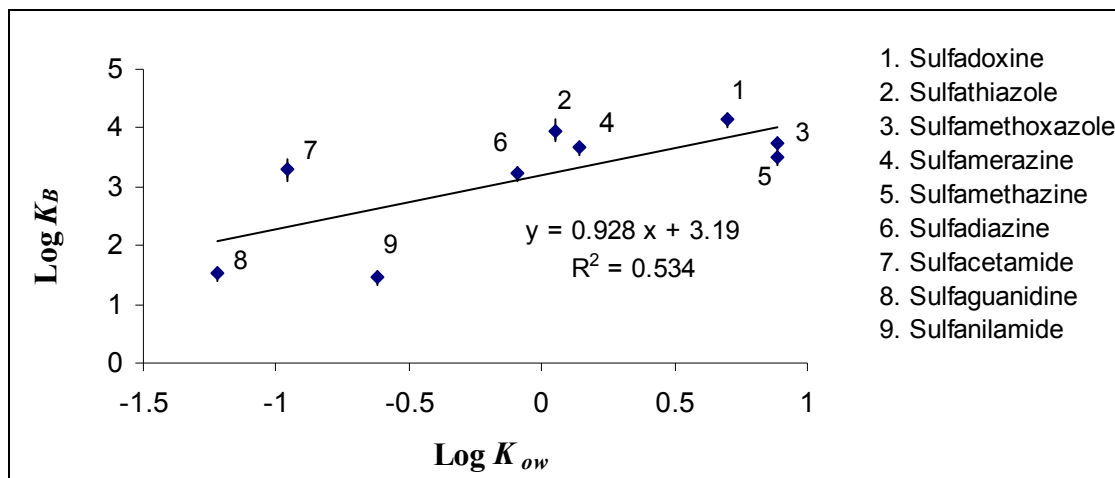


**Fig. 3.5.** Linear Free Energy Relationship indicating the correlation ( $r^2 = 0.53$ ) between  $\text{Log } K_B$  and  $\text{Log } K_{OW}$  for sulfonamide antibiotics binding to CTABr.

Two of these three also have low  $\text{Log } K_B$  values, however sulfacetamide gives a binding constant similar to the high  $\text{Log } K_{OW}$  compounds. An explanation of the interactions can be derived from observing the plot of  $\text{Log } K_B$  against  $\log \text{p}K_{a2}$  for the sulfonamides, as seen in Fig. 3.6.

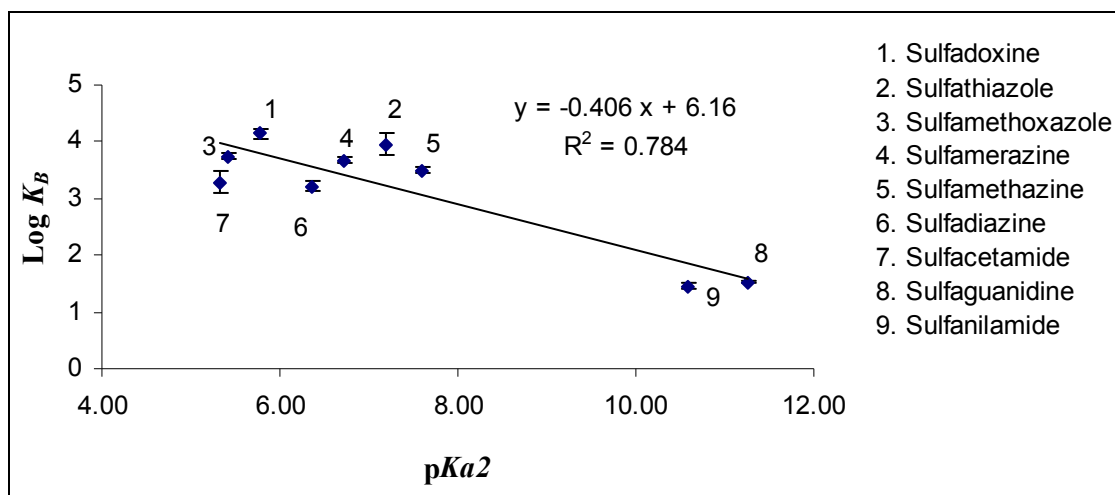


**Fig. 3.6.** Linear Free Energy Relationship depicting the correlation ( $r^2 = 0.78$ ) between  $\text{Log } K_{OW}$  and  $\text{p}K_{a2}$  for sulfonamide antibiotics binding to CTABr.

This plot gives a much stronger correlation ( $r^2 = 0.78$ ) without significant outliers, suggesting that micelle binding is significantly related to the tendency of the compounds to be deprotonated and to form a negatively charged species.<sup>34</sup> The sulfonamides have amine groups that can be protonated or de-protonated, as shown in Fig. 3.7.

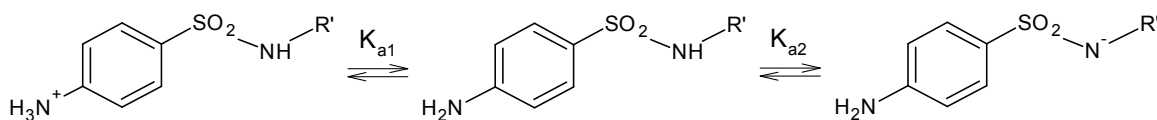


**Fig. 3.7.** Protonation/deprotonation equilibria of sulfonamides showing positive, neutral and negative forms. At pH values of 7 and above, only the neutral and negative forms will be found in equilibrium, as determined by  $K_{a2}$ . Note that the negative charge is shown on the secondary nitrogen atom, but is shared through resonance structures with the oxygens on the sulfonate group

The pH of these solutions was between 7.8 and 8.5. In this range, most of the sulfonamides will be in the de-protonated or negatively charged form (Fig. 3.7, right-hand-side). Sulfaguanidine and sulfanilamide have  $pK_{a2}$  values above 10, however, and will be in the neutral form in these experiments. This shows that the key interaction between the sulfonamides and the CTABr micelles is a charge-charge interaction between the negative form of the sulfonamide and the positive CTABr headgroups. Zarei et. al. reported that  $pK_a$  value of sulfonephthalein dyes was increased with increasing concentration of anionic, neutral and cationic surfactants.<sup>35</sup> This suggests that bound sulfonamide will have lower  $pK_a$  values than reported in solution, which is favorable for binding to cationic micelles.

The relationship of binding to both  $pK_{a2}$  and  $\text{Log } K_{OW}$  can further be characterized if we assume that only the negative form of the sulfonamide binds to the micelles. A modified  $\text{Log } K_B$  can be calculated using the proportion of sulfonamide in the negative form at the pH of the experiment,<sup>36</sup> as calculated from the pH and  $pK_{a2}$  values, to calculate a free negative sulfonamide concentration

for the denominator in Equation 8 (see appendix A1.2). The modified  $\text{Log } K_B$  results are plotted against  $\text{Log } K_{OW}$  in Fig. 3.8.

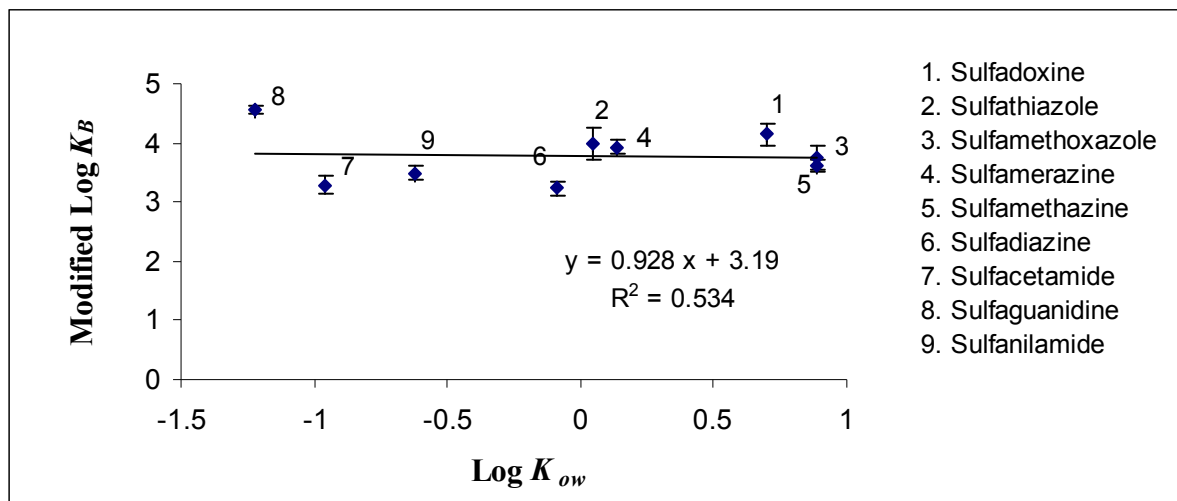


**Fig. 3.8.** Modified  $\text{Log } K_B$  plotted against  $\text{Log } K_{OW}$  for the sulfonamides. The modified  $\text{Log } K_B$  values were calculated by assuming only the negative forms will bind to the positive CTABr micelles.

This shows clearly that micelle binding is not related to  $\text{Log } K_{OW}$  for these compounds, with  $\text{Log } K_{OW}$  in the range of -1 to 1. A plot of  $\text{Log } K_B$  vs.  $\text{p}K_{a2}$  is the best option for estimating  $\text{Log } K_B$  for this compound group.

A multivariate regression using  $\text{p}K_{a2}$  and  $\text{Log } K_{OW}$  provided a small but not significant improvement in prediction of  $\text{Log } K_B$  (not shown). Similar groups of ionizable polar organic compounds will probably show similar behaviour, though the equation for the  $\text{Log } K_B$  vs  $\text{p}K_a$  plot for other groups may be different. It was also noted that SED experiments using these sulfonamides and negatively-charged sodium dodecylsulfate micelles showed no detectable binding, giving the same retentate and permeate side concentrations after 24 h (results not shown).

### ***3.3.3 Use of micellar binding constants to describe MEUF potential***

The binding constants indicate the affinity of the individual sulfonamide compounds for CTABr micelles, and thereby indicate the potential effectiveness of a MEUF process based on cationic surfactants for their removal from wastewater streams. One way to describe the potential for MEUF treatment is to consider the proportion of sulfonamide on the retentate side after 24 h. The four strongest bound compounds (sulfadoxine, sulfathiazole, sulfamethoxazole, sulfamerazine) are over 95% retained, while sulfamethazine is 94% retained. Sulfadiazine and sulfacetamide are 89-90% retained, while weakly bound sulfaguanidine and sulfanilamide are not significantly retained at 53%. Actual performance of MEUF may be significantly different, as it will depend on specific parameters including surfactant concentration and flow rate. A general statement can be made that systems with  $\text{Log } K_B$  values greater than 3.0 are good candidates for MEUF using CTABr. It should also be noted that these results are consistent with those reported by Exall et al.<sup>10</sup>, where sulfaguanidine was poorly removed while sulfamerazine and sulfathiazole were effectively removed, corresponding to their  $\text{Log } K_B$  values of 1.53, 3.67 and 3.96, respectively. In the case of sulfaguanidine and sulfanilamide treatment with CTABr in MEUF, improved retention of these compounds may be possible with an increase in the pH of the effluent.

### **3.4 Conclusions**

The binding constants between various sulfonamide antibiotics and CTABr were determined using semi-equilibrium dialysis. This illustrated the potential for MEUF with CTABr to remove these contaminants from water if a portion of the compounds carry a negative charge. We constructed a linear free energy plot demonstrating the correlation between  $\text{Log } K_B$  (in CTABr) and  $\text{Log } K_{OW}$  as well as between  $\text{Log } K_B$  and  $\text{p}K_{a2}$ . Collectively, this information could

be used to estimate a Log  $K_B$  value for additional sulfonamides and similar compounds, provided the pH and the  $pK_{a2}$  values were known. The general approach used here should work for other compound groups, though the specific relationship between Log  $K_B$  and other parameters would need to be determined. Practical MEUF may need to consider other surfactants that are less toxic or provide a greater opportunity for recovery, but for sulfonamide removal a cationic surfactant is likely essential.

### 3.5 References

1. Kolpin, D. W.; Furlong, E. T.; Meyer, M. T.; Thurman, E. M.; Zaugg, S. D.; Barber, L. B.; Buxton, H. T. *Environ. Sci. Technol.* **2002**, 36 (6), 1202-1211.
2. Monteiro S. C.; Boxall A. B. A. *Rev. Environ. Contam. Toxicol.* **2010**, 202, 53-154.
3. Watkinson, A. J.; Murby, E. J.; Kolpin, D. W.; Costanzo, S. D. *Sci. Total Environ.* **2009**, 407(8), 2711-2723.
4. Kümmerer, K. *Chemosphere*, **2009**. 75, 417-435.
5. Miao, X. S.; Bishay, F.; Chen, M.; Metcalfe C. D. *Environ. Sci. Technol.* **2004**, 38, 3533-3541.
6. Zhang, T.; Li, B. *Environ. Sci. Technol.* **2011**, 41(11), 951-998.
7. Lin, A. Y. C.; Lin, C. F.; Chiou, J. M.; Hong, P. K. A. *J Hazard Mater.* **2009**, 171, 452.
8. Bielska, M.; Szymanowski, J. *Water Research*, **2006**, 40, 1027-1033.
9. Huang, J.; Peng, L.; Zeng, G.; Li, X.; Zhao, Y.; Liu, L.; Li, F.; Chai, Q. *Separation and Purification Technology*, **2014**, 125, 83-89.
10. Exall, K.; Balakrishnan, V. K.; Toito, J.; McFadyen, R. *Sci. Total Environ.* **2013**, 461-462, 371-376.
11. Dunn, R. O.; Scamehorn, J. F.; Christian, S. D. *Sci. Technol.* **1985**, 20 (4), 257-284.
12. Baek, K.; Yang, J. W. *Chemosphere*, **2004**, 57 (9), 1091-1097.
13. Zeng, G. M.; Xu, K.; Huang, J. H.; Li, X.; Fang, Y. Y.; Qu, Y. H. *J Membrane Sci.* **2008**, 310 (1-2), 149-160.



14. Purkait, M. K.; DasGupta, S.; De, S. *Sep. Purif. Technol.* **2004**, *37* (1), 81-92.
15. Farias, T.; de Menorval, L. C.; Zajac, J.; Rivera, A. *Colloids and Surfaces A: Physicochem. Eng. Aspects* **2009**, *345*, 51-57.
16. Dhar, S.; Rana, D. K.; Sarkar, A.; Mandal, T. K. Ghosh, S.; Battacharya, S. C. *Colloids and Surfaces A: Physicochem. Eng. Aspects* **2009**, *349* (1-3) 117-124.
17. Bunton, C. A.; Sepulveda, L. *J Phys Chem.* **1979**, *83*(6), 680-683.
18. Xu, K.; Ren, H. Q.; Zeng, G. M.; Ding, L. L.; Huang, J. H. *Colloids and Surfaces A: Physicochem. Eng. Aspects* **2010**, *356*, 150-155.
19. Waters, L. J.; Kasprzyk-Hordern, B. *J Therm Anal Calorim.* **2010**, *102*(1), 343-347.
20. Terabe, S.; Otsuk, K.; Ichikawa, K.; Tsuchiya, A.; Ando, T. *Anal. Chem.* **1984**, *56*, 111-113.
21. Terabe, S.; Otsuk, K.; Ando, T. *Anal. Chem.* **1985**, *57*, 834-841.
22. Vindevogel, J.; Sandra, P. *Introduction to Micellar Electrokinetic Chromatography, Htithig, Heidelberg*, **1992**.
23. Rouse, J. D.; Sabatini, D. A.; Deed, N. E.; Brown, R E.; Harwell, J. H. *Environ. Sci. Technol.* **1995**, *29*, 2484-2489.
24. Sun, L.; Chen, L.; Sun, X.; Du, X.; Yue, Y.; He, D.; Xu, H.; Zeng, Q.; Wang, H.; Ding, L. *Chemosphere*, **2009**, *77* 1306-1312.
25. Cifuentes, A.; Bernal, J. L.; Diez-Masa, J. C. *Anal. Chem.* **1997**, *69*, 4271-4274.
26. Vautier-Giongo, C.; Bales, B. L. *J. Phys. Chem. B* **2003**, *107*(23), 5398-5403.
27. "US National Library of Medicine" ChemIDPlus database.  
<http://toxnet.nlm.nih.gov/cgi-bin/sis/search>. (Accessed Nov. 10, 2015).
28. Sanli, S.; Altun, Y.; Sanli, N.; Alsancak, G.; Beltran, J. L. *J Chem Eng Data*, **2009**, *54*(11), 3014-3021.
29. Shalaeva, M.; Kenseth, J.; Lombardo, F.; Bastin, A. *J Pharm Sci.* **2008**, *97*, 2581-2606.
30. Quina, F. H.; Alonso, E. O.; Farah, J. P. S. *J. Phys. Chem.* **1995**, *99* (30), 11708-11714.
31. Abraham, M. H. *Chem. Soc. Rev.* **1993**, *22* (2), 73-83.
32. Treiner, C.; Mannebach, M. H. *J. Coll. Interface Sci.* **1987**, *118* (1), 243-251.
33. Treiner, C.; Chattopadhyay, K. *J. Coll. Interface Sci.* **1986**, *109* (1), 101-108.

34. Abraham, M. H.; Chadha, H. S.; Dixon, J. P.; Rafols, C.; Treiner, C. *J. Chem. Soc. Perkin Trans 2*, **1995**, 887-894.
35. Zarei, K.; Atabati, M.; Abdinasab, E. *Eurasian J. Anal. Chem.* **2009**, *4*(3), 314-327.
36. Mehling, T.; Kloss, L.; Ingram, T.; Smirnova, I. *Langmuir*, **2013**, *29*, 1035–1044.

## Chapter 4

# Understanding binding of sulfonamide antibiotics to CTABr micelles using $^1\text{H}$ NMR spectroscopy

### 4.1 Introduction

Sulfonamides are organic compounds which form a class of antibiotic pharmaceutical compounds. In recent years, the occurrence and fate of pharmaceutically active compounds (PhACs) in the aquatic environment has been considered as one of the emerging environmental issues.<sup>1-5</sup> Low concentrations (<1 ppb) of sulfonamides have been detected in surface water as well as in the influent and effluent of wastewater treatment plants.<sup>6-11</sup> These compounds are only partially removed by conventional wastewater treatment systems. A number of advanced treatment options have been investigated for removal of PhACs from wastewater, but none is in common use. Micellar enhanced ultrafiltration (MEUF) has been proposed to be an effective removal technique for a variety of trace contaminants in wastewater,<sup>12-14</sup> and has recently been reported for a small number of sulfonamides.<sup>15</sup>

MEUF depends on contaminants binding to micelles, so understanding the contaminant-micelle interaction and knowing the contaminant-micelle binding constant is key to predicting the removal efficiency of particular contaminants in a MEUF system. We recently reported on the use of semi-equilibrium dialysis (SED) to determine the binding constant of several sulfonamides with cetyltrimethylammonium bromide (CTABr) micelles.<sup>16</sup>

We noted that the binding constants were good predictors of MEUF performance for the three sulfonamides examined by Exall et al.<sup>15</sup> The SED results led to the suggestion that sulfonamides bind to cationic CTABr micelles when the former are in an anionic form, which would be consistent with the sulfonamides interacting with the CTABr headgroup region. The

SED experiments do not, however, provide any specific information regarding the binding interaction or the locus of the sulfonamide molecule in the micelle structure.

$^1\text{H}$  NMR can be an important tool for characterizing a molecular species in the free and bound states.<sup>17</sup> For organic compounds associating with micelles,  $^1\text{H}$  NMR has been used to probe the local environment of specific protons of a molecule bound to a micellar system.<sup>18</sup> In the case of molecules bound to cationic surfactant micelles, proximity to the positively charged head group of the micelle results in decreased electron density, and this deshielding effect is associated with an increase in chemical shift (downfield shift) for a proton in the headgroup region or Stern layer.<sup>18</sup> In contrast, if a proton penetrates past the headgroups into the upper “palisade” region of the hydrocarbon chains, or further into the hydrophobic centre of the micelle, higher electron density results in shielding and an upfield chemical shift for the proton.<sup>18</sup> For complex molecules with multiple protons, there may be some protons that show upfield chemical shifts on binding, while others show downfield shifts. A proton that sits exactly on the border between the Stern layer and the palisade region may exhibit no chemical shift at all, even though the molecule is bound. Gaidamauskas et al.<sup>18</sup> used the pattern of upfield and downfield shifts for multiple protons in a molecule to propose a locus and orientation for 2,6-pyridinedicarboxylate anions interacting with CTABr micelles, as only certain orientations provided the correct combination of proton shifts in each direction.

$^1\text{H}$  NMR spectroscopy also utilizes the determination of binding constants,<sup>17</sup> such as in host-guest inclusion complexes.<sup>19,20</sup> If the chemical shift of a proton changes between free and bound forms, a plot of chemical shift vs. concentration of binding agent can be used to determine the binding constant. Typically, NMR does not report separate chemical shifts for bound and free species for systems at equilibrium, because the individual molecules will alternate between bound and free states many times on the NMR timescale. Instead, the observed chemical shift

will be the weighted average of the chemical shifts of the free and bound forms.<sup>21</sup> Standard binding equations to determine the “fraction bound” have been combined with the measured average chemical shift to calculate the binding constant. Only a few papers have appeared using <sup>1</sup>H NMR to examine binding of organic compounds to micelles, and we have not seen any previous reports where micelle binding constants were determined using <sup>1</sup>H NMR chemical shift measurements.

This paper describes the interaction of nine sulfonamide compounds with CTABr micelles in solution as characterized using <sup>1</sup>H NMR measurements of sulfonamide-micelle complexes. These results can be combined with previous binding constant measurements<sup>16</sup> to propose a locus and orientation for the sulfonamide molecules in the micelle structure, analogous to the work of Gaidamauskas et al.<sup>18</sup> The <sup>1</sup>H NMR data are also used to estimate the binding constant between the sulfonamides and the micelle pseudo-phase to assess the ability of <sup>1</sup>H NMR to predict MEUF performance.

## **4.2 Materials and methods**

### ***4.2.1 Materials***

Cetyltrimethylammonium bromide (CTABr) and the sulfonamides sulfadoxine, sulfathiazole, sulfamethoxazole, sulfamerazine, sulfadiazine, sulfamethazine, sulfacetamide, sulfaguanidine, and sulfanilamide were purchased from Sigma-Aldrich Chemicals (Oakville, ON). D<sub>2</sub>O was purchased from both Cambridge Isotope Laboratories and CDN Isotopes. Deionized water was obtained from a Milli-Q system (Millipore, Etobicoke, ON).

### 4.2.2 Sample preparation

Stock solutions of sulfonamides were prepared by addition of approximately 5 mg of sulfonamide to 25 mL D<sub>2</sub>O, followed by sonication at 35±1 °C to aid dissolution. Samples were sonicated again prior to use. The ~5x10<sup>-4</sup> M concentration (see Table 4.1) was chosen to be as low as possible while still providing a reliable peak in the NMR spectrum.

**Table 4.1. Sample preparation of sulfonamides in D<sub>2</sub>O**

Sulfonamides	M.W (g/mole)	Conc. (M)
1. Sulfadoxine	310.3	5.2 x 10 <sup>-4</sup>
2. Sulfathiazole	255.32	8.2 x 10 <sup>-4</sup>
3. Sulfamethoxazole	253.28	2.4 x 10 <sup>-4</sup>
4. Sulfamerazine	264.31	7.6 x 10 <sup>-4</sup>
5. Sulfamethazine	278.33	5.0 x 10 <sup>-4</sup>
6. Sulfadiazine	250.28	5.4 x 10 <sup>-4</sup>
7. Sulfacetamide	214.24	5.8 x 10 <sup>-4</sup>
8. Sulfaguanidine	214.24	6.7 x 10 <sup>-4</sup>
9. Sulfanilamide	172.2	5.1 x 10 <sup>-4</sup>

CTABr solutions were prepared via serial dissolution of a 20 mM of CTABr stock solution prepared by dissolving 0.7289 g of CTABr (MW = 364.45 g/mol) in 100 mL D<sub>2</sub>O. Dissolution was aided by placing the solution in an ultrasonic bath at 35 °C for 30 minutes. Prior to further use, CTABr stock solutions were sonicated again, as a precipitate would often form if solutions were left at room temperature for a period of longer than one day.

### 4.2.3 <sup>1</sup>H NMR studies

CTABr studies ranged from sub-micellar concentrations to an order of magnitude greater than the CMC (~ 1 mM, see below). Samples were prepared in D<sub>2</sub>O (see Table 4.1) and sonicated prior to being placed in 5 mm probe head NMR tubes for analysis. Samples were analyzed on a Bruker

500 MHz NMR spectrometer operating at 499.40 MHz with a digital resolution of 0.18 Hz. Chemical shifts( $\delta$ ) were measured relative to the HOD peak present at approximately  $\delta=4.7$  ppm (samples were held held at  $298.0 \pm 0.1$  K to ensure that HOD peak remained at a constant position).  $^1\text{H}$  NMR spectra were generated quantitatively as the average of 64 individual scans using a 45 degree pulse of  $7.5 \mu\text{s}$  with a relaxation time ( $t_1$ ) of 2.7 s. The NMR time scale for the sulfonamide was estimated to be between 0.1-0.3 s by examining the free induction decay data.

#### 4.2.4 CMC determination

The critical micelle concentration (CMC) of CTABr in  $\text{D}_2\text{O}$  was determined by measuring conductivity of CTABr concentrations from 0 mM to 6 mM using a Jenway- 470 Conductivity Meter (VWR, Mississauga, ON). CMC of CTABr in  $\text{D}_2\text{O}$  was reported to decrease by 0.18mM compare to  $\text{H}_2\text{O}$ .<sup>22</sup>

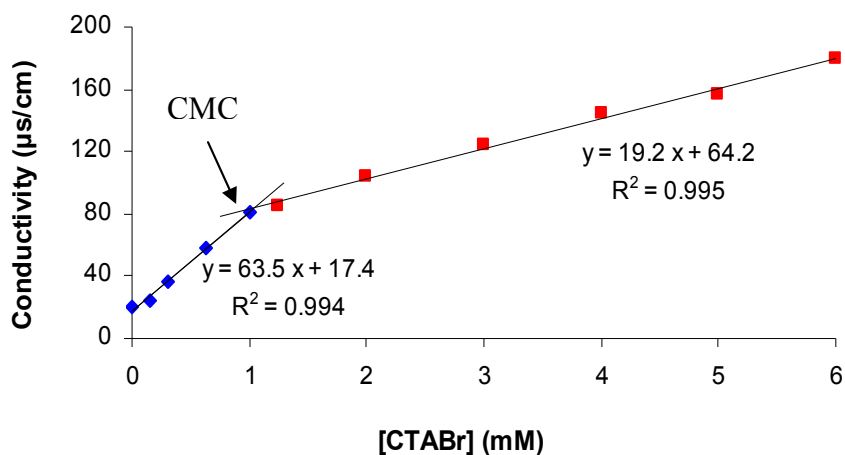


**Fig. 4.1.** Conductivity of CTABr solutions in  $\text{D}_2\text{O}$ . The discontinuity between two linear ranges indicates the CMC value of CTABr ( $\sim 1.1$  mM).

CMC determined in this work was 1.1 mM, which is about 0.17 mM greater than previously reported values of 0.93 mM<sup>23</sup> and 0.92 mM.<sup>16</sup> This suggests the error in this CMC measurement

is greater than 0.2 mM . This will contribute to the error in the calculated  $\text{Log } K_B$  values. But the magnitude of the error will be less than reported standard deviation.

## 4.3 Results and discussion

### 4.3.1 NMR spectra in $\text{D}_2\text{O}$ with CTABr

NMR spectra of the sulfonamides were recorded in  $\text{D}_2\text{O}$  with and without CTABr present. Individual peaks were assigned based on reference data, and were identified in pure  $\text{D}_2\text{O}$  and in 10 mM CTABr (well above the CMC), as shown for sulfamethazine in Fig. 4.2.

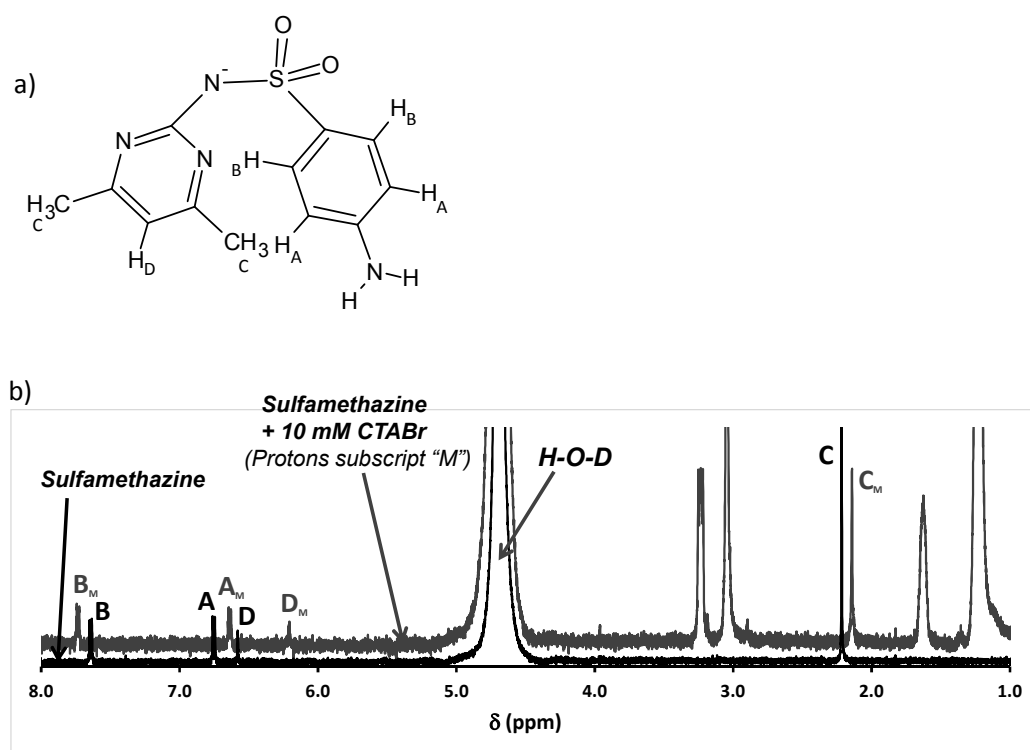
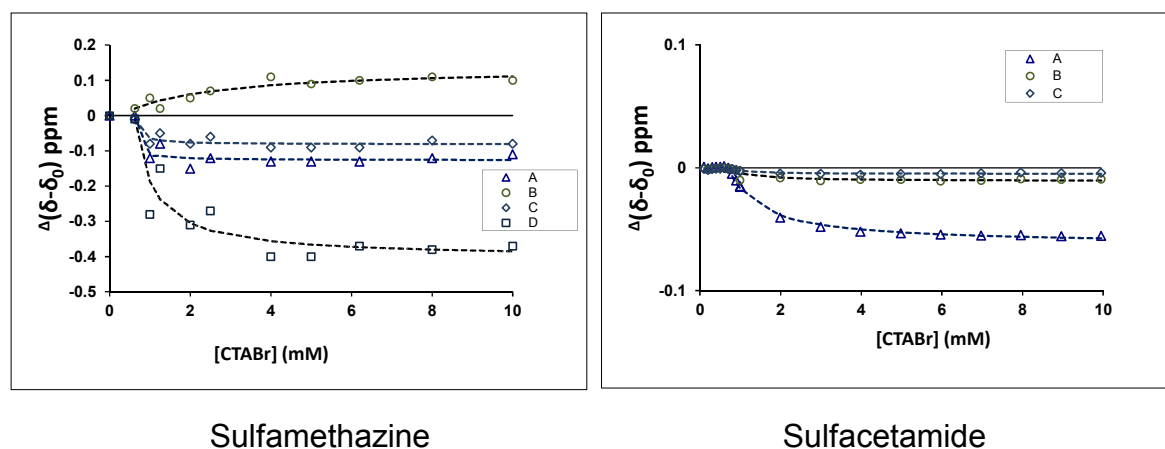


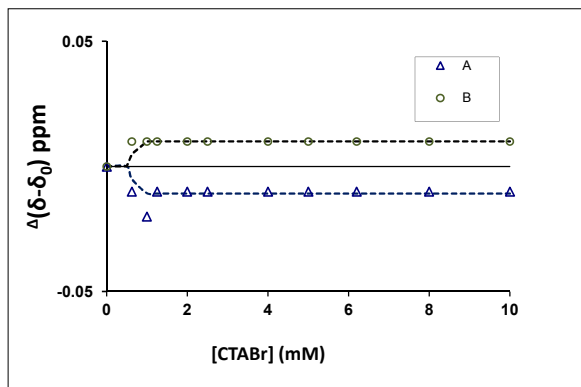
**Fig. 4.2.** a) Sulfamethazine structure with non-exchangeable protons labelled. b) NMR spectra of sulfamethazine in  $\text{D}_2\text{O}$  (lower spectrum) and in 10 mM CTABr in  $\text{D}_2\text{O}$  (upper spectrum). Peak labels correspond to proton labels in a). Labels with subscript "M" indicate peaks in presence of CTABr micelles.



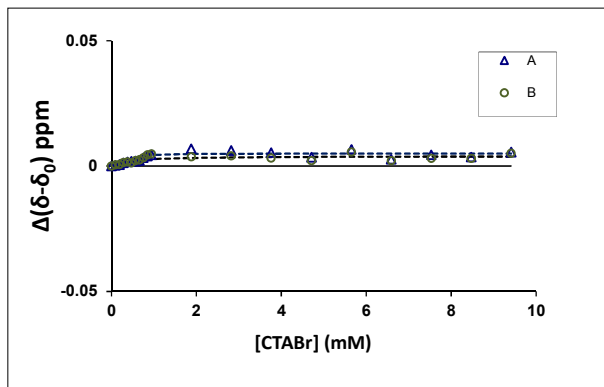
The change in position of the protons, with some shifting upfield and some shifting downfield, can be used to suggest a locus and orientation of the molecule within the micelle. With increasing CTABr concentration, the NMR chemical shift values of the various protons on the sulfonamides migrated (Fig. 4.2) either upfield or downfield.

For example, as CTABr concentration increased from 0 mM to 10 mM, protons A, C and D of sulfamethazine experienced an upfield shift, whereas proton B showed a moderate downfield shift (Fig. 4.2). The chemical shift changes measured for all protons in all nine sulfonamides are plotted in Fig. 4.3.

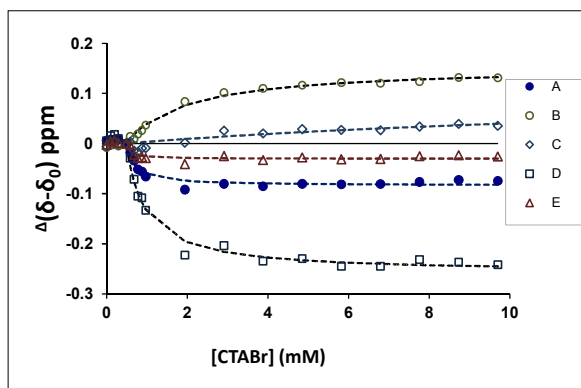




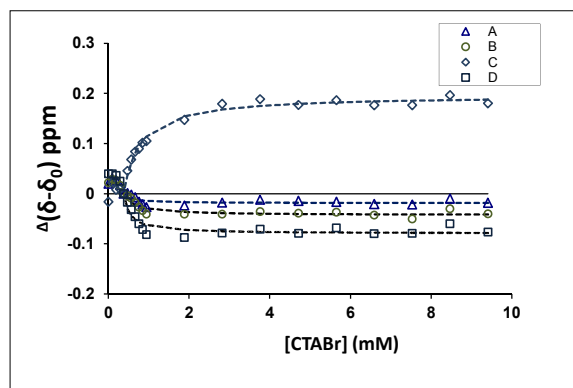
Sulfanilamide



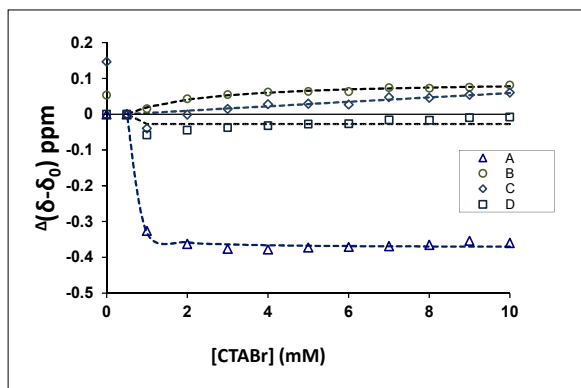
Sulfaguanidine



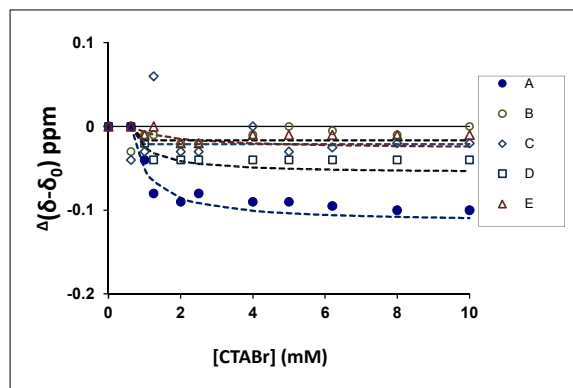
Sulfamerazine



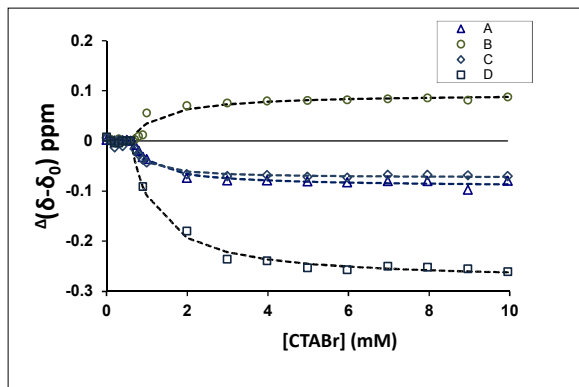
Sulfamethoxazole



Sulfathiazole



Sulfadoxine



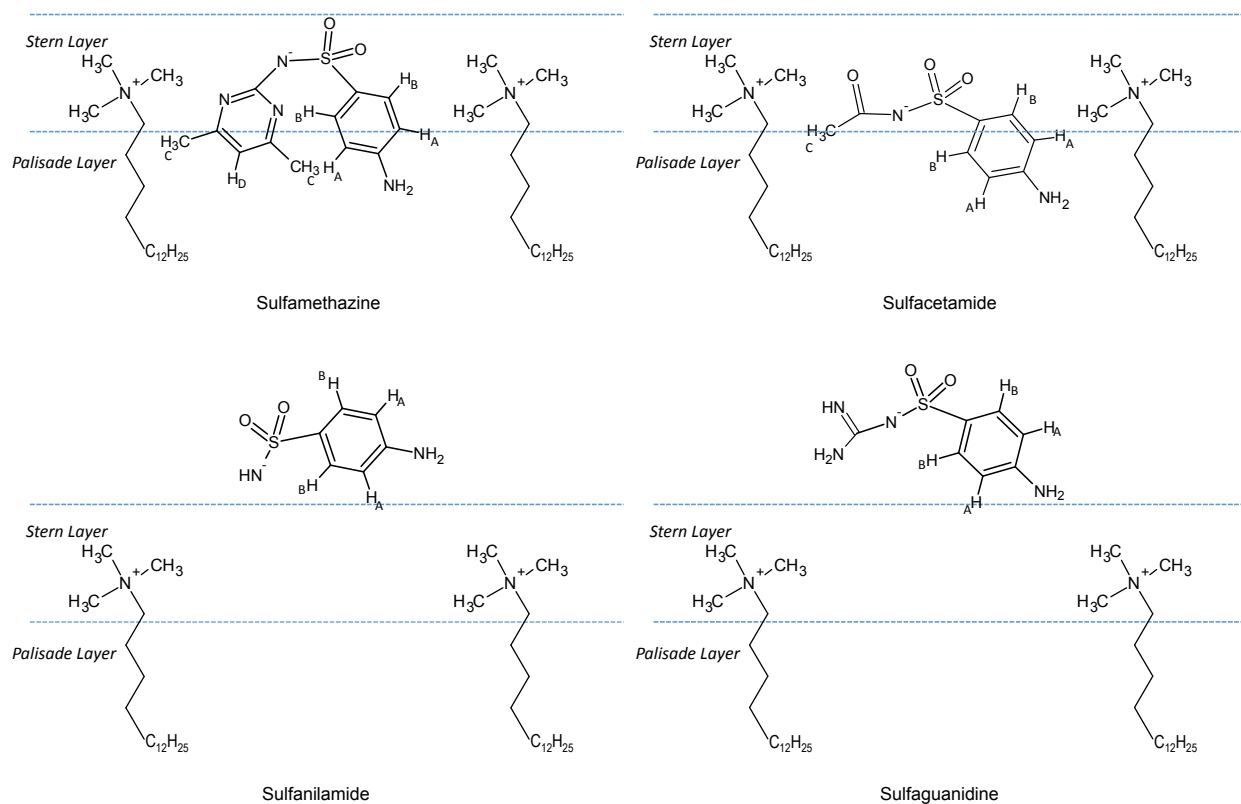
Sulfadiazine

**Fig. 4.3.** Change in relative chemical shift of hydrogens as a function of CTABr concentration. Relative chemical shift values are shown where the chemical shift for each proton in the absence of CTABr was subtracted from each measured chemical shift. Dashed lines were drawn using fit parameters and Equation 4.1 below.

#### 4.3.2 Determining Locus and orientation of the sulfonamide

The chemical shift change ( $\Delta\delta$ , ppm) patterns in Fig. 4.3 can be used to propose a locus and orientation for each bound sulfonamide molecule within the micelle. Following the description of Gaidamauskas et al.<sup>18</sup> the shift can be related to protons ending up in the head-group region (downfield shift to larger  $\delta$  values) or in the hydrocarbon center of the micelle (upfield shift to smaller  $\delta$  values). Protons shifting only slightly upfield are likely just into the “palisade” region, which is the outer portion of the hydrocarbon center close to the headgroups, where the hydrocarbon chains are relatively structured and less hydrophobic than in the micelle interior. Protons that show no significant shift that are on molecules where adjacent protons do shift are most likely just on the border between the palisade and headgroup region, where the level of shielding happens to be similar to bulk solution. Molecules where no protons are shifting are more likely weak binders, where the fraction associated with micelles is too small for the average chemical shift to be noticeably affected. The illustrations in Fig. 4.4 were derived by manipulation of simple structure diagrams to show an arrangement that corresponds most closely

with the observed pattern of chemical shifts across the protons. For example, sulfamethazine is placed with the D proton in the palisade layer and the B protons in the Stern layer, consistent with their upfield and downfield shifts, respectively. Then the molecule is located such that the A and C protons are just below the Stern-palisade interface, consistent with their slight upfield shift (compared with the D proton). Note that the structures with two aromatic rings appear congested in these two dimensional representations, but in three-dimensional space the rings would not be co-planar and would have greater separation. It should also be noted that when structures have equivalent protons located in different positions (e.g. the B protons in sulfacetamide), rapid translational and internal motion mean the NMR spectrum will show a peak position corresponding to the average of the available positions.



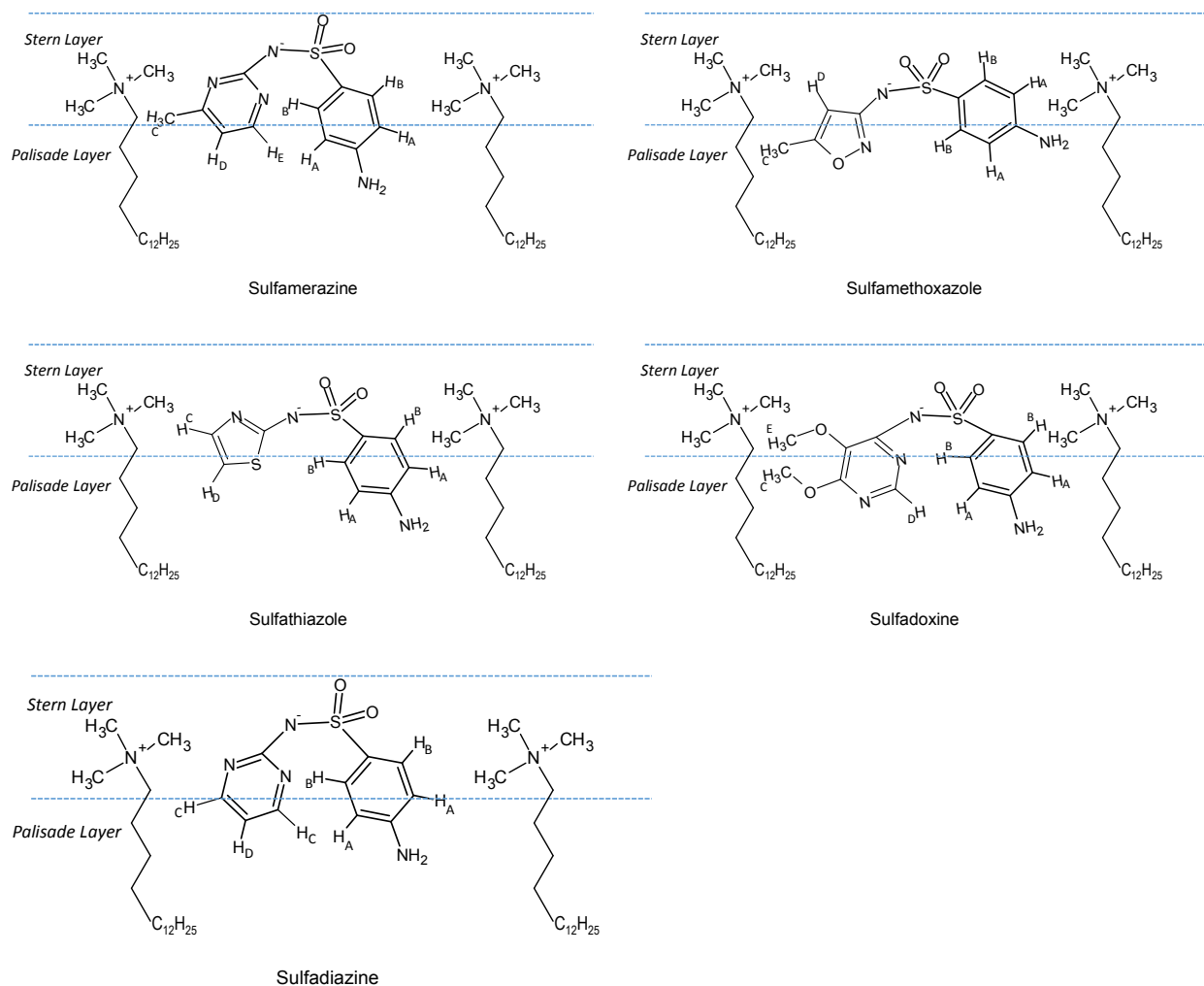


**Fig. 4.4.** Proposed locus and orientation of sulfonamide molecules in CTABr micelles according to the chemical shift patterns shown in Fig. 4.3.

The orientations depicted in Fig. 4.4 can be used to provide an overall description of sulfonamide binding with the micelles. Each sulfonamide features an aniline group attached to an anionic sulfonamide ( $\text{NSO}_2^-$ ) group, and for all strongly bound forms, the aniline group penetrates partly into the palisade layer while the negative sulfonamide group remains near the charged CTABr groups in the headgroup region (Stern layer), analogous to the proposed binding of 2,6-pyridinedicarboxylate anions described by Gaidamauskas et al.<sup>18</sup> Six of the seven strongly bound sulfonamides feature a second aromatic group attached to the sulfonamide “N”, with that second

group also penetrating into the micelle interior. The other strongly bound sulfonamide, sulfacetamide, features a  $\text{CH}_3\text{C}=\text{O}$  group which is also relatively non-polar and may contribute positively to micelle interactions. For the compounds where no binding was detected, sulfaguanadine and sulfanilamide, the second group is  $\text{C}(\text{NH})\text{NH}_2$  and  $\text{H}$ , respectively. In our previous report,<sup>16</sup> the weaker binding of these two sulfonamides was discussed in terms of  $\text{p}K_a$  values and the tendency of the sulfonamides to be negatively charged or neutral. An additional contribution could be the lack of interaction between these small and more polar second groups and the hydrophobic micelle interior, compared with the second groups on the strongly bound sulfonamides. Unfortunately, we are not able to observe chemical shifts for the protons on these two second groups directly as they are exchangeable with  $\text{D}_2\text{O}$ .

#### ***4.3.3 Determination of binding constant of sulfonamides with CTABr micelles***

As CTABr was added to the sulfonamide solutions, the chemical shift of non-exchangeable sulfonamide protons generally followed a pattern. At very low values, there was no change in chemical shift. As the CTABr concentration approached and then exceeded the CMC, a chemical shift change started for most protons, either in an upfield or downfield direction. Then at higher CTABr concentrations the chemical shift “leveled off” at a maximal value. This general pattern is consistent with increasing micelle formation and subsequent partitioning of a greater fraction of sulfonamide into the micelles.<sup>19</sup> In some cases, chemical shifts were noted at CTABr concentrations below the CMC, which could be a result of sulfonamides influencing the critical micelle concentration or it could indicate binding of the sulfonamide by both pre-micellar aggregates and by micelles.<sup>24</sup> The chemical shift observed at each CTABr concentration is an average of the chemical shift values of bound and free sulfonamides, where the NMR reports the average for molecules that rapidly exchange between bound and free forms on the NMR

timescale.<sup>18,21</sup> Given this explanation of the measured chemical shift, and following the approach used for derivation of Equation 8 in Ch. 3, Equation 1 was derived for the relationship between chemical shift and micelle binding constant  $K_B$ .

$$\delta = \frac{\delta_0 + \delta_M K_B M_V (C_S - C_{CMC})}{1 + K_B M_V (C_S - C_{CMC})} \quad \text{Equation (4.1)}$$

Where,  $\delta$  = Chemical shift of proton at  $C_S$ ;

$\delta_0$  = Initial chemical shift of the proton when  $C_S = 0$ ;

$\delta_M$  = Chemical shift of the proton in a fully bound state;

$K_B$  = Binding constant;

$M_V$  = Molar volume of the surfactant;

$C_S$  = Total concentration of the surfactant; and

$C_{CMC}$  = Critical micelle concentration of the surfactant

An important factor for Equation 4.1 is that the maximum chemical shift ( $\delta_M$ ) cannot be measured directly, so there are two unknown parameters in the equation ( $\delta_M$  along with  $K_B$ ). Rather than calculating  $K_B$  directly from the equation, both  $\delta_M$  and  $K_B$  were determined by an iterative fitting procedure to minimize the sum of the squares of residuals using the “Solver” utility of Microsoft Excel. The resulting fits are shown as the dashed lines in Fig. 4.3, indicating that the data followed this equation. The noise or random variations in chemical shift values in these experiments was about 0.018 ppm, so  $K_B$  values were determined only for protons with a total shift greater than 0.05 ppm (S/N>3).

This minimum shift can be used with typical parameters in Equation 4.1 to estimate the minimum binding constant that can be measured. If a maximum chemical shift change ( $\delta_M$ ) of 0.28 ppm is assumed (largest seen in Figure 4.3), then a log  $K_B$  value of 1.8 would give an observed change of 0.05 ppm at 10 mM CTABr. Therefore log  $K_B = 1.8$  is the estimated

minimum value that can be measured. For sulfanilamide and sulfaguanidine, the chemical shift changes for all protons were much less than 0.05 ppm, so  $\log K_B$  values for these are reported as  $<1.8$ .

It can be noted that the  $\log K_B$  values for these two compounds were previously found by SED to be close to 1.5.<sup>16</sup>

The  $\log K_B$  values calculated for the 7 sulfonamides with sufficiently large chemical shifts are shown in Table 4.2. For these sulfonamides, all but sulfadoxine had two or more protons that could be used for determining the binding constant (total chemical shift change greater than 0.05 ppm). The average and standard deviation of the  $\log K_B$  values determined in this way for each compound are given in Table 4.2. The binding experiments for sulfamerazine were done as triplicate independent trials, and the  $\log K_B$  and error values for this compound determined from the triplicate data. Note that the error value from the triplicates ( $\pm 0.19$ ) is in the range of the errors determined from multiple protons ( $\pm 0.095$  to  $\pm 0.25$ ), so the estimated errors seem reasonable. Since sulfadoxine only had one measured  $\log K_B$  value, the error term in Table 4.2 (0.15) is the average of the other six measured values, which should be regarded as a very rough estimate of the actual error value.



**Table 4.2. Log  $K_B$  values as determined by NMR shown with corresponding values determined by semi-equilibrium dialysis.<sup>16</sup> NMR values were determined by fitting data to Equation 4.1 as shown in Fig. 4.3. Values for sulfaguanidine and sulfanilamide represent the minimum Log  $K_B$  that can be measured with the NMR method. Errors are standard deviations (see text).**

Compound	Log $K_B$ by SED <sup>16</sup>	Log $K_B$ by NMR (this work)
1. Sulfadoxine	4.14 ± 0.08	3.95 ± 0.15
2. Sulfathiazole	3.96 ± 0.20	3.56 ± 0.25
3. Sulfamethoxazole	3.75 ± 0.06	3.88 ± 0.10
4. Sulfamerazine	3.67 ± 0.06	3.39 ± 0.19
5. Sulfamethazine	3.50 ± 0.06	3.66 ± 0.18
6. Sulfadiazine	3.22 ± 0.10	3.51 ± 0.07
7. Sulfacetamide	3.29 ± 0.19	3.60 ± 0.10
8. Sulfaguanidine	1.53 ± 0.03	≤ 1.80
9. Sulfanilamide	1.46 ± 0.05	≤ 1.80

The results in Table 2 show good agreement with the log  $K_B$  values determined by semi-equilibrium dialysis.<sup>16</sup> This indicates that the NMR method is able to estimate Log  $K_B$  values with reasonable efficacy. The main disadvantages of the NMR method are that precision is generally lower (larger standard deviations) and that binding constants below log  $K_B=1.8$  cannot be measured. There may be systems where semi-equilibrium dialysis cannot be used, and this could be the preferred method. The results can also be compared with reported MEUF efficacy. Exall et al.<sup>15</sup> reported that MEUF with CTABr was effective for removal of sulfathiazole and sulfamerazine, but not for removal of sulfaguanidine. This is completely consistent with the binding constants measured here, with sulfathiazole and sulfamerazine in the Log  $K_B = 3.4-3.6$  range while sulfaguanidine had Log  $K_B < 1.8$ .

#### 4.4 Conclusions

The interactions between sulfonamide antibiotic compounds and CTABr micelles were examined using  $^1\text{H}$  NMR. The chemical shift changes of various non-exchangeable protons on the sulfonamide molecules provided a means of approximating the locus and orientation of the molecules within a model micelle structure. Some protons for bound sulfonamides were located either in the headgroup region (Stern layer) or just below in the palisade region of the micelles, consistent with the previous observation<sup>16</sup> that negatively-charged forms of sulfonamides would bind with cationic CTABr micelles. The sulfonamide group itself would be located in the headgroups region where it can associate with the cationic headgroups by charge-charge interactions.

The estimation of binding constants using the NMR chemical shift data showed that this method can be used to determine micelle binding constants for molecules that give an NMR signal in both free and bound forms, as long as the chemical shift of some protons of bound molecules changes appreciably (more than 0.05 ppm for this study).

While not as precise or sensitive as some other methods, there may be cases where NMR spectroscopy is a convenient method to follow compound binding while providing information about the chemical interactions between compounds and micelles at the same time. In some cases, the NMR spectroscopy results may be more accurate since bound and free molecules are simultaneously measured at equilibrium. The results can contribute to the prediction if a particular micelle/contaminant combination is a good candidate for MEUF treatment, and the unique information regarding binding interactions may be useful in tuning the MEUF process for a given group of compounds.

## 4.5 References

1. Stan, H. J.; Heberer, T. *Analisis*, **1997**, *25(7)*, 20–23.
2. Halling-Sorensen, B.; Nielsen, N.; Lansky, P. F.; Ingerslev, F.; Hansen, L.; Lutzhoft, H. C.; Jorgensen, S. E. *Chemosphere*, **1998**, *36*, 357–394.
3. Daughton, C. G.; Ternes, T. A. *Environ. Health Perspect*, **1999**, *107*, 907–938.
4. Daughton, C. G., Jones-Lepp, T. *Pharmaceuticals and Personal Care Products in the Environment: Scientific and Regulatory Issues*. Symposium Series 791, American Chemical Society, Washington DC. 2001.
5. Kummerer, K. *Chemosphere*, **2001**, *45*, 957–969.
6. Kolpin, D. W.; Furlong, E. T.; Meyer, M. T.; Thurman, E. M.; Zaugg, S. D.; Barber, L. B.; Buxton, H. T. *Environ. Sci. Technol.* **2002**, *36 (6)*, 1202- 1211.
7. Monteiro S. C.; Boxall A. B. A. *Rev. Environ. Contam. Toxicol.* **2010**, *202*, 53-154.
8. Watkinson, A. J.; Murby, E. J.; Kolpin, D. W.; Costanzo, S. D. *Sci. Total Environ.* **2009**, *407(8)*, 2711-2723.
9. Kummerer, K. *Chemosphere*, **2009**, *75*, 417-435.
10. Miao, X. S.; Bishay, F.; Chen, M.; Metcalfe C.D. *Environ. Sci. Technol.* **2004**, *38*, 3533-3541.
11. Zhang, T.; Li, B. *Crit. Rev. Environ. Sci. Technol.* **2011**, *41(11)*, 951-998.
12. Zeng, G. M.; Xu, K.; Huang, J. H.; Li, X.; Fang, Y. Y.; Qu, Y. H. *J. Membrane Sci.* **2008**, *310 (1-2)*, 149-160.
13. Purkait, M. K.; DasGupta, S.; De, S. *Sep. Purif. Technol.* **2004**, *37 (1)*, 81-92.
14. Dunn, R. O.; Scamehorn, J. F.; Christian, S. D. *Sep. Sci. Technol.* **1985**, *20 (4)*, 257-284.
15. Exall, K.; Balakrishnan, V. K. ; Toito, J.; McFadyen, R. *Sci Total. Environ.* **2013**, *461–462*, 371–376.
16. Sarker, A. K.; Cashin, P. J.; Balakrishnan, V. K.; Exall, K.; Chung, H. K. Buncel, E.; Brown, R.S. *Sep. Purif. Technol.* **2016**, *162*, 134-141.
17. Funasaki, N.; Nomura, M.; Ishikawa, S.; Neya, S. *J. Phys. Chem. B* **2001**, *105*, 7361-7365.
18. Gaidamauskas, E.; Cleaver, D. P.; Chatterjee, P. B.; Crans, D.C. *Langmuir*, **2010**, *26(16)*, 13153–13161.

19. Fielding, L. *Tetrahedron*, **2000**, *56*, 6151-6170.
20. Schneider, H. J.; Yatsimirsky, A. K. *Principles and Methods in Supramolecular Chemistry*; John Wiley and Sons: New York, 2000; Chapter E4.
21. Ramstad, T.; Hadden, C. E.; Martin, G. E.; Speaker, S. M.; Teagarden, D. L.; Thamann, T. J. *Int. J. Pharma.* **2005**, *296*, 55–63.
22. Chang, N.J.; Kaler, E.W. *J. Phys. Chem.* **1985**, *89*(14), 2996-3000.
23. Cifuentes, A.; Bernal, J. L.; Diez-Masa, J. C. *Anal. Chem.* **1997**, *69*, 4271-4274.
24. Menger, F. M.; Portnoy, C. E. *J. Am. Chem. Soc.* **1967**, *89*(18), 4698-4703.

## Chapter 5

### Determining binding of polycyclic aromatic hydrocarbons to CTABr micelles using semi-equilibrium dialysis

#### 5.1 Introduction

Polycyclic aromatic hydrocarbons (PAHs) are widely distributed in the environment due to numerous sources. They are commonly found in crude oil, petroleum, coal tar, shale oil, and oil sands bitumen. Through various mechanisms, the PAHs may end up contaminating water, which is a great concern due to their toxic, mutagenic and carcinogenic properties.<sup>1</sup> Therefore, there is a demand to develop effective treatment methods to remove PAHs from contaminated water. There are several treatment options which are typically considered for the removal of organic contaminants from wastewater that include adsorption, advanced oxidation processes (AOPs), ultrafiltration (UF), nanofiltration (NF), and reverse osmosis (RO).<sup>2,3</sup> However, most of these treatment methods use complicated equipment and are associated with high capital and operating costs, and production of secondary pollution (toxic sludge, etc.).

Membrane filtration processes, such as ultrafiltration (UF), are increasingly employed in water and wastewater treatment. The UF membrane is characterized by relatively large pore sizes, which reduces fouling and allows use of lower pressures, but does not remove small dissolved molecules like PAHs. In this context, micellar enhanced ultra filtration (MEUF) has been shown to be an effective removal technique for small molecules.<sup>4-6</sup>

In MEUF, contaminants partition to the micellar phase, followed by ultrafiltration of the solution to remove the micelles and bound contaminants.<sup>7, 4</sup> For the formation of micelles in the MEUF system, many commercially-produced surfactants have been used. MEUF enhances the

performances of ultra filtration by retaining smaller contaminants that would normally pass through conventional ultra filtration membranes. Low molecular wt. PAHs can easily pass through the ultra filtration membrane, but the same molecular size PAHs bound to micelles will remain in the retentate side.

This technique, described in detail by Dunn et al.,<sup>6</sup> makes use of the tendency for surfactants in water to spontaneously aggregate to form micelles at concentrations above the critical micelle concentration (CMC). Formation of a micelle generates several new zones into which molecules may partition, depending on the polarity of the molecule. The interior, low polarity (hydrophobic) region of the micelle can solubilize less polar molecules. In the case of an ionic surfactant, the outer charged layer will also interact strongly with oppositely charged ions or molecules with strong dipoles.

Semi Equilibrium Dialysis (SED) is a UF-based method where no pressure is applied. In the SED method using surfactants, the membrane retains the micelles and bound molecules, while allowing unbound species and free surfactant molecules to come to near-equilibrium conditions on both sides of the membrane. SED uses a separation cell and then separately examines “retentate” and “permeate” sides of the cell. “Semi-equilibrium” means it is assumed that free molecules and free surfactant molecules are at equilibrium across the membrane after 24 h, but there will not be any micelles on the permeate side. The difference between the small molecule concentrations in the permeate and retentate solutions reflects the amount that is bound to the micelles.<sup>6</sup> Partition of the PAHs between retentate and permeate side depends on the pore size of the dialysis membrane and the physicochemical properties of the PAHs.

## 5.2 Experimental

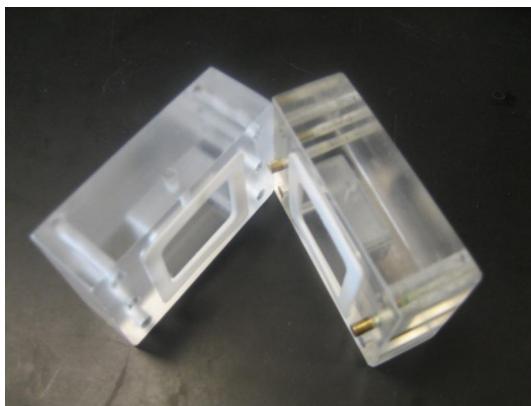
### 5.2.1 Materials and Methods

Cetyltrimethylammonium bromide (CTABr) and the PAHs naphthalene, phenanthrene, pyrene and fluorene were purchased from Sigma-Aldrich Chemicals (Oakville, ON). Deionized water was obtained from a Milli-Q system (Millipore, Etobicoke, ON). Pierce brand snakeskin dialysis tubing was purchased from Fisher Scientific (Ottawa, ON) with a molecular weight cut-off (MWCO) of 7000 Da.

A dual-monochromator, SpectraMax M2 spectrofluorometer (Molecular Devices, Sunnyvale, CA) equipped with a xenon flash lamp and 45 mm standard height cells with 1-cm path length, and 9 nm bandwidth was employed for the fluorescence measurements. SoftMax Pro 5 software was used to analyze all emission spectra and quartz fluorescence cell (28F-Q-10 (0.7 ml)) was used to take sample readings. For the conductivity measurement, a Jenway-470 conductivity meter (VWR International, Mississauga, ON) was used.

#### *Semi-equilibrium Dialysis*

Semi-equilibrium dialysis cells were produced in-house, consisting of two halves machined in methacrylate polymer, each with an internal volume of approximately 5 mL (See Figure 5.1). The two halves were separated by a dialysis membrane held in place by a Teflon gasket on either side. The dialysis membrane (MWCO 7000 Da) was cut from tubing and hydrated in deionized water for five minutes prior to use. Samples were introduced into the dialysis cell and removed for analysis via a threaded hole located in the top of each half, which was kept sealed with a stainless steel screw during the experiment.



(a)

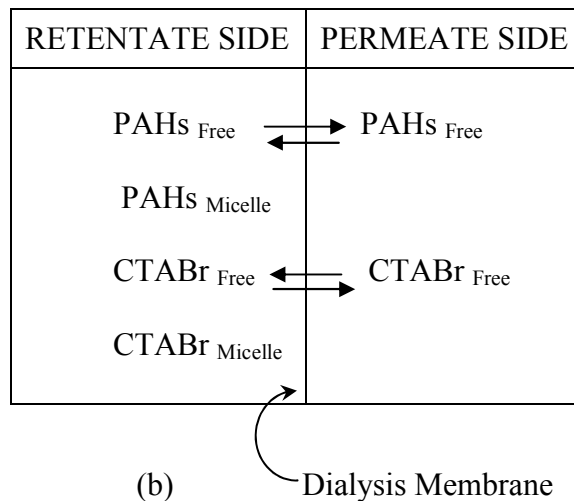


**Fig. 5.1.** (a) Semi-equilibrium dialysis cell and (b) illustration of separation behaviour across the dialysis membrane after addition of CTABr micelle/PAHs mixture to left hand side.

Stock solutions with 20 ppm PAHs were prepared by adding 0.0020 g of each PAH to a 100-ml volumetric flask and dissolving in a 50:50 ethanol-water mixture. A 20 mM stock of solution CTABr was prepared by adding 0.7289 g to a 100 ml flask and dissolving in deionized water. In the permeate side of the dialysis cell, 4.00 mL of deionized water was added, and in the retentate side, 0.10 mL of 8 ppm of PAHs solution, 1.90 mL of deionized water and 2.00 mL of the 20 mM of CTABr solution were added, resulting in a total volume of 4.00 mL on each side of the dialysis membrane. Cells were allowed to equilibrate for 24 h, at which time samples were removed from each side and analyzed using the SpectraMax M2 spectrofluorometer and Jenway-470 conductivity meter.



### 5.2.2 Spectrofluorometric measurement

Fixed excitation values of the PAHs were set up in the Spectra Max M2 spectrofluorometer for emission scans. The optimal excitation and emission wavelengths for detection of each PAH were selected as the maxima of the excitation and emission spectra (see Appendix C1). PAH concentrations in the SED experiment were measured based on separate lower range and higher range calibration curves (Table-5.1a,b). Lower range calibration was used for the permeate side samples and higher range calibration was used for the retentate side samples. Lower range and higher range calibration curves (Appendix C2) were prepared with different concentrations of each of the PAHs in 50:50 ethanol: water mixed solvent (see Table 5.1a,b).

**Table 5.1(a). Lower range calibration data of PAHs**

PAHs	Concentration range (ppb)	Slope	Intercept	R <sup>2</sup>	LOD <sup>a</sup> (ppb)
Naphthalene	0-25	0.532	0.476	0.988	3.71
Fluorene	0-25	12.76	4.84	0.999	2.55
Pyrene	0-7	8.34	3.97	0.984	1.28
Phenanthrene	0-40	0.388	0.878	0.990	5.49

**Table 5.1(b). Higher range calibration data of PAHs**

PAHs	Concentration range (ppb)	Slope	Intercept	R <sup>2</sup>	LOD <sup>a</sup> (ppb)
Naphthalene	0-300	0.412	4.08	0.995	28.8
Fluorene	0-400	9.29	106	0.997	30.0
Pyrene	0-500	5.39	79.4	0.997	31.7
Phenanthrene	0-400	0.306	3.17	0.998	22.3

LOD<sup>a</sup> = Limit of detection

2.00 mL was taken from both the retentate and permeate sides and added to 2.00 mL of 100% ethanol in order to keep the PAHs dissolved in the solution. The standard PAH solutions were

prepared in the same (50:50) ethanol-water mixture. Three spectrofluorometric measurements were done for each of three SED replicate solutions.

### 5.2.3 Conductivity measurement

We measured the conductivity of solutions with varying amounts of CTABr added, as shown in Fig.5.2. PAH stock solutions were in 50:50 ethanol-water mixtures, and dilution into the SED cell resulted in 1.25% of ethanol in the SED experiment. Therefore standard solutions and SED solutions for conductivity measurement were all prepared with 1.25% ethanol. 1.00 mL samples collected from the SED cell were too small for conductivity measurement, so they were diluted with 3.00 mL of 1.25% ethanol and conductivity measured to determine the CTABr concentration.

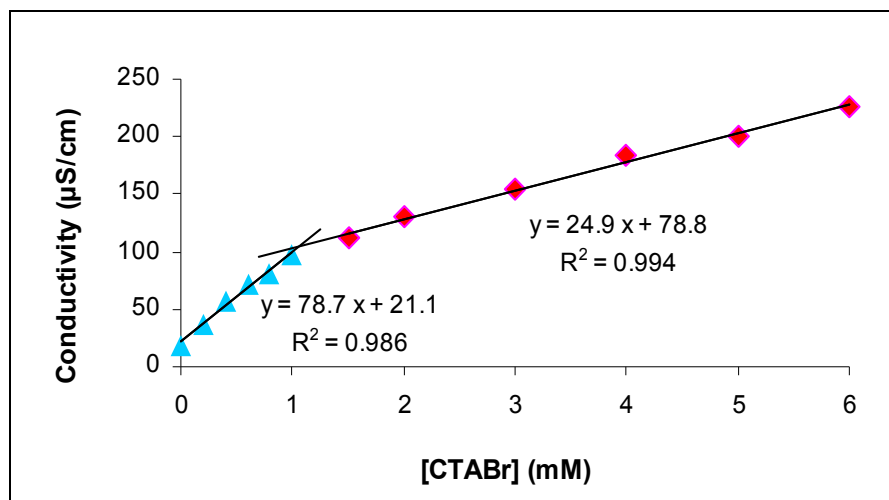


**Fig. 5.2.** Determination of critical micelle concentration (CMC) of CTABr in 1.25% ethanol by identifying the concentration where discontinuity of the two conductivity plot between lower and higher concentration range calibration curve was observed. The measured CMC value of CTABr is 1.1 mM.

### 5.2.4 Characterizing SED method

Samples were withdrawn from the permeate side of the SED cell at regular intervals and conductivity measured to determine CTABr concentration in the permeate. Experimental procedures remained same as discussed before. 4.00 mL solution were collected from the permeate side after 2 h, 4 h, 6 h, 8 h, 12 h, 18 h and 24 h and conductivity measured. The concentration of the CTABr was determined using the low concentration calibration function (see Fig. 5.2). A plot of CTABr concentration vs. time (Fig. 5.3) shows that free surfactant concentration was below the CMC level at 24 h, and no micelles were detected on the permeate side. These results confirm that the conditions for semi-equilibrium were achieved in these experiments.

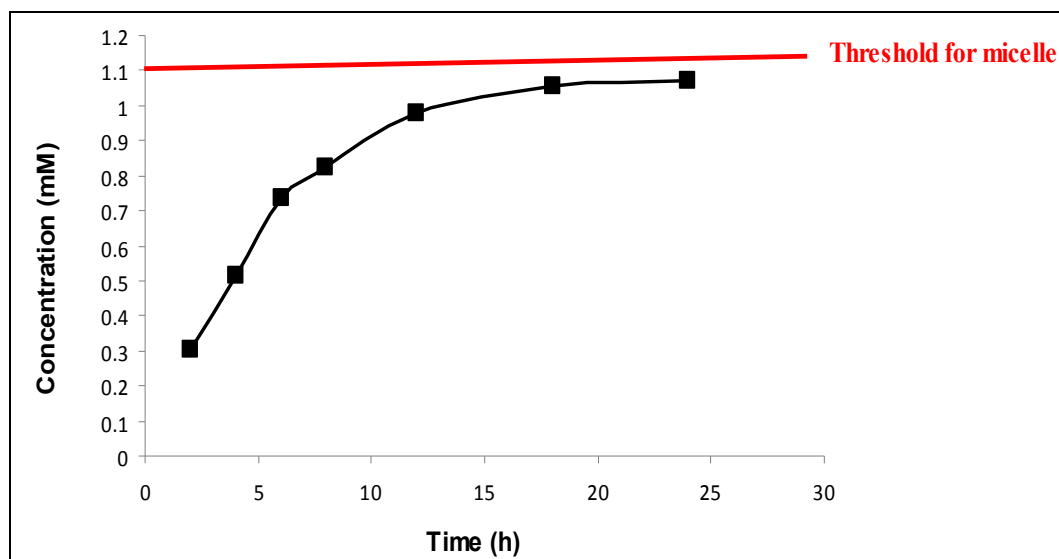


**Fig. 5.3.** Equilibrium experiment of CTABr in SED  
(Free CTABr molecules are in equilibrium at 24 h)

## 5.3 Results and discussion

### 5.3.1 Surfactant concentration, CMC and PAHs concentration

Fig 5.2 was used to determine the critical micelle concentration (CMC) of CTABr by identifying the concentration where a discontinuity in the conductivity plot was observed. The measured CMC value of 1.1 mM (Fig. 5.2) is in good agreement with the previously reported value of 0.93 mM.<sup>8</sup> The CMC value is a little bit higher than the previously reported values as we added organic solvent (1.25% ethanol) was added into the surfactant solution in order to maintain same matrix solution as the SED experiment (Table 5.2a-d). Fig.5.2 also provided calibration curves which were used to determine CTABr concentrations in the SED experiments (Table 5.2a-d). The results show that the concentration of the CTABr in the retentate side is higher than the CMC, confirming the presence of micelles on the retentate side. However, the measured permeate side concentrations are slightly higher than the CMC value that theoretically indicating the presence of micelles in the permeate side. The equilibrium experiment (Fig.5.3) suggested that there were no micelles in the permeate side after the SED experiment at 24 h. The higher numbers in Table 5.2 might be caused by error in dilution factors and instrumental error.

**Table 5.2 (a). Analysis of fluorene by spectrofluorometry and CTABr using conductivity in SED experiments at 24 h.**

Fluorene	Fluorene concentration		CTABr concentration	
	Retentate side	Permeate side	Retentate side	Permeate side
	(mole/L)	(mole/L)	(mole/L)	(mole/L)
Trial-1	$9.76 \times 10^{-7}$	$1.12 \times 10^{-8}$	0.0115	0.00158
	$9.84 \times 10^{-7}$	$1.15 \times 10^{-8}$	0.0115	0.00158
	$9.86 \times 10^{-7}$	$1.02 \times 10^{-8}$	0.0115	0.00158
Trial-2	$6.38 \times 10^{-7}$	$9.45 \times 10^{-9}$	0.0113	0.00164
	$6.51 \times 10^{-7}$	$9.80 \times 10^{-9}$	0.0113	0.00164
	$6.84 \times 10^{-7}$	$9.81 \times 10^{-9}$	0.0113	0.00164
Trial-3	$8.90 \times 10^{-7}$	$1.01 \times 10^{-8}$	0.0118	0.00161
	$8.89 \times 10^{-7}$	$1.04 \times 10^{-8}$	0.0118	0.00161
	$8.92 \times 10^{-7}$	$1.10 \times 10^{-8}$	0.0118	0.00161

**Table 5.2(b). Analysis of pyrene by spectrofluorometry and CTABr using conductivity in SED experiments at 24 h.**

Pyrene	Pyrene concentration		CTABr concentration	
	Retentate side	Permeate side	Retentate side	Permeate side
	(mole/L)	(mole/L)	(mole/L)	(mole/L)
Trial-1	$8.87 \times 10^{-7}$	$1.54 \times 10^{-9}$	0.0103	0.00147
	$8.22 \times 10^{-7}$	$1.41 \times 10^{-9}$	0.0103	0.00147
	$8.86 \times 10^{-7}$	$1.99 \times 10^{-9}$	0.0103	0.00147
Trial-2	$8.72 \times 10^{-7}$	$2.54 \times 10^{-9}$	0.0112	0.00165
	$8.83 \times 10^{-7}$	$2.40 \times 10^{-9}$	0.0112	0.00165
	$8.80 \times 10^{-7}$	$2.81 \times 10^{-9}$	0.0112	0.00165
Trial-3	$9.13 \times 10^{-7}$	$2.27 \times 10^{-9}$	0.0115	0.00168
	$9.51 \times 10^{-7}$	$2.52 \times 10^{-9}$	0.0115	0.00168
	$9.21 \times 10^{-7}$	$2.67 \times 10^{-9}$	0.0115	0.00168

**Table 5.2(c). Analysis of naphthalene by spectrofluorometry and CTABr using conductivity in SED experiments at 24 h.**

Naphthalene	Naphthalene concentration		CTABr concentration	
	Retentate side	Permeate side	Retentate side	Permeate side
	(mole/L)	(mole/L)	(mole/L)	(mole/L)
Trial-1	$5.57 \times 10^{-7}$	$2.34 \times 10^{-7}$	0.0112	0.00164
	$6.08 \times 10^{-7}$	$2.17 \times 10^{-7}$	0.0112	0.00164
	$5.62 \times 10^{-7}$	$2.31 \times 10^{-7}$	0.0126	0.00164
Trial-2	$3.55 \times 10^{-7}$	$1.91 \times 10^{-7}$	0.0126	0.00188
	$3.76 \times 10^{-7}$	$1.83 \times 10^{-7}$	0.0126	0.00188
	$4.07 \times 10^{-7}$	$1.82 \times 10^{-7}$	0.0122	0.00188
Trial-3	$6.29 \times 10^{-7}$	$2.08 \times 10^{-7}$	0.0122	0.00166
	$7.03 \times 10^{-7}$	$2.04 \times 10^{-7}$	0.0122	0.00166
	$6.42 \times 10^{-6}$	$2.13 \times 10^{-7}$	0.0122	0.00166

**Table 5.2 (d). Analysis of phenanthrene by spectrofluorometry and CTABr using conductivity in SED experiments at 24 h.**

Phenanthrene	Phenanthrene concentration		CTABr concentration	
	Retentate side	Permeate side	Retentate side	Permeate side
	(mole/L)	(mole/L)	(mole/L)	(mole/L)
Trial-1	$8.74 \times 10^{-7}$	$1.06 \times 10^{-7}$	0.0112	0.00161
	$9.10 \times 10^{-7}$	$1.00 \times 10^{-7}$	0.0112	0.00161
	$9.05 \times 10^{-7}$	$9.81 \times 10^{-8}$	0.0112	0.00161
Trial-2	$9.95 \times 10^{-7}$	$1.13 \times 10^{-7}$	0.0126	0.00188
	$9.80 \times 10^{-7}$	$1.21 \times 10^{-7}$	0.0126	0.00188
	$1.00 \times 10^{-6}$	$1.14 \times 10^{-7}$	0.0126	0.00188
Trial-3	$8.20 \times 10^{-7}$	$9.70 \times 10^{-8}$	0.0124	0.00187
	$8.19 \times 10^{-7}$	$9.86 \times 10^{-8}$	0.0124	0.00187
	$8.36 \times 10^{-7}$	$1.01 \times 10^{-7}$	0.0124	0.00187

The PAH concentrations were also measured (Table 5.2 a-d) by spectrofluorometry for all solutions. A mass balance calculation shows that, of the total PAH added to the SED cell, 48% naphthalene, 90% phenanthrene, 91% pyrene and 71% fluorene are detected in either the retentate or permeate solution after 24 h. PAH, which are known to have low solubility, might be lost by adsorption to the membrane or walls of the SED cell, or by precipitation during the 24 h SED experiment.

### 5.3.2 Determination of MDL and LOQ

Method detection limits were statistically determined as the minimum concentration of a PAH that gave a signal greater than the 99% confidence level of a blank sample. These were determined from analysis of nine replicate samples containing a known, low level concentrations of the analytes. MDL was determined by multiplying the sample standard deviation of the 9 replicates by the 99% t-value with eight degrees of freedom, which is 2.896, and determining the concentration that would give this signal. Limit of quantitation (LOQ) was determined for the signal that is 10 times the standard deviation of the replicates.

**Table 5.3. Method detection limit**

PAHs	Average Permeate Concentration (M)	MDL (M)	LOQ (M)	S/N
Naphthalene	$2.07 \times 10^{-7} \pm 1.9 \times 10^{-8}$	$5.55 \times 10^{-8}$	$1.92 \times 10^{-7}$	10.8
Fluorene	$1.04 \times 10^{-8} \pm 7.1 \times 10^{-10}$	$2.06 \times 10^{-9}$	$7.12 \times 10^{-9}$	14.6
Phenanthrene	$1.05 \times 10^{-7} \pm 8.6 \times 10^{-9}$	$2.48 \times 10^{-8}$	$8.57 \times 10^{-8}$	12.3
Pyrene	$2.24 \times 10^{-9} \pm 4.9 \times 10^{-10}$	$1.43 \times 10^{-9}$	$4.93 \times 10^{-9}$	4.54

Results found from the spectrofluorometric analysis (Table 5.2) were all above the method detection limits (Table 5.3). Pyrene was the only analyte with some results below the LOQ value, indicating a larger expected error in pyrene measurements. It was noted that the calculated Log  $K_B$  value for Pyrene (Table 5.4) did have a larger error than two of the other PAHs.

### **5.3.3 Determination of the binding constant of PAHs**

The SED method was used to determine binding constants for the four PAHs, with Log  $K_B$  results listed in Table 5.4. PAHs and CTABr concentrations were measured in the retentate and permeate compartments at 24 h after the SED was started. CTABr retentate concentrations were also used in the calculation. The calculations used the parameters defined in Equation 8, as derived from a simple partition binding model in Equation 1.

To determine binding constants using SED, the concentrations of PAHs and CTABr in both permeate and retentate were analyzed after 24 h of equilibration time and use in Equation 8. Table 5.2 shows the concentration difference between the permeate and retentate for both the PAHs and CTABr, indicating that the micellar phase was unable to pass through the membrane. The concentration of CTABr in the permeate was approximately equal to the CMC of the surfactant, with only small variations due to the presence of the PAH in solution. The concentration of CTABr in the retentate was approximately an order of magnitude higher than that in the permeate, and was consistent between replicates for different PAH.

An equation relating the results in Table 5.2 to  $K_B$  is derived according to:

$$K_B = \frac{[PAH]_M}{[PAH]_A} \quad (5.1)$$

Where,  $K_B$  is the binding constant or equilibrium partition constant,  $[PAH]_A$  is the concentration of free PAH in aqueous solution, and  $[PAH]_M$  is the concentration of PAH within the volume of the micelles. This latter term can be further defined by:

$$[PAH]_M = \frac{n_{PAH,M}}{Vol_M} \quad (5.2)$$

Where  $n_{PAH,M}$  is the number of PAH molecules associated with micelles and  $Vol_M$  is the volume of the micelle phase. The volume of the micelle phase can be approximated by:

$$Vol_M = n_{CTABr,M} \times M_V \quad (5.3)$$

Where  $n_{CTABr,M}$  is the number of CTABr surfactant molecules that are in micelle form and  $M_V$  is the molar volume of CTABr, with a reported<sup>9</sup> value of  $3.64 \times 10^{-1} \text{ L/mol}$ . These can be substituted into the equation for  $K_B$ :

$$K_B = \frac{n_{PAH,M}}{[PAH]_A \times n_{CTABr,M} \times M_V} \quad (5.4)$$

Under the assumptions for SED,  $[PAH]_A$  is the same in the retentate and permeate solutions and is simply  $[PAH]_{\text{Permeate}}$ , which is measured directly. To get  $n_{PAH,M}$ , it is assumed that the concentration of PAH in the retentate ( $[PAH]_{\text{Retentate}}$ ) is the total of the aqueous and micelle-bound concentrations, so the micelle-bound concentration is:

$[PAH]_{\text{Retentate}} - [PAH]_{\text{Permeate}}$  and:

$$n_{PAH,M} = \{[PAH]_{\text{Retentate}} - [PAH]_{\text{Permeate}}\} \times V_{\text{retentate}} \quad (5.5)$$

For the value of  $n_{CTABr,M}$ , it is assumed that all CTABr above CMC on the retentate side is in micelle form, and therefore:

$$n_{CTABr,M} = \{[CTABr]_{\text{Retentate}} - CMC\} \times V_{\text{Retentate}} \quad (5.6)$$

Substituting 5 and 6 into 4 gives:

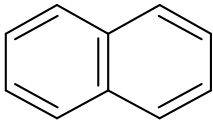
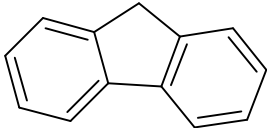
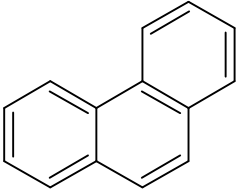
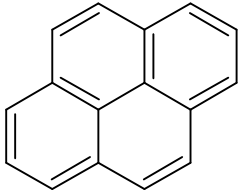
$$K_B = \frac{\{[PAH]_{\text{Retentate}} - [PAH]_{\text{Permeate}}\} \times V_{\text{Retentate}}}{[PAH]_{\text{Permeate}} \times \{[CTABr]_{\text{Retentate}} - CMC\} \times V_{\text{Retentate}} \times M_V} \quad (5.7)$$

Which simplifies to a final working equation for calculating  $K_B$ :

$$K_B = \frac{\{[PAH]_{\text{Retentate}} - [PAH]_{\text{Permeate}}\}}{[PAH]_{\text{Permeate}} \times \{[CTABr]_{\text{Retentate}} - CMC\} \times M_V} \quad (5.8)$$



**Table 5.4. Binding constant between PAH and CTABr determined by SED analysis**

<b>PAHs</b>	<b>Structure</b>	<b>Log <math>K_{OW}</math><sup>10</sup></b>	<b>Calculated Log <math>K_B</math></b>
Naphthalene		3.36	$2.61 \pm 0.15$
Fluorene		4.12	$4.36 \pm 0.05$
Phenanthrene		4.57	$3.31 \pm 0.04$
Pyrene		5.18	$5.07 \pm 0.12$

The Log  $K_B$  values determined through SED demonstrate a positive relationship with Log  $K_{OW}$  of the PAHs. A free energy relationship can be plotted to support that Log  $K_B$  values may be estimated for additional molecules where Log  $K_{OW}$  is known.

The use of  $K_{OW}$  as a model parameter for describing the binding forces between small hydrophobic molecules and macromolecules or hydrophobic phases has already been established.<sup>11</sup> Correlation of the binding constants with the Log  $K_{OW}$  constants is shown in Fig. 5.4.

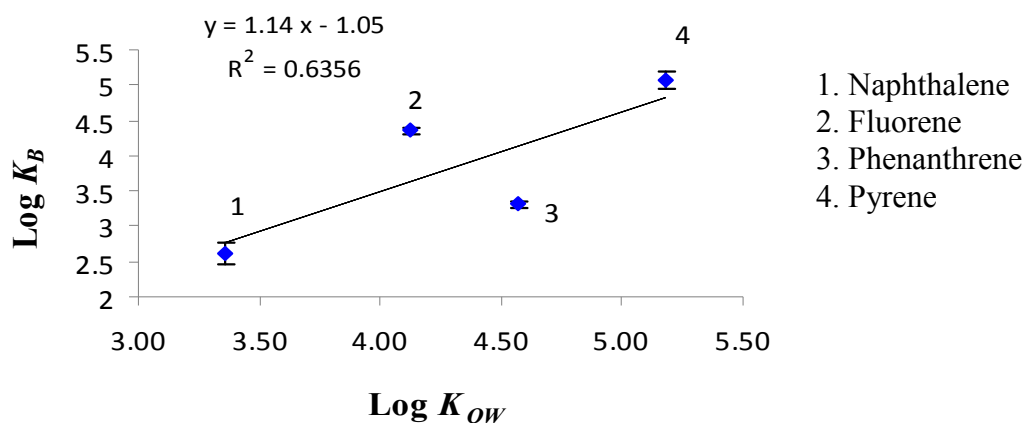


**Fig. 5.4.** Binding correlation of PAHs with Log  $K_{OW}$ .

The binding constants from SED analysis indicate the affinity of the individual PAH compounds for CTABr micelles. The  $K_B$  calculation uses measured concentrations after 24 h and should be independent of mass balance results. The results show that the concentrations of the PAHs in the retentate side are much higher than in the permeate side. After 24 h in the SED cell, approximately 72% naphthalene, 90% phenanthrene, 99.7% pyrene and 98.8% fluorene remained in the retentate side. This supports the idea that PAH can be removed from contaminated water by MEUF. Real wastewater samples have a mixture of PAH and other organic compounds, but the mixture is unlikely to affect micelle binding as the PAH concentrations used here result in 1% of the micelles being bound with PAH molecules (calculation not shown).

Pyrene shows stronger binding and has a higher Log  $K_{OW}$  value compared with fluorene, naphthalene and phenanthrene. This indicates that compounds with more hydrophobic character are expected to have strong binding affinity. However, fluorene and phenanthrene do not support a strong correlation with Log  $K_{OW}$ . Results indicate that fluorene has relatively higher binding to micelles than phenanthrene, even though phenanthrene has more hydrophobic character (higher Log  $K_{OW}$ ) than fluorene. Normally, PAH with a higher  $K_{OW}$  would be expected to bind more

strongly with micelles. A study of micellar electrokinetic chromatography (MEKC) using charged and neutral surfactants reported migration times for six PAHs, including fluorene and phenanthrene, and all eluted in order of their relative  $K_{OW}$  values.<sup>12</sup> Another MEKC study using SDS micelles measured capacity factors, which are proportional to binding constants, for a number of PAHs and other hydrophobic compounds.<sup>13</sup> The capacity factors for fluorene and phenanthrene also matched their relative  $K_{OW}$  values. Interestingly, in this work, some pairs of compounds had relative capacity factors that did not match the  $K_{OW}$  order, indicating that under some conditions the micelle binding might not match the order predicted by  $K_{OW}$ . Similar results are reported by Palmer and Terabe.<sup>14</sup> A study using SDS and CTABr micelles in micellar liquid chromatography with various water/solvent mixtures measured capacity factors and calculated binding constants and also reported larger binding constants for phenanthrene than fluorene for both systems.<sup>15</sup>

Another micellar liquid chromatography study using CTABr and various water/alcohol mixtures was conducted by Ramos-Lledo et al.<sup>16</sup> This work showed that while phenanthrene had a higher binding constant than fluorene under most conditions, some combinations of ethanol: water or propanol: water actually showed stronger binding of fluorene than phenanthrene. This at least confirms the possibility that these compounds can have micelle interactions under some conditions that do not follow the order predicted by their  $K_{OW}$  values. Therefore, additional studies are needed to explain this result in this work. Other physiochemical parameters such as surfactant structure, aggregation number, micelle geometry, ionic strength, temperature, and the size and shape of the PAH might be contributing factors to the  $K_B$  trend being different than the  $K_{OW}$  trend.<sup>17</sup>

#### ***5.3.4 Statistical analysis of the variances of binding constant***

Statistical analysis of the variances was done in order to determine whether two different approaches of the experimental design produce variances that are statistically different. Experiments included testing three replicates of the three different trials (3x3–replicates). But, results were also treated as 9 independent replicates (9x1). The comparison was used to determine if the variance in results came mainly from preparing multiple experiments or from doing multiple fluorescence measurements of each trial. The F-test in a one-way analysis of variance was used to assess whether the results grouped by trial (eliminating variability due to multiple fluorescence measurements) differed from results using 9 independent values (variance due to multiple fluorescence measurements included with variance from multiple trials).

***Table 5.5. Variances of the binding constant with 9 replicates***

<b>PAHS</b>	<b>Total replicate</b>	<b>Log <math>K_B</math></b>	<b>Variances (<math>S_1^2</math>)</b>
Naphthalene	9	$2.61 \pm 0.15$	0.023
Fluorene	9	$4.36 \pm 0.05$	0.0025
Phenanthrene	9	$3.31 \pm 0.04$	0.0016
Pyrene	9	$5.07 \pm 0.12$	0.0144

**Table 5.6. Variances of the binding constant with 3 replicates and compare variances between 9 replicates and 3 replicates through F test, in which  $F_{Critical} (F_{0.05,(8)(2)})$  value is 19.37. ( $S_1^2$  values collected from table 5.5 )**

PAHs	Trial	Replicates	Log $K_B$	Variances ( $S_2^2$ )	$F_{expt}$ = $(S_1^2/S_2^2)$
Naphthalene	Trial-1	3	$2.64 \pm 0.06$	0.0036	6.39
	Trial-2	3	$2.42 \pm 0.07$	0.0049	4.69
	Trial-3	3	$2.75 \pm 0.04$	0.0016	14.4
Fluorene	Trial-1	3	$4.41 \pm 0.03$	0.0009	2.78
	Trial-2	3	$4.30 \pm 0.01$	0.0001	25.0
	Trial-3	3	$4.38 \pm 0.02$	0.00032	7.81
Phenanthrene	Trial-1	3	$3.35 \pm 0.03$	0.0009	1.78
	Trial-2	3	$3.29 \pm 0.02$	0.0004	4.00
	Trial-3	3	$3.28 \pm 0.01$	0.0001	16.0
Pyrene	Trial-1	3	$5.17 \pm 0.07$	0.0049	2.94
	Trial-2	3	$4.94 \pm 0.03$	0.0009	16.0
	Trial-3	3	$4.97 \pm 0.03$	0.0009	16.0

Table 5.6 shows the error in binding constants due to the variable fluorescence results of triplicate samples collected from each trial. At the 95% confidence level, all of the F experimental values are less than F-critical (19.37) (see Table 5.6). The variances of the binding constant determined from 9 replicates are not significantly different from the variances of binding constants determined from 3 trials. This indicates that replicate fluorescence measurements have relatively high precision, and a single fluorescence measurement of each triplicate trial would provide the same final result. Most of the error in Log  $K_B$  came from differences between SED trials, which can include variations in surfactant concentration (micelle formation), time for equilibrium distribution of the dissolved PAHs in the SED cell, dilution factors, temperature, and solution pH. It is not recommended to do single trials with 3 fluorescence replicates.

## 5.4 Conclusions

The binding constants between various PAHs and CTABr were obtained using semi-equilibrium dialysis. This illustrated the potential for MEUF to remove these contaminants from water. The correlation between  $\text{Log } K_B$  (in CTABr) and  $\text{Log } K_{OW}$  indicates a strong tendency for PAHs with a more hydrophobic character to have a greater affinity for binding with CTABr micelles. It generally supports the idea that  $\text{Log } K_B$  values may be estimated for additional molecules where  $\text{Log } K_{OW}$  is known, but hydrophobic character only does not explain the binding potential of each PAH molecule, rather binding must also depend on other physiochemical properties of the compounds.

## 5.5 References

1. Maila, M. P.; Cloete, T. E. *Int. Biodeter.Biodegr.* **2002**, *50*(2), 107-113.
2. Bolong, N.; Ismail, A. F.; Salim, M. R.; Matsuura, T. *Desalination*, **2009**, *239*, 229–246.
3. Rossnera, A.; Snyderb, S. A.; Knappec, D. R.U. *Water Research*, **2009**, *43*, 3787–3796.
4. Zeng, G. M.; Xu, K.; Huang, J. H.; Li, X.; Fang, Y. Y.; Qu, Y. H. *J. Membrane Sci.* **2008**, *310*, 149-160.
5. Purkait, M. K.; DasGupta, S.; De, S. *Sep. Purif. Technol.* **2004**, *37* (1), 81-92.
6. Dunn, R. O.; Scamehorn, J. F.; Christian, S. D. *Sep. Sci. Technol.* **1985**, *20* (4), 257-284.
7. Baek, K.; Yang, J. W. *Chemosphere*, **2004**, *57* (9), 1091-1097.
8. Cifuentes, A.; Bernal, J. L. ; Diez-Masa, J. C. *Anal. Chem.* **1997**, *69*, 4271-4274.
9. Vautier-Giongo, C.; Bales, B. L. *J. Phys. Chem. B* **2003**, *107*(23), 5398-5403.
10. Kayal, S. I.; Connell, D. W. *Aust. J. Mar. Freshwater Res.* **1990**, *41*, 443-56.
11. Leo, A.; Hansch, C. *J. Org. Chem.* **1971**, *36*(11), 1539-1544.
12. do Rosario, P. M. A.; Nogueira, J. M. F. *Electrophoresis*, **2006**, *27*, 4694–4702.

13. Garcia, M. A.; Diez-Masa, J. C.; Marina, M. L. *J. Chromatogr. A*, **1996**, *742*, 251-256.
14. Palmer, C. P.; Terabe, S. *Anal. Chem.* **1997**, *69*, 1852-1860.
15. Rodriguez Delgado, M. A.; Sanchez, M. J.; Gonzalez, V.; Montelongo, F. G. *Chromatographia*, **1994**, *38(5/6)*, 342-348.
16. Ramos-Lledó, P.; San Andrés, M. P. Vera, S. *J. Chromatogr. Sci.* **1999**, *37*, 429-435.
17. Shamsi, S. A.; Akbay, C.; Warner, I. M. *Analytical Chemistry*, **1998**, *70(14)*, 3078-3083.

## Chapter 6

### Determining binding of polycyclic aromatic hydrocarbons to micelles formed by SDS and SOL using semi-equilibrium dialysis

#### 6.1 Introduction

Polycyclic aromatic hydrocarbons (PAHs) are widely distributed in the environment as a result of the incomplete combustion of organic matter.<sup>1</sup> Many PAHs and their epoxides are highly toxic, mutagenic and/or carcinogenic<sup>2</sup> to microorganisms as well as to humans. PAHs are neutral aromatic compounds and their octanol-water partition coefficients ( $K_{OW}$ ) are relatively high, indicating a relatively high potential for adsorption to suspended particulates in air, water, and for bioconcentration in organisms.<sup>3</sup> PAHs could be discharged from the effluent of wastewater treatment plants to natural aquatic environments in dissolved form or adsorbed to flocculant particles.<sup>4</sup> PAHs found in municipal wastewater normally come from the discharge of petroleum products like petroleum fuels and lubricants, the discharge of urban storm water runoff containing PAHs from asphalt and car exhaust particles<sup>5,6</sup> and household wastes, which can account for 50–60 % of the total sewer load for pyrene and phenanthrene.<sup>7</sup> Although various treatment options are considered for the removal of organic contaminants from wastewater that include adsorption, advanced oxidation processes (AOPs), ultrafiltration (UF), nanofiltration (NF), and reverse osmosis (RO),<sup>8,9</sup> they have many limitations. Micellar enhanced ultra filtration (MEUF) has been found to be an effective removal technique for small dissolved molecules like PAHs.<sup>10-12</sup> In MEUF, contaminant partition occurs to the micellar phase, followed by ultra filtration of the solution to remove the micelles and bound contaminants.<sup>10-13</sup>



Semi-equilibrium dialysis (SED) is a micellar based ultra filtration method which has been employed for the treatment of PAHs with CTABr surfactant in the previous chapter (chapter 5). Some of the surfactant that has been added in MEUF will end up in the permeate solution, where it might cause secondary pollution to the environment. Considering the potential fate of the surfactants, anionic surfactants are preferred for MEUF as they generally have lower toxicity and are more biodegradable.<sup>14</sup> In Ch. 5 it was shown that PAHs were strongly bound with CTABr cationic micelles due to hydrophobic interactions, rather than through charge-charge interactions as noted for the negatively charged sulfonamides in Ch. 3 and 4. Since surfactant charge is not important, it can be assumed that anionic surfactants can also bind with PAH. Sodium dodecyl sulfate (SDS) is an anionic surfactant that has been used for the extraction of PAH and other oil components from soil and other matrices.<sup>15</sup> SDS has also been used in a number of MEUF and related studies,<sup>16</sup> while other sulfonate surfactants have been used specifically with PAH.<sup>17</sup>

Another promising option might be useful for using switchable surfactant to reuse or minimize secondary pollutants generated from the MEUF method. The switchable surfactants are molecules that can be reversibly converted between surface active and inactive forms by application of triggers.<sup>18</sup> Switchable surfactants are very useful for extracting a hydrophobic or hydrophilic substance from a mixture when in the “on” (usually charged) state, and then can be switched "off " to help recover the extracted substance and surfactant, for example if they precipitate.<sup>19</sup> Switchable surfactants of many designs have been published since the mid-1980s.<sup>20</sup> The designs differ primarily in the kind of trigger used for switching. CO<sub>2</sub> is one of the preferred triggers used for switching, with advantages over other triggers (photo-switching, addition of

acids or oxidants), as it is inexpensive, nonhazardous, non-accumulating in the system, and it can easily be removed.<sup>21</sup>

CO<sub>2</sub> bubbled into water can re-protonate anionic surfactants such as soaps (sodium alkanoates).<sup>22</sup> It was reported that the switching of anionic surfactants such as long-tail carboxylates and phenolates is fully reversible with only CO<sub>2</sub> addition and CO<sub>2</sub> removal.<sup>21</sup> Recyclable CO<sub>2</sub>-triggered switchable cationic surfactants were also reported by Jessop and co-workers.<sup>18, 23</sup>

Sodium laurate (SOL), a commercially available alkanoate switchable surfactant, was chosen for this research project. This research is solely focused on determining binding of PAH in SOL micelles with SOL in the “on” (anionic) state, and does not deal with switching. The binding constants of PAHs with both SDS and SOL micelles are examined. We also extended our research to develop a correlation between the binding constants and the octanol-water partition constants for the estimation of binding constants of other PAH. In this research work, SDS and SOL binding with PAH were studied using semi-equilibrium dialysis (SED), where the dialysis membranes retained the micelles and associated PAH molecules, while allowing free surfactant monomers and unbound PAH to come to near-equilibrium distribution on both sides of the membrane. The difference between the total PAH concentration in the retentate and permeate solutions reflects the amount that is bound to the micelles.<sup>12</sup>

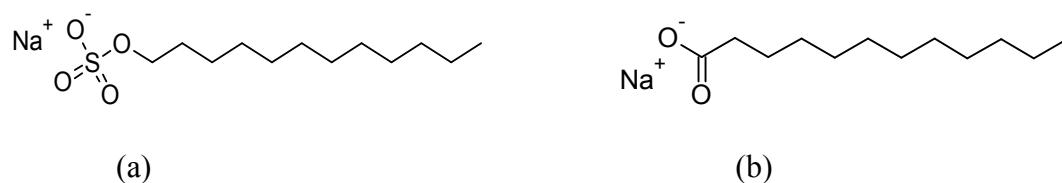


**Fig.6.1.** Chemical structure of (a) Sodium dodecyl sulphate (SDS); and (b) Sodium laurate (SOL).

## 6.2 Experiment

### 6.2.1 Materials and Method

SDS, SOL and the PAHs naphthalene, phenanthrene, pyrene and fluorene were purchased from Sigma-Aldrich Chemicals (Oakville, ON). Deionized water was obtained from a Milli-Q system (Millipore, Etobicoke, ON). Pierce brand snakeskin dialysis tubing was purchased from Fisher Scientific (Ottawa, ON) with a molecular weight cut-off (MWCO) of 7000 Da.

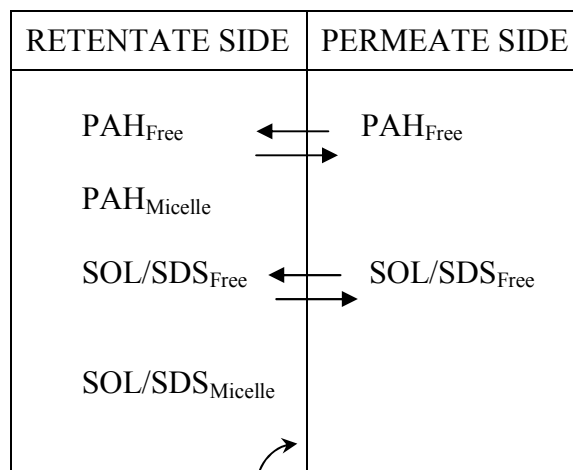
A dual-monochromator, SpectraMax M2 spectrofluorometer (Molecular Devices, Sunnyvale, CA) equipped with a xenon flash lamp and 45 mm standard height cells with 1-cm path length, and 9 nm bandwidth was employed for the fluorescence measurements. SoftMax Pro 5 software was used to analyze all emission spectra and quartz fluorescence cell (28F-Q-10 (0.7 ml)) was used to take sample readings. For the conductivity measurements, a Jenway-470 conductivity meter (VWR International, Mississauga, ON) was used.

#### *Semi-equilibrium Dialysis.*

Semi-equilibrium dialysis cells were made in-house, consisting of two halves machined in methacrylate polymer, each with an internal volume of approximately 5 mL (See Fig. 6.2). The two halves were separated by a dialysis membrane held in place by a Teflon gasket on either side. The dialysis membrane (MWCO 7000 Da) was cut from tubing and hydrated in deionized water for five minutes prior to use. Samples were introduced into the dialysis cell and removed for analysis via a threaded hole located in the top of each half, which was kept sealed with a stainless steel screw during the experiment.



(a)



(b) Dialysis Membrane

**Fig. 6.2.** (a) Semi-equilibrium dialysis cell and (b) illustration of separation behaviour across the dialysis membrane after addition of SDS micelle/PAH mixture or SOL micelle/PAH mixture (in a separate experiment) to the left hand side.

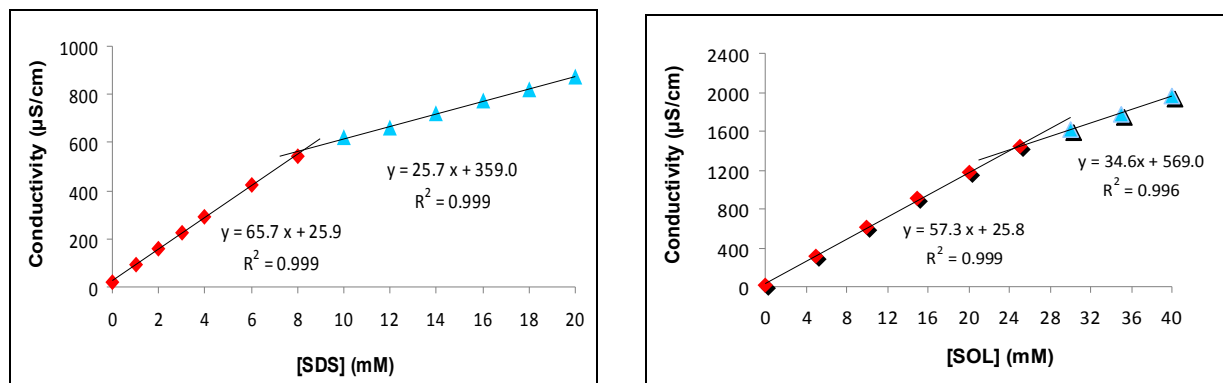
Stock solutions with 20 ppm PAH were prepared by adding 0.0020 g of each PAH to a 100-mL volumetric flask and dissolving in a 50:50 ethanol-water mixture. A 40 mM SDS and 100 mM SOL stock solution were prepared by dissolving 1.154 g of SDS and 2.223 g of SOL in a 100-mL volumetric flask with deionized water. In the permeate side of the SED cell, 4.00 mL of deionized water was added, and in the retentate side, 0.10 mL of 8 ppm of PAHs solution, 1.90 mL of deionized water and 2.00 mL of the 40 mM SDS solution were added, resulting in a total volume of 4.0 mL on each side of the dialysis membrane. In the SOL experiment, 2.00 mL of 100 mM of SOL solution was added in the retentate side in place of the SDS. Cells were allowed to equilibrate for 24 h for SDS analysis while cells were allowed to equilibrate for 12 h for SOL analysis, at which point samples were removed from each side and analyzed by spectrofluorometry and conductivity.

### ***6.2.2 Spectrofluorometric measurement***

Fixed excitation values of the PAHs were set up in the Spectra Max M2 spectrofluorometer for emission scans. The optimal excitation and emission wavelengths for detection of each PAH were selected as the maxima of the excitation and emission spectra (see Appendix C1). PAH concentrations in the SED experiment were measured based on separate lower range and higher range calibration curves. Lower range calibration was used for the permeate side samples and higher range calibration was used for the retentate side samples. Lower range and higher range calibration curves (Appendix C2) were prepared with different concentrations of each of the PAHs in 50:50 ethanol: water mixed solvent. The concentration range and other calibration parameters of the different PAHs were the same as described in chapter 5 (Table 5.1 a,b). 2.00 mL was taken from both the retentate and permeate sides and added to 2.00 mL of 100% ethanol in order to keep the PAHs dissolved in the solution. The standard PAH solutions were prepared in the same (50:50) ethanol-water mixture. Three spectrofluorometric measurements were done for each of three SED replicate solutions.

### ***6.2.3 Conductivity measurement***

The conductivity of solutions with varying concentrations of SDS and SOL were determined, with results shown in Fig. 6.3. PAH stock solutions were in 50:50 ethanol-water mixture, and dilution into the SED cell resulted in 1.25% of ethanol in the SED experiment. Therefore standard solutions and SED solutions for conductivity measurements were all prepared with 1.25% ethanol. 1.00 mL samples collected from the SED cell were too small for the conductivity measurements, so they were diluted with 3.00 ml of 1.25% ethanol and conductivity measured to determine the SDS and SOL concentration.



(a)

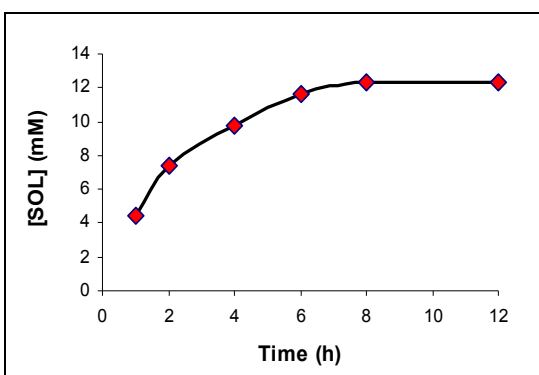
(b)

**Fig. 6.3.** Determination of critical micelle concentration (CMC) of SDS and SOL in 1.25% ethanol by identifying the concentration where discontinuity of the two conductivity plot between lower and higher concentration range calibration curve was observed. (a) The measured CMC value of SDS is 8.1 mM. (b) The measured CMC value of SOL is 23 mM.

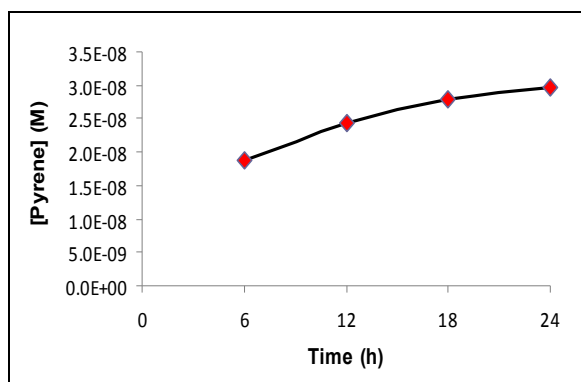
#### 6.2.4 Characterizing SED method

In separate experiments, samples were withdrawn from the permeate side of the SED cell at regular intervals and conductivity was measured to determine SOL concentration in the permeate. Experimental procedures remained same as discussed before. A 4.00 mL sample was collected from the permeate side after 1 h, 2 h, 4 h, 6 h, 8 h and 12 h and measured conductivity. It is required to conduct SED experiment in a condition where retentate side concentration of the surfactant should be more than half of the surfactant concentration initially added in order to form micelle. Upper limit of surfactant depends on solubility. A 100 mM standard stock SOL solution was prepared. It is difficult to prepare higher than 100 mM SOL in solution due to SOL precipitation. The retentate side concentration of the SOL was close to the CMC value after 18-24 h, therefore, PAHs experiments in SOL were conducted at 12 h, and SOL equilibrium measurements were recorded up to 12 h instead of 24 h.

After each conductivity measurement, the solution was returned to the cell. The concentration of the SOL was determined using the low concentration calibration function (see Fig. 6.3(b)). A plot of SOL concentration vs. time (Fig. 6.4 (a)) shows that free surfactant concentration was well below the CMC level at 12 h, and no micelles were detected on the permeate side. Fig. 6.4(a) shows that SOL surfactant reached equilibrium by 12 h. In separate experiments, small samples were withdrawn from the permeate side of the SED cell at regular intervals and analyzed for PAH concentration using spectrofluorometry. The results for pyrene are shown in Fig. 6.4 (b), and confirm that the free pyrene concentrations reached equilibrium between the sides by 24 h. These results show that the conditions for semi-equilibrium were achieved in these experiments.



(a)



(b)

**Fig. 6.4.** (a) Conductivity measurement over time showing diffusion of SOL surfactant in the SED cell from the retentate to the permeate. The surfactant concentration in the permeate was well below the CMC up to 12 h. SOL concentration was measured by conductivity meter (b) Concentration of pyrene on permeate side of SED cell to confirm equilibration of free pyrene by 24 h. Pyrene concentration was determined by spectrofluorometry.

## 6.3 Results and discussion

### 6.3.1 Surfactant concentration, CMC and PAH concentrations

Fig. 6.3 was used to determine the critical micelle concentration (CMC) of SDS and SOL by identifying the concentration where a discontinuity in the conductivity plot was observed. The measured CMC value of 8.1 mM for SDS (Fig. 6.3a) is in good agreement with the previously reported value of 8.3 mM<sup>24</sup> and 23 mM for SOL (Fig. 6.3b) is in good agreement with the previously reported value of 24 mM.<sup>15</sup> Fig. 6.3 also provided calibration curves which were used to determine SDS and SOL concentrations in SED experiments (Table 6.1 ).

The results show that the concentration of the SDS and SOL in the retentate side is higher than the CMC, confirming the presence of micelles on the retentate side. In the permeate side, both of the SDS and SOL concentrations were found to be well below the CMC values. This confirms that there is no micelle in the permeate side after 24 h for SDS and 12 h for SOL. This is well supported by the equilibrium experiment shown in Fig. 6.4 a,b.

**Table 6.1(a). Analysis of PAH by spectrofluorometry and SDS using conductivity in SED experiments at 24 h.**

PAHs	Spectrofluorometric analysis		Conductivity analysis	
	Retentate side (mole/L)	Permeate side (mole/L)	Retentate side (mole/L)	Permeate side (mole/L)
Naphthalene	$4.44 \times 10^{-7}$ $\pm 8.1 \times 10^{-8}$	$1.85 \times 10^{-7}$ $\pm 7.60 \times 10^{-8}$	0.00951	0.00517
Fluorene	$7.22 \times 10^{-7}$ $\pm 6.1 \times 10^{-8}$	$3.29 \times 10^{-8}$ $\pm 4.26 \times 10^{-9}$	0.0121	0.00660
Phenanthrene	$8.58 \times 10^{-7}$ $\pm 1.3 \times 10^{-8}$	$8.81 \times 10^{-8}$ $\pm 1.2 \times 10^{-8}$	0.0124	0.00681
Pyrene	$7.81 \times 10^{-7}$ $\pm 6.7 \times 10^{-8}$	$1.56 \times 10^{-8}$ $\pm 1.7 \times 10^{-9}$	0.0124	0.00665



**Table 6.1(b). Analysis of PAH by spectrofluorometry and SOL using conductivity in SED experiments at 12 h.**

PAHs	Spectrofluorometric analysis		Conductivity analysis	
	Retentate side (mole/L)	Permeate side (mole/L)	Retentate side (mole/L)	Permeate side (mole/L)
Naphthalene	$6.13 \times 10^{-7}$ $\pm 1.40 \times 10^{-7}$	$3.66 \times 10^{-7}$ $\pm 2.1 \times 10^{-8}$	0.0357	0.0179
Fluorene	$4.20 \times 10^{-7}$ $\pm 2.2 \times 10^{-8}$	$4.14 \times 10^{-8}$ $\pm 1.9 \times 10^{-9}$	0.0351	0.0172
Phenanthrene	$5.31 \times 10^{-7}$ $\pm 4.2 \times 10^{-8}$	$1.96 \times 10^{-7}$ $\pm 2.5 \times 10^{-8}$	0.0354	0.0170
Pyrene	$4.08 \times 10^{-7}$ $\pm 5.4 \times 10^{-8}$	$2.71 \times 10^{-8}$ $\pm 8.2 \times 10^{-9}$	0.0354	0.0163

The PAHs concentrations of all solutions were also measured (Table 6.1 a,b) by spectrofluorometry. After 24 h in the SED cell with SDS micelles, approximately 71% naphthalene, 91% phenanthrene, 98% pyrene and 96% fluorene remained in the retentate side using SDS surfactant. In the SOL experiments after 12 h of equilibration, approximately 63% naphthalene, 73% phenanthrene, 94% pyrene and 91% fluorene remained in the retentate side. These results indicate that both SDS and SOL micelles bind PAH in the SED system, and binding constants can be determined. It also shows that SDS is better than SOL for the treatment of PAH especially for the naphthalene and phenanthrene. Naphthalene is not a good binding candidate for either of the surfactants, and SOL is less effective for this particular compound.

### **6.3.2 Determination of the binding constant of PAH**

The SED method was used to determine binding constants for the four PAHs, with  $\text{Log } K_B$  results listed in Table 6.2. The concentrations of PAHs and SDS as well as PAHs and SOL in both permeate and retentate were used to calculate  $K_B$  using Equation 8, which is derived as follows:

$$K_B = \frac{[PAH]_M}{[PAH]_A} \quad (6.1)$$

where,  $K_B$  is the binding constant or equilibrium constant,  $[PAH]_A$  is the concentration of free sulfonamide in aqueous solution, and  $[PAH]_M$  is the concentration of sulfonamide within the volume of the micelles. This latter term can be further defined by:

$$[PAH]_M = \frac{n_{PAH,M}}{Vol_M} \quad (6.2)$$

where  $n_{PAH,M}$  is the number of sulfonamide molecules associated with micelles and  $Vol_M$  is the volume of the micelle phase. The volume of the micelle phase can be approximated by:

$$Vol_M = n_{SDS,M} \times M_V \quad (6.3)$$

where  $n_{SDS,M}$  is the number of SDS surfactant molecules that are in micelle form and  $M_V$  is the molar volume of SDS, with a reported<sup>25</sup> value of 0.288 L/mol. These can be substituted into the equation for  $K_B$ :

$$K_B = \frac{n_{PAH,M}}{[PAH]_A \times n_{SDS,M} \times M_V} \quad (6.4)$$

Under the assumptions for SED,  $[PAH]_A$  is the same in the retentate and permeate solutions and is simply  $[PAH]_{Permeate}$ , which is measured directly. To get  $n_{PAH,M}$ , it is assumed that the concentration of Sulfonamide in the retentate ( $[PAH]_{Retentate}$ ) is the total of the aqueous and micelle-bound concentrations, so the micelle-bound concentration is  $[PAH]_{Retentate} - [PAH]_{Permeate}$  and:

$$n_{PAH,M} = \{[PAH]_{Retentate} - [PAH]_{Permeate}\} \times V_{retentate} \quad (6.5)$$

For the value of  $n_{SDS,M}$ , it is assumed that all SDS above CMC on the retentate side is in micelle form, and therefore:

$$n_{SDS,M} = \{[SDS]_{Retentate} - CMC\} \times V_{Retentate} \quad (6.6)$$

Substituting 5 and 6 into 4 gives:

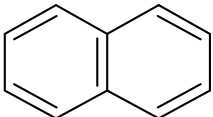
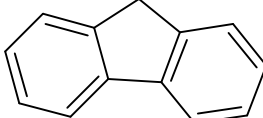
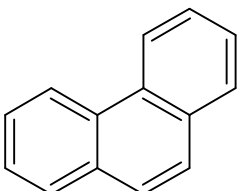
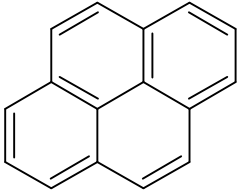
$$K_B = \frac{\{[PAH]_{Retentate} - [PAH]_{Permeate}\} \times V_{Retentate}}{[PAH]_{Permeate} \times \{[SDS]_{Retentate} - CMC\} \times V_{Retentate} \times M_V} \quad (6.7)$$

which simplifies to a final working equation for calculating  $K_B$ :

$$K_B = \frac{\{[SDS]_{Retentate} - [SDS]_{Permeate}\}}{[SDS]_{Permeate} \times \{[SDS]_{Retentate} - CMC\} \times M_V} \quad (6.8)$$

Same working equation was used for the calculation of  $K_B$  of PAH in SOL micelle.

**Table 6.2. Binding constant of PAHs in SOL and SDS**

<i>PAHs</i>	<i>Structure</i>	<i>Log K<sub>ow</sub><sup>26</sup></i>	<i>Log K<sub>B</sub></i> <i>(SDS Micelle)</i>	<i>Log K<sub>B</sub></i> <i>(SOL Micelle)</i>
Naphthalene		3.36	3.07 ± 0.26	2.11 ± 0.4
Fluorene		4.12	4.13 ± 0.06	3.36 ± 0.04
Phenanthrene		4.57	3.74 ± 0.07	2.62 ± 0.10
Pyrene		5.18	4.48 ± 0.05	3.53 ± 0.09

Since PAH concentrations in SOL were measured at 12 h, it is possible the PAH were not completely equilibrated, and the retentate concentrations may have been low. This might contributed higher  $K_B$  values, however, Fig. 6.4 (b) suggests that the concentration of pyrene at 12 h was over 80% of the equilibrium concentration. The Log  $K_B$  values determined through SED demonstrate a positive relationship with Log  $K_{OW}$  of the PAHs. This linear free energy plot

supports the idea that  $\text{Log } K_B$  values may be estimated for some additional molecules where  $\text{Log } K_{OW}$  is known.  $K_{OW}$  has been established<sup>27</sup> as a model parameter for describing the binding forces between small hydrophobic molecules and macromolecules. Correlation of the binding constants with the  $\text{Log } K_{OW}$  constants is shown in Fig. 6.5.

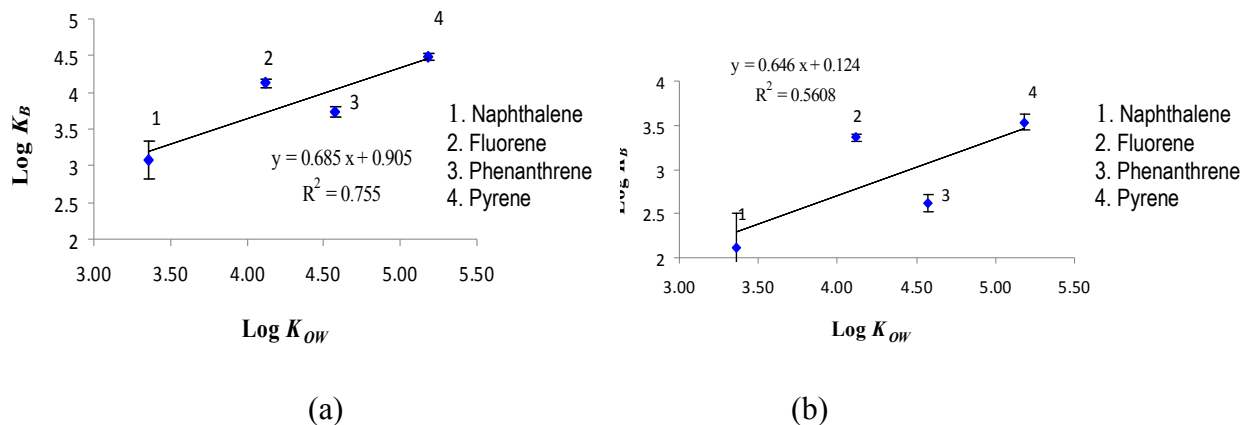


**Fig. 6.5. (a)** Binding correlation of PAHs in SDS with the  $\text{Log } K_{OW}$  **(b)** binding correlation of PAHs in SOL with  $\text{Log } K_{OW}$ .

The binding constants from SED analysis indicate the affinity of the individual PAH compounds for SDS and SOL micelles. Pyrene, with the higher  $\text{Log } K_{OW}$  value, shows stronger binding than fluorene, naphthalene and phenanthrene. This indicates that the more hydrophobic character of the compound has a strong influence on binding. However, fluorene exhibited the next highest tendency to bind to SOL and SDS micelles indicating that it possesses comparatively greater potential for removal *via* MEUF than other PAHs.

Results indicate that fluorene has relatively higher binding to micelles than phenanthrene, even though phenanthrene has more hydrophobic character (higher  $\text{Log } K_{OW}$ ) than fluorene. As discussed in Chapter 5, PAH with a higher  $K_{OW}$  would normally be expected to bind more strongly with micelles. However, other physiochemical parameters such as surfactant structure,

aggregation number, micelle geometry, ionic strength, temperature, and the size and chemistry of the PAH might result in a different pattern in  $\text{Log } K_B$  than predicted using  $\text{Log } K_{OW}$ . From the results in this Chapter, it can be stated that the charge on the headgroup does not influence this overall behaviour, as the identical trend of fluorene binding more than phenanthrene was observed for the anionic SDS and SOL micelles as for the cationic CTABr micelles in Ch. 5. Binding of PAHs in SDS micelles had a significantly better correlation with  $\text{Log } K_{OW}$  than binding in SOL micelles, so there may be clues in the differences between these surfactants that will help to explain these results in the future.

#### **6.4 Conclusions**

The SED system has been employed for the determination of binding constants for selected PAHs using SDS and SOL surfactant. Like CTABr binding of PAH described in Ch. 5, the hydrophobic driver is dominant for the binding of PAH in both SDS and SOL micelles. Since cationic surfactants like CTABr are more toxic than anionic surfactants like SDS, this anionic surfactant would be a better choice to treat PAH in MEUF as it provides similar binding. On the other hand, SOL, an anionic surfactant that is switchable, was shown to be less effective for the binding of PAH, so a weaker candidate for the MEUF method.

The correlation between  $\text{Log } K_B$  (in SDS) and  $\text{Log } K_B$  (in SOL) with  $\text{Log } K_{OW}$  supported the idea that  $\text{Log } K_B$  values may be estimated for some additional molecules where  $\text{Log } K_{OW}$  is known. However, hydrophobic character alone cannot explain the binding potential of all individual molecules, as evidenced by the relative results for fluorene and phenanthrene, but rather binding also depends on other physiochemical properties of the compounds.

## 6.5 References

1. Samanta, S. K.; Singh, O.V.; Jain, R. K. *TRENDS in Biotechnology*, **2002**, 20 (6), 243-248.
2. Maila, M. P.; Cloete, T. E. *Int. Biodeter.Biodegr.* **2002**, 50(2), 107-113.
3. "Polycyclic aromatic hydrocarbon" Health Canada. <http://www.hc-sc.gc.ca/> (accessed 06/2013).
4. Qi, W.; Liu, H.; Pernet-Coudrier, B.; Qu, J. *Environ. Sci. Pollut. Res.* **2013**, 20, 4254–4260.
5. Tanaka, H.; Onda, T.; Ogura, N. *Environ Sci Technol.* **1990**, 24, 1179–1186.
6. Wang, W. T.; Simonich, S.; Giri, B.; Xue, M.; Zhao, J.; Chen, S.; Shen, H.; Shen, G.; Wang, R.; Cao, J.; Tao, S. *Environ. Pollut.* **2011**, 159(1), 287–293.
7. Mattsson, J.; Avergård, I.; Robinson, P. *Vatten*, **1991**, 47, 204–211.
8. Bolong, N.; Ismail, A. F.; Salim, M. R.; Matsuura, T. *Desalination*, **2009**, 239, 229–246.
9. Rossnera, A.; Snyderb, S. A.; Knappec, D. R. U. *Water Research*, **2009**, 43, 3787–3796.
10. Zeng, G. M.; Xu, K.; Huang, J. H.; Li, X.; Fang, Y. Y.; Qu, Y. H. *J. Membrane Sci.* **2008**, 310, 149-160.
11. Purkait, M. K.; DasGupta, S.; De, S. *Sep. Purif. Technol.* **2004**, 37 (1), 81-92.
12. Dunn, R. O.; Scamehorn, J. F.; Christian, S. D. *Sep. Sci. Technol.* **1985**, 20 (4), 257-284.
13. Baek, K.; Yang, J. W. *Chemosphere*, **2004**, 57 (9), 1091-1097.
14. Zeng, G.; Fu, H.; Zhong, H.; Yuan, X.; Fu, M.; Wang, W.; Huang, G. *Biodegradation*, **2007**, 18, 303–310.
15. Ceschia, E.; Harjani, J. R.; Liang, C.; Ghoshouni, Z.; Andrea, T.; Brown, R.S.; Jessop, P. G. *RSC Adv.* **2014**, 4, 4638-4645.
16. Chaiko, M. A.; Nagarajan, R.; Ruckenstein, E. *Colloid Interface Sci.* **1984**, 99(1), 168-182.
17. Rouse, J. D.; Morita, T.; Furukawa, K.; Shiau, B. J. *Coll. Surf. A: Physicochemical and Engineering Aspects*, **2008**, 325(3), 180-185.
18. Liu, Y.; Jessop, P. G.; Cunningham, M.; Eckert, C. A.; Liotta, C. L. *Science*, **2006**, 313, 958–960.

19. Jessop, P. G. "Reversibly Switchable Surfactants and Methods of Use Thereof," *PCT Int. Appl.* **2007**, WO 2007/056859 A1.
20. Holmberg, K. in *Reactions and Synthesis in Surfactant Systems*, ed. J. Texter, Marcel Dekker, New York, 2001, pp. 45–58.
21. Jessop, P. G.; Mercer, S. M.; Heldebrant, D. J. *Energy Environ. Sci.* **2012**, *5*, 7240-7253.
22. Lottermoser, A. *Trans. Faraday Soc.* **1935**, *31*, 200–204.
23. Jessop, P. G. *Reversibly switchable surfactants and methods of use thereof.*" U.S. Patent No. 8,283,385. 9 Oct. 2012.
24. Cifuentes, A.; Bernal, J. L.; Diez-Masa, J. C. *Anal. Chem.* **1997**, *69*, 4271-4274.
25. Vautier-Giongo, C.; Bales, B. L. *J. Phys. Chem. B* **2003**, *107*(23), 5398-5403.
26. Kayal, S. I.; Connell, D. W. *Aust. J. Mar. Freshwater Res.* **1990**, *41*, 443-56.
27. Leo, A.; Hansch, C. *J. Org. Chem.* **1971**, *36*(11), 1539-1544.

## Chapter 7

### Summary and Future Work

#### 7.1 Summary of chapters

The aim of this research is to develop a model using SED to guide MEUF method development for the removal of trace organic contaminants from wastewater. This is done by characterization of binding in the micelle-contaminants complex. In chapter 3, we used SED with CTABr, a cationic surfactant, to study binding of sulfonamides from solution, and to examine relationships between binding constants and  $K_{OW}$  and  $pK_{a2}$ . The resulting plots indicate that charge-charge interactions are the driving force in this binding process, and micelle binding is significantly related to the tendency of the compounds to be deprotonated to form a negatively charged species. In chapter 4, we used NMR spectroscopy to characterize bound complexes. NMR confirmed that the sulfonamides are strongly associated with the head-group (Stern layer) region of the micelles, consistent with anionic sulfonamides interacting with cationic headgroups. Orientation of the molecule can be suggested from the relative chemical shift changes of the various protons. It's also possible to model the binding coefficient, which generally confirms the values from SED. In chapter 5, we examined the same CTABr surfactant for binding PAHs to predict whether MEUF can remove PAHs from wastewater. Results indicate that hydrophobic interactions are responsible for binding of PAHs in CTABr micelles. Unlike sulfonamides, PAHs are neutral compounds whose binding was also characterized by examining relationships with the hydrophobic parameter  $K_{OW}$ , which was strongly related to this binding. Results have supported this assumption in general but did not demonstrate good correlation with hydrophobicity for all compounds. In chapter 6, we examined binding with anionic SDS and SOL micelles, SOL being a switchable surfactant. Similarly, results showed significant binding and suggested that MEUF



can effectively remove PAHs using both of the surfactants. Like CTABr micelle, hydrophobic interactions are the main driving force of the binding of PAH with SDS and SOL micelles. SDS showed stronger binding and better correlation with  $K_{OW}$  than SOL. Results also supported the idea that binding of PAHs increases with increasing hydrophobicity. However, the correlation with  $K_{OW}$  was weak, with the trend among PAHs for binding sometimes being different from the trend in  $K_{OW}$ . Other physiochemical properties of the individual compounds must also be contributing to the trend in binding affinity.

## 7.2. General conclusions

Over the last three decades, wastewater treatment technologies have been improved significantly but, at the same time, water pollution has significantly increased due to rapidly growing modern industries and expanded human activities around the world.<sup>1</sup> Membrane technology has found several industrial applications, especially for ultrafiltration.<sup>2</sup> Ultra filtration is useful for water clarification and disinfection, without by-products, in a single step and with a constant permeate quality.<sup>2</sup> It removes bacteria, viruses, proteins and some sugars from effluents after treatment.<sup>3</sup> However, various literature reports suggest that ultra filtration can not remove low molecular weight species such as sulfonamides and PAH from wastewater. MEUF, a type of ultra filtration, is very effective for the treatment of trace organic compounds in wastewater.<sup>4-6</sup>

In this research, we proposed SED as a means of characterizing binding, which was used to predict MEUF performance. The SED method is a non-pressure driven method, however it includes contaminants binding with micelles and being separated in a manner similar to the conventional MEUF system. We examined the potential of MEUF to remove ionic and neutral organic contaminants from wastewater. SED was used to determine binding constants, which are

key to predicting MEUF performance and characterizing contaminant binding to micelles. SED was done on sulfonamides in anionic and neutral form. Sulfonamides are found to bind strongly with cationic micelles only if they are in the negative form, so charge-charge interactions dominate in this binding process. NMR spectroscopy confirmed the association of the negative groups in the sulfonamides with the cationic head groups of CTABr micelles.

SED was also done on neutral PAH compounds. We found that PAHs bind strongly with all cationic and anionic micelles due to hydrophobic interactions. We found higher correlation between binding constants and  $K_{OW}$  for PAH than for sulfonamides. This is consistent with the hydrophobic parameter ( $K_{OW}$ ) because sulfonamides have lower  $K_{OW}$  values than PAH. Unlike sulfonamides, we did not use NMR spectroscopy for binding characterization of PAHs in micelles. This is because NMR is less sensitive and cannot detect low concentrations of PAH in the solution.

We used varieties of surfactants that include cationic and anionic surfactants in this SED study in order to determine suitable surfactants best fit in our system. We found cationic surfactant is the best fit for the negatively charged contaminants. In case of neutral contaminants, both cationic and anionic surfactants can be used for the treatment. Even though both cationic and anionic surfactants work in our system, anionic surfactants may be recommended as they are less toxic. We also used switchable anionic surfactant for binding with PAH in the SED method. We used sodium laurate (SOL) as switchable surfactant which has worked in our system but it was found comparatively less effective than other surfactants. However, switchable surfactants can be used to recover the extracted substance and surfactant, for example, if they can be made to precipitate.<sup>7</sup> We need separate experiments where switching "off" and "on" can be applied in order to justify this theory in our system, in future experiments.

The lowest binding constant ( $\text{Log } K_B$ ) we measured by SED was  $1.46 \pm 0.05$ . The lower limit to binding constant depends on the standard deviation of the measurements of both retentate and permeate side concentrations. This is because a term in the equation is the difference between the retentate and permeate side concentrations. Upper limit to binding constant depends on the LOD of the permeate site concentration as LOD is much higher than standard deviation. As for example, we measured permeate side concentration of pyrene is  $2.24 \times 10^{-9}$  M which is close to the LOD (1.28 ppb or  $6.3 \times 10^{-9}$  M). Therefore, the upper limit for  $\text{Log } K_B$  may be the  $\text{Log } K_B$  of pyrene, which was measured as 5.07.

SED experiments were done with simple solutions but SED can be done on real water samples as long as the analysis method can handle the matrix. SED is a simple, inexpensive experiment that needs only a sensitive analysis method to be available for contaminants of interest. We can estimate binding efficiency of the unknown contaminants through the SED predictive binding model.

### **7.3. Future work**

We determined binding constants between selected sulfonamide antibiotics and CTABr using semi-equilibrium dialysis (SED). The general approach used here should work for other group of compounds. We need to apply this method to the specific group of compounds which can form negative charge in the solution subsequently we need to compare and verify the binding correlation with our results. We constructed free energy relationship with different parameters that include  $\text{Log } K_{OW}$  and  $\text{p}K_{a2}$ . This linear free energy relationship might be influenced by pH, temperature and other thermodynamic entities. We need to investigate this in our SED method.

We also determined binding constants between selected PAH which are neutral in nature, with cationic, anionic and switchable surfactants. We need to find other neutral compounds and test them in the SED system in order to confirm the suitability of this method for the neutral compounds. PAH experiments in the SED indicate that binding constants are not following the expected order of hydrophobic trend. Fluorene shows higher binding affinity than other PAH. We need to find more scientific information and data that will well support our results.

The main purpose of this research is to use SED to predict removal efficiency of the contaminants in the MEUF. We conducted SED experiments with the selected sulfonamides and PAH prepared solution in the laboratory. We need to use the real wastewater samples with same selected contaminants to compare with our results. Therefore, future work would be applying our SED method for sulfonamide and PAH in the real wastewater treatment system equipped with pressure and associated logistics similar to the other advanced treatment system in order to verify whether the  $K_B$  values we determined are good for predicting the performance of MEUF.

There are lots of other environmental contaminants that need to be tested and validated in the SED method. Sulfonamides are mainly related to sewage contamination, our next interest is the treatment of wastewater released from Canadian oil sands, which is recognized as one the most contentious environmental issues in Canada. Untreated oil sands produced waters (OSPW), including the water in tailings ponds, is a major environmental concern. OSPW are a very complex mixture of different toxic organic and inorganic contaminants.<sup>8</sup>

We did not test our SED method on inorganic contaminants yet. Future work will be also testing inorganic contaminants in the SED to find out whether it can be used for predicting binding efficiency in the MEUF as well.

It is important to select appropriate surfactants for binding with contaminants in the SED method. Some surfactants have very high CMC that might cause less total binding of the contaminants as fewer micelles will be produced in the retentate side of the SED cell at equilibrium. Some surfactants are toxic and some are expensive. We used several surfactants in the SED method. We need to test more surfactants with same contaminants that we used in our research in order to find better correlation and binding. The same tests should be repeated in real samples and compared with the prepared laboratory samples. Other contaminants should be tested with various surfactants as well. It would be future work to identify appropriate surfactants which will give better binding to contaminants as well as it being less toxic. Cost, toxicity, Critical Micelle Concentration (CMC), solubility, and transport permeability through the membrane will be taken into account for finding suitable surfactants. CMC can be changed by certain parameters such as pH, temperature or addition of chemicals. So, it would be future work to control CMC under certain condition especially for the surfactants which have higher CMC and the surfactants which can precipitate at room temperature.

We also used switchable surfactants but we did not apply switch "off" and "on" technique in our SED method. It would be an important tool to recover pollutants from SED. Therefore, it refers to future work to find applicable switchable surfactants in the SED system. The membrane is also an important ingredient of the SED experiment. Different membranes have different pore size and cut-off point of the molecule. Moreover, high concentrations of certain organic materials can react with membrane polymer matrixes to cause degradation or swelling.<sup>9</sup> It needs to be investigated in future to identify any degradation product was produced in our system. In our research, we also noticed that fluorine has relatively higher binding affinity to micelle than other

PAH. We need many more experiments with more PAH to develop a constructive relationship with  $K_{OW}$  to find this answer. This would be another future research.

#### 7.4 References

1. Chun, Y.; Khay-chun, T.; Yan-rong, X. *J. Environ. Sci.* **2002**, *14(1)*, 1-6.
2. Ciardelli, G.; Corsi, L.; Marcucci, M. *Resour., Conserv and Recy.* **2000**, *31*, 189–197.
3. Gadani V, Irwin R, Mandra V. *Desalination*, **1996**, *106*, 47–53.
4. Zeng, G. M.; Xu, K.; Huang, J. H.; Li, X.; Fang, Y. Y.; Qu, Y. H. *J Membrane Sci.* **2008**, *310 (1-2)*, 149-160.
5. Purkait, M. K.; DasGupta, S.; De, S. *Sep. Purif. Technol.* **2004**, *37 (1)*, 81-92.
6. Dunn, R. O.; Scamehorn, J. F.; Christian, S. D. *Sep. Sci. Technol.* **1985**, *20 (4)*, 257-284.
7. Jessop, P. G. Reversibly switchable amidine surfactants and methods of use thereof. *PCT Int. Appl.* **2007**, WO 2007/056859.
8. Langlais, B.; Reckhow, D.; Brink, D. *Ozone in Water Treatment-Application and Engineering*; Lewis Publishers: Chelsea, Michigan. 1991, pp 224-229.
9. Nausbaum, I.; Riedinger, A. B. *In Water Treatment Plant Design*; Sanks, R. L., Ed.; Ann Arbor Science: Ann Arbor, Mich. 1978; pp 623-652.

## Appendix A

### Additional data for chapter 3

*Table A1.1. Sample preparation of sulfonamides*

Sulfonamides	M.W(g/mole)	Wt taken(g)	Volume, H <sub>2</sub> O (ml)	Conc. (M)	Conc.(mM)
Sulfacetamide	214.24	0.0040	100	0.000187	0.187
Sulfadiazine	250.28	0.0049	100	0.000196	0.196
Sulfaguanidine	214.24	0.0026	100	0.000121	0.121
Sulfamerazine	264.31	0.0042	100	0.000159	0.159
Sulfamethoxazole	253.28	0.0036	100	0.000142	0.142
Sulfathiazole	255.32	0.0039	100	0.000153	0.153
Sulfanilamide	172.20	0.0026	100	0.000151	0.151
Sulfamethazine	278.33	0.0036	100	0.000129	0.129
Sulfadoxin	310.30	0.0034	100	0.000110	0.110

*Table A1.2. Modified Log K<sub>B</sub>*

Sulfonamide	HPLC analysis		pH	Conductivity analysis	
	[Sulfonamide] <sub>Retentate</sub> (M)	[Sulfonamide] <sub>Permeate</sub> (M)		[Sulfonamide <sup>-</sup> ] <sub>Permeate</sub> (M)	log K <sub>B</sub> (pH adjusted)
1. Sulfadoxine	4.06 ± 0.18 (x10 <sup>-5</sup> )	0.70 ± 0.07 (x10 <sup>-6</sup> )	8.06	0.69 ± 0.07 (x10 <sup>-6</sup> )	4.14 ± 0.20
2. Sulfathiazole	5.25 ± 0.60 (x10 <sup>-5</sup> )	1.40 ± 0.14 (x10 <sup>-6</sup> )	8.22	1.30 ± 0.13 (x10 <sup>-6</sup> )	3.99 ± 0.26
3. Sulfamethoxazole	3.72 ± 0.23 (x10 <sup>-5</sup> )	1.38 ± 0.14 (x10 <sup>-6</sup> )	8.49	1.37 ± 0.14 (x10 <sup>-6</sup> )	3.75 ± 0.19
4. Sulfamerazine	5.83 ± 0.29 (x10 <sup>-5</sup> )	2.50 ± 0.13 (x10 <sup>-6</sup> )	8.09	1.38 ± 0.13 (x10 <sup>-6</sup> )	3.93 ± 0.11
5. Sulfamethazine	5.79 ± 0.29 (x10 <sup>-5</sup> )	3.79 ± 0.16 (x10 <sup>-6</sup> )	7.84	2.78 ± 0.12 (x10 <sup>-6</sup> )	3.63 ± 0.10
6. Sulfadiazine	4.10 ± 0.20 (x10 <sup>-5</sup> )	5.61 ± 0.41 (x10 <sup>-6</sup> )	8.05	5.49 ± 0.40 (x10 <sup>-6</sup> )	3.23 ± 0.12
7. Sulfacetamide	4.78 ± 0.24 (x10 <sup>-5</sup> )	5.30 ± 0.53 (x10 <sup>-6</sup> )	8.17	5.29 ± 0.53 (x10 <sup>-6</sup> )	3.29 ± 0.16
8. Sulfaguanidine	3.72 ± 0.19 (x10 <sup>-5</sup> )	32.7 ± 3.3 (x10 <sup>-6</sup> )	8.27	0.030 ± 0.003 (x10 <sup>-6</sup> )	4.56 ± 0.08
9. Sulfanilamide	3.61 ± 0.30 (x10 <sup>-5</sup> )	31.8 ± 2.4 (x10 <sup>-6</sup> )	8.37	0.29 ± 0.02 (x10 <sup>-6</sup> )	3.49 ± 0.11

**Table A1.3. Free sulfadiazine concentrations in the permeate side with different time (h)**

<b>Time (h)</b>	<b>Conc. Permeate (M)</b>
0.00	1.00E-10
0.50	6.98E-05
1.00	7.41E-05
2.00	9.38E-05
2.50	9.71E-05
3.00	1.09E-04
3.50	1.10E-04
4.00	1.10E-04
4.50	1.22E-04
5.00	1.27E-04
5.50	1.29E-04
6.00	1.30E-04
6.50	1.35E-04
7.25	1.41E-04
8.00	1.45E-04
22.00	1.74E-04
23.00	1.76E-04

**Table A1.4. Free surfactant (CTABr) concentration in the both permeate and retentate side with different time (h)**

<b>Time(h)</b>	<b>Conductivity (<math>\mu</math>S/cm)</b>	
	<b>Permeate</b>	<b>Retentate</b>
0.17	38.4	321
2	79.1	313
4	119	289
6	134	286
24	142	265
48	167.7	260
72	175.7	272
96	145	258



**Table A1.5. CMC determination through lower range and higher range calibration curve**

CTABr(mM)	Conductivity ( $\mu\text{S}/\text{cm}$ )
0	20.1
0.2	52
0.4	70
0.6	86.9
0.8	110
1	118.6
1.2	129
1.6	142.5
2.2	162.5
3	181.5
4	196.8

**A2. HPLC Chromatogram**

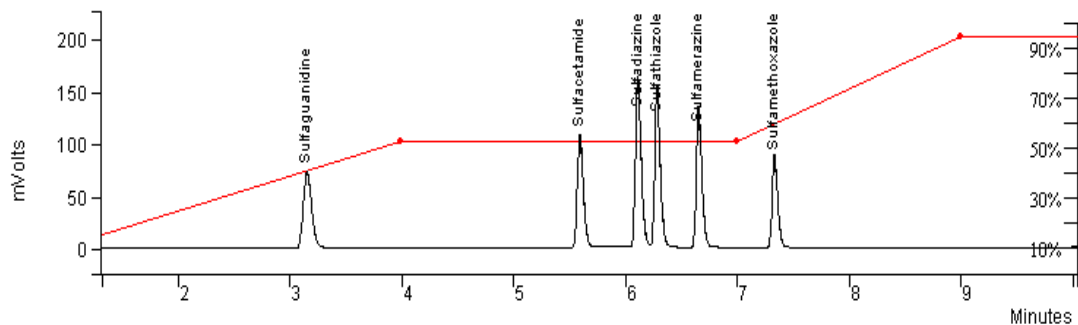


**Fig. A2.1.** HPLC Chromatogram of the STD six sulfonamides (Sulfaguanidine, Sulfacetamide, Sulfadiazine, Sulfathiazole, Sulfamerazine, Sulfamethoxazole)

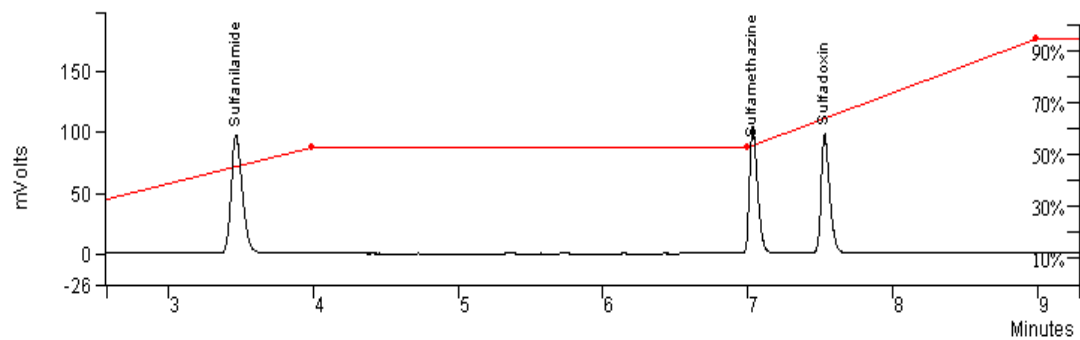


**Fig. A2.2.** HPLC Chromatogram of the STD three sulfonamides (Sulfanilamide, Sulfamethazine, Sulfadoxin)

## Appendix B

### Additional data for chapter 4

*Table B1.1. CMC determination of CTABr in D<sub>2</sub>O through lower range and higher range calibration curve*

CTABr(mM)	Conductivity (μS/cm)
0	20.1
0.15	24.5
0.3	36.3
0.6	57.6
1	81.2
1.25	85.4
2	103.8
3	124
4	144.3
5	157.3
6	179.3

*Table B1.2. Chemical shift of the different protons of Sulfadoxine*

CTABr Conc. (mM)	Proton A		Proton B		Proton C		Proton D		Proton E	
	δ <sub>0</sub>	δ	δ <sub>0</sub>	δ	δ <sub>0</sub>	δ	δ <sub>0</sub>	δ	δ <sub>0</sub>	δ
0	6.74	6.74	7.57	7.57	7.75	7.75	3.84	3.84	3.69	3.69
0.625	6.74	6.74	7.57	7.54	7.75	7.71	3.84	3.84	3.69	3.69
1.00	6.74	6.7	7.57	7.56	7.75	7.72	3.84	3.82	3.69	3.68
1.25	6.74	6.72	7.57	7.62	7.75	7.87	3.84	3.86	3.68	3.68
2.0	6.74	6.65	7.57	7.55	7.75	7.72	3.84	3.80	3.69	3.67
2.5	6.74	6.66	7.57	7.55	7.75	7.72	3.84	3.80	3.69	3.67
4.0	6.74	6.65	7.57	7.56	7.75	7.75	3.84	3.80	3.69	3.68
5.0	6.74	6.65	7.57	7.57	7.75	7.72	3.84	3.80	3.69	3.68
6.2	6.74	6.59	7.57	7.5	7.75	7.66	3.84	3.74	3.69	3.62
8.0	6.74	6.64	7.57	7.56	7.75	7.73	3.84	3.80	3.69	3.68
10.0	6.74	6.64	7.57	7.57	7.75	7.73	3.84	3.80	3.69	3.68

**Table B1.3. Chemical shift of the different protons of Sulfamethazine**

CTABr Conc. (mM)	Proton A		Proton B		Proton C		Proton D	
	$\delta_0$	$\delta$	$\delta_0$	$\delta$	$\delta_0$	$\delta$	$\delta_0$	$\delta$
0	6.76	6.76	7.63	7.63	2.22	2.22	6.58	6.58
0.625	6.76	6.76	7.63	7.65	2.22	2.21	6.58	6.57
1.00	6.76	6.64	7.63	7.68	2.22	2.14	6.58	6.3
1.25	6.76	6.68	7.63	7.65	2.22	2.17	6.58	6.43
2.0	6.76	6.61	7.63	7.68	2.22	2.14	6.58	6.27
2.5	6.76	6.64	7.63	7.7	2.22	2.16	6.58	6.31
4.0	6.76	6.63	7.63	7.74	2.22	2.13	6.58	6.18
5.0	6.76	6.63	7.63	7.72	2.22	2.13	6.58	6.18
6.2	6.76	6.63	7.63	7.73	2.22	2.13	6.58	6.21
8.0	6.76	6.64	7.63	7.74	2.22	2.15	6.58	6.2
10.0	6.76	6.65	7.63	7.73	2.22	2.14	6.58	6.21

**Table B1.4. Chemical shift of the different protons of Sulfanilamide**

CTABr Conc. (mM)	Proton A		Proton B	
	$\delta_0$	$\delta$	$\delta_0$	$\delta$
0	6.82	6.82	7.59	7.59
0.625	6.82	6.81	7.59	7.6
1.00	6.82	6.80	7.59	7.6
1.25	6.82	6.81	7.59	7.6
2.0	6.82	6.81	7.59	7.6
2.5	6.82	6.81	7.59	7.6
4.0	6.82	6.81	7.59	7.6
5.0	6.82	6.81	7.59	7.6
6.2	6.82	6.81	7.59	7.6
8.0	6.82	6.81	7.59	7.6
10.0	6.82	6.81	7.59	7.6

## B2. NMR Spectrum (500 MHz, D<sub>2</sub>O)

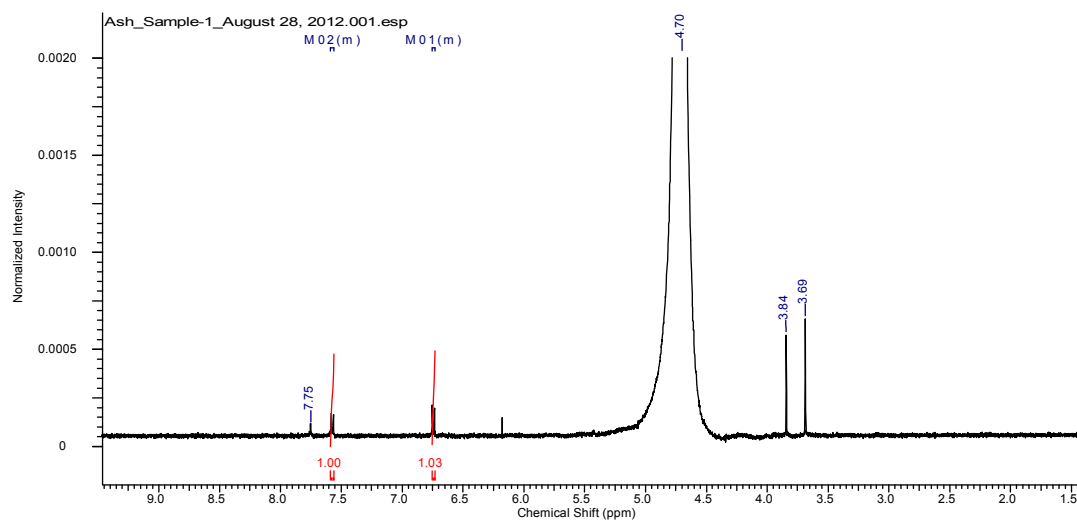


Fig. B2.1. Sulfadoxine

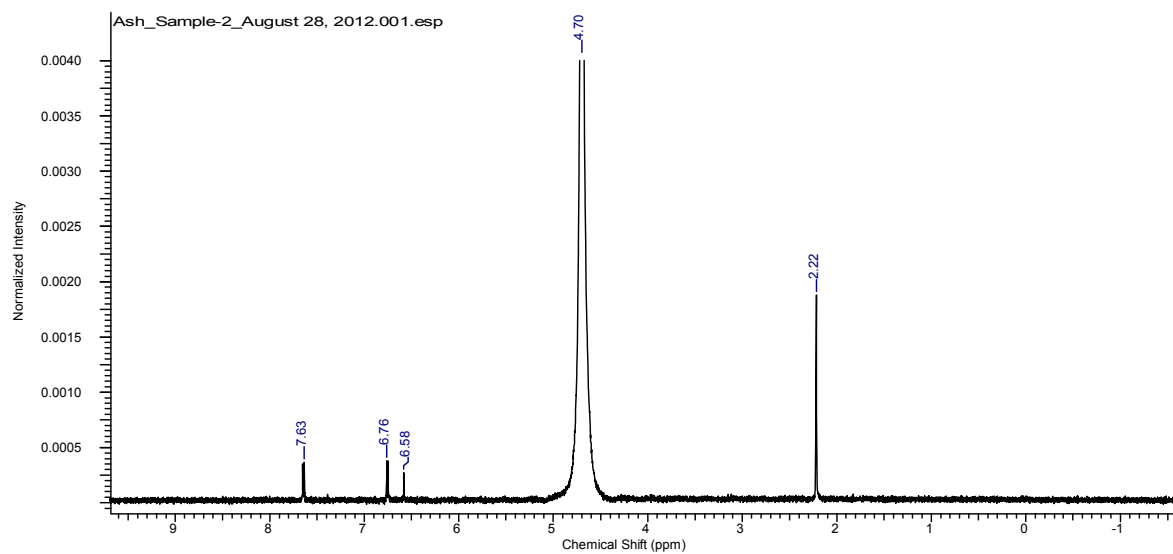
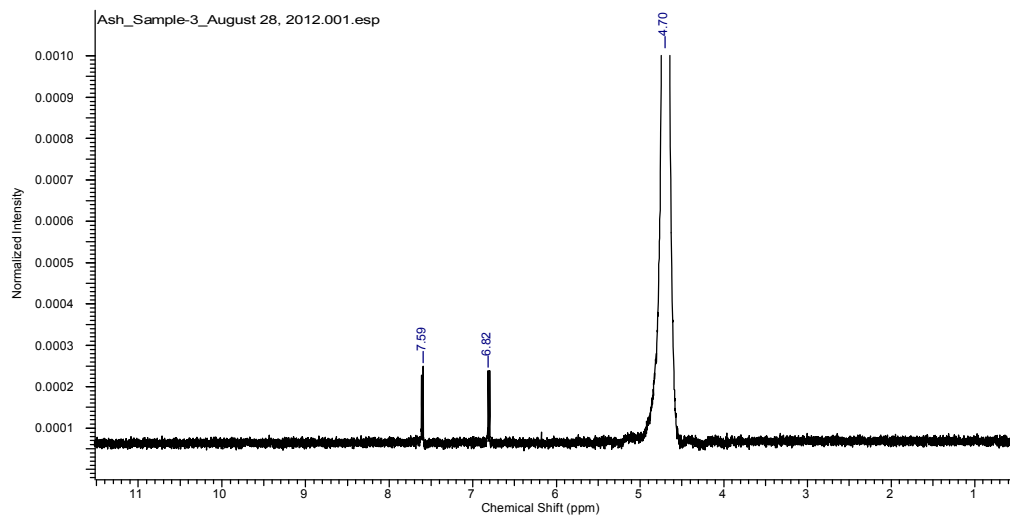
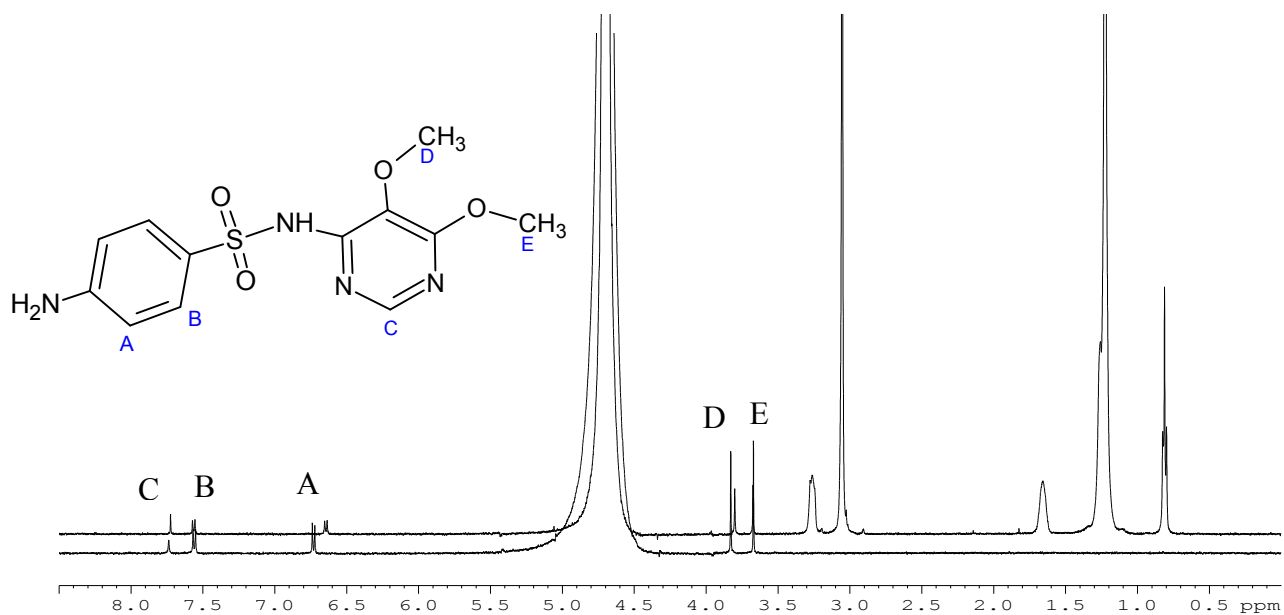


Fig. B2.2. Sulfamithazine



**Fig.B2.3.** Sulfanilamide

*NMR Spectrum of Sulfadoxine (500 MHz, D<sub>2</sub>O)*



**Fig. B2.4.** Chemical shift changes of Sulfadoxine with CTABr concentrations (10 mM)

*NMR Spectrum of Sulfanilamide (500MHz, D<sub>2</sub>O)*

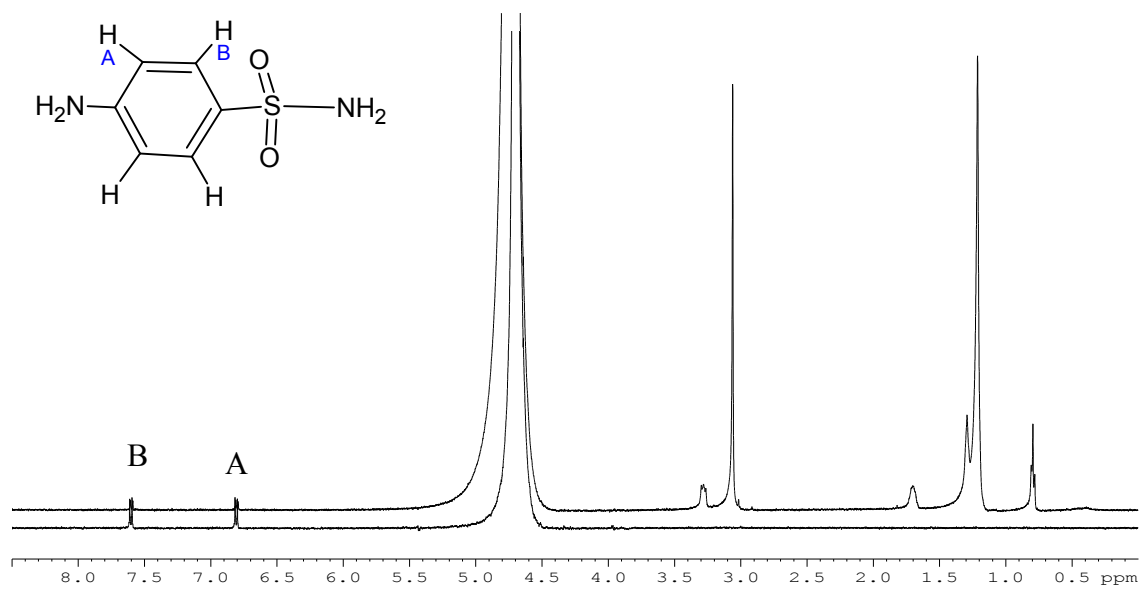


**Fig. B2.5.** Chemical shift changes of sulfanilamide with CTABr concentrations (10mM)

## Appendix C

### Additional data for chapter-5

#### *C1. Emission spectrum of PAHs*

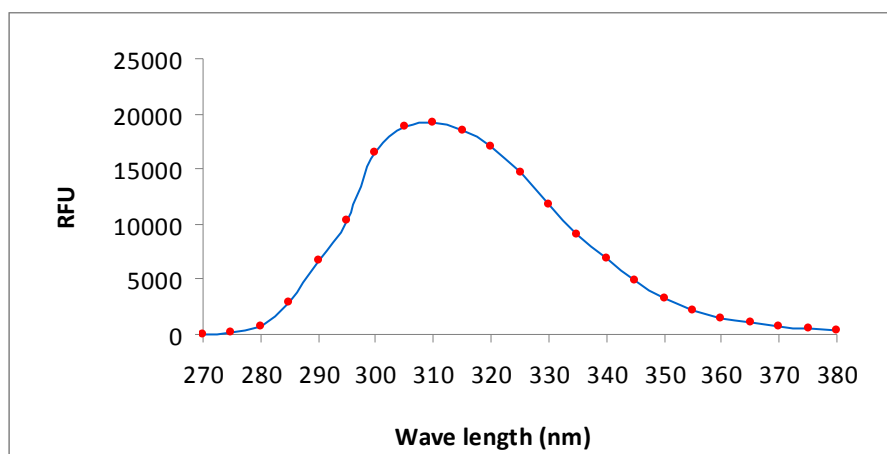


**Fig. C1.1.** Emission spectrum of Fluorene (Ex: 258 nm; emission range: 270-380nm; Emission max: 310 nm)

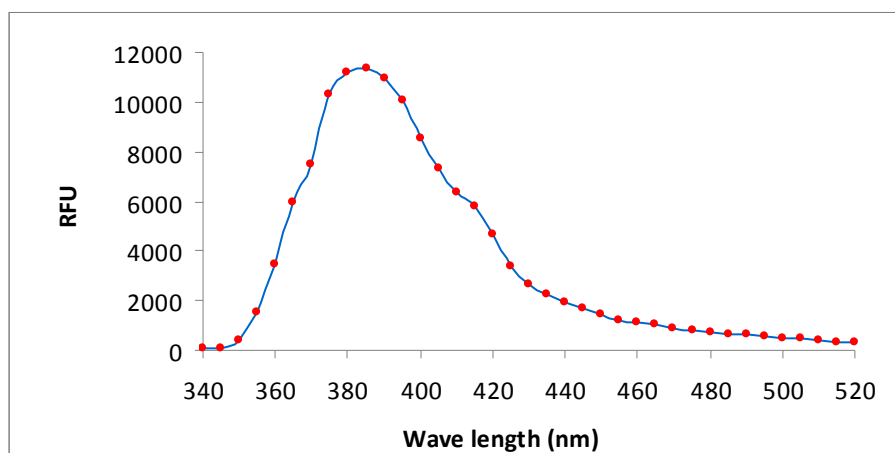


**Fig. C1.2.** Emission spectrum of Pyrene (Ex: 260 nm; emission range: 340-520 nm; Emission max: 358 nm)



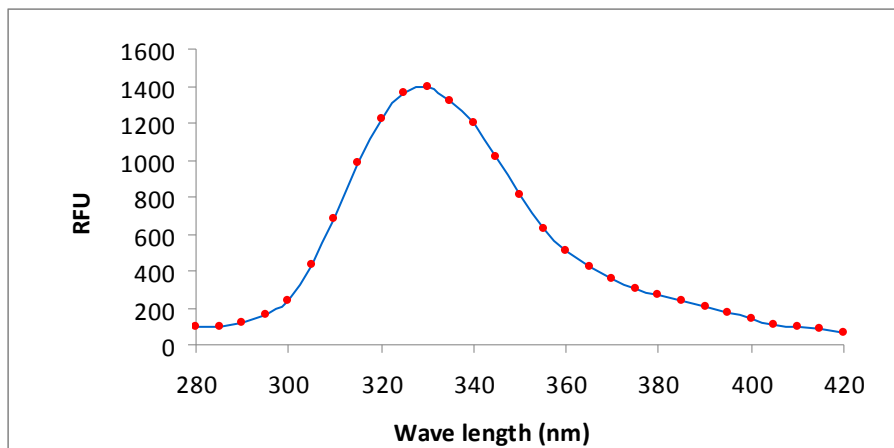


**Fig. C1.3.** Emission spectrum of Naphthalene (Ex: 270 nm; emission range: 280-420 nm; Emission max: 330 nm)

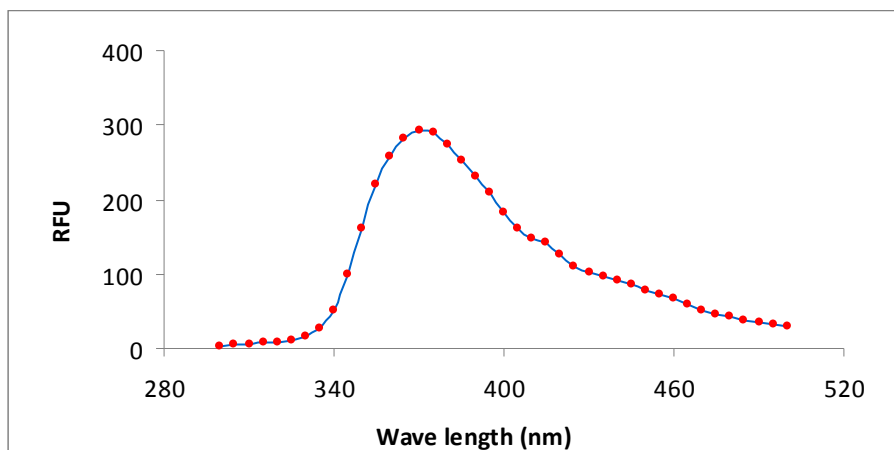


**Fig. C1.4.** Emission spectrum of Phenanthrene (Ex: 250 nm; emission range: 300-500 nm; Emission max: 370 nm)

## C2. Calibration curve of PAHs

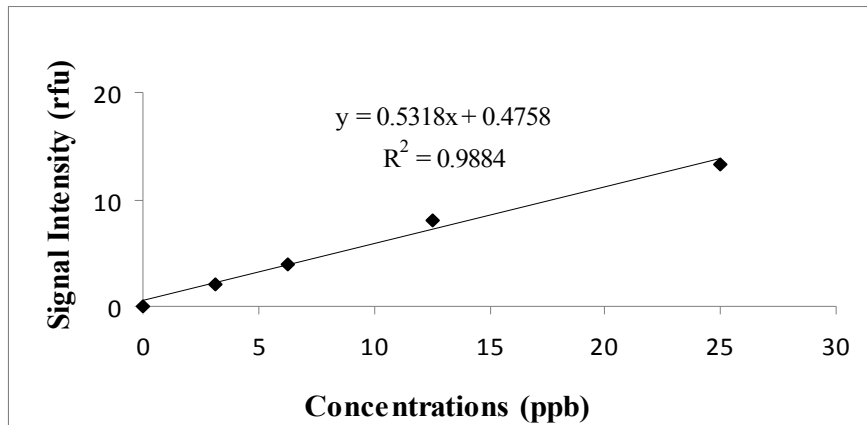


Fig. C2.1. Low range calibration curve of Naphthalene

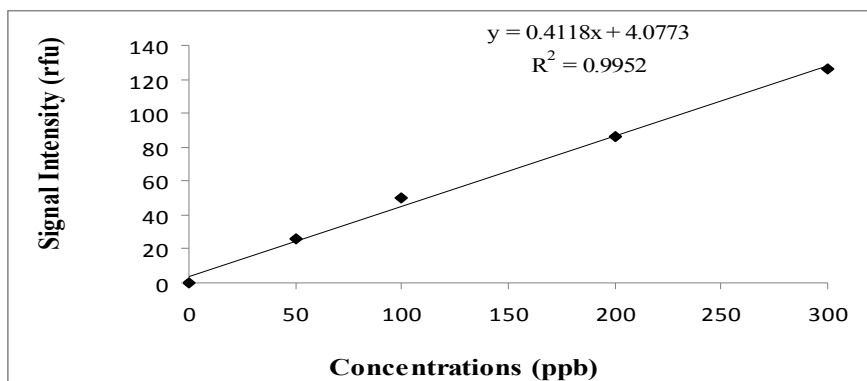


Fig. C2.2. High range calibration curve of Naphthalene

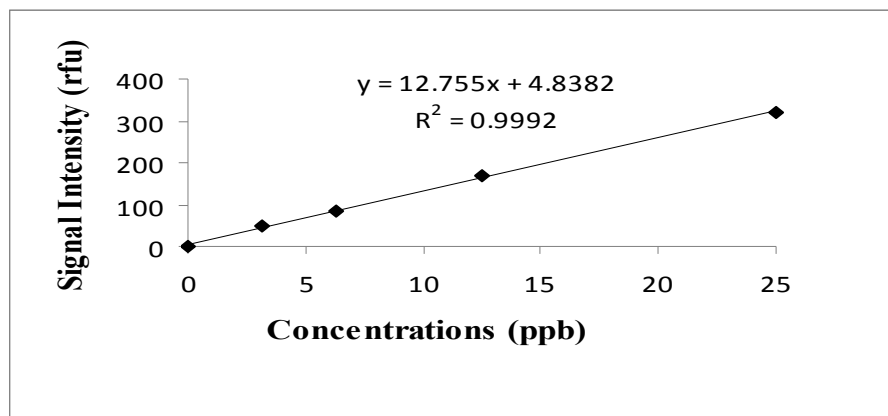


Fig. C2.3. Low range calibration curve of Fluorene

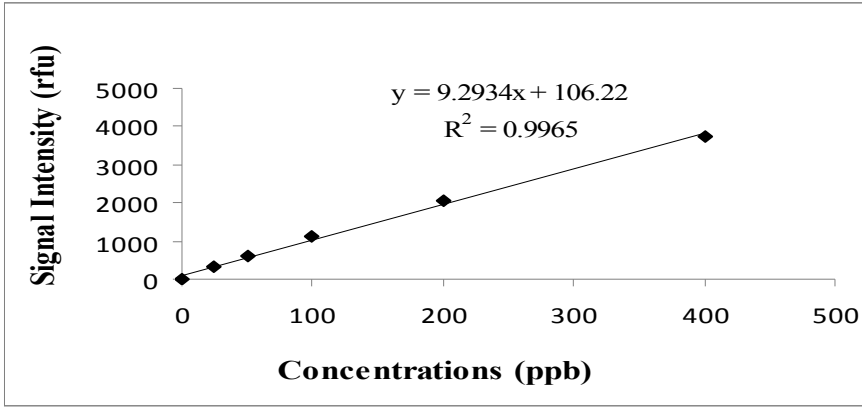


Fig. C2.4. High range calibration curve of Fluorene

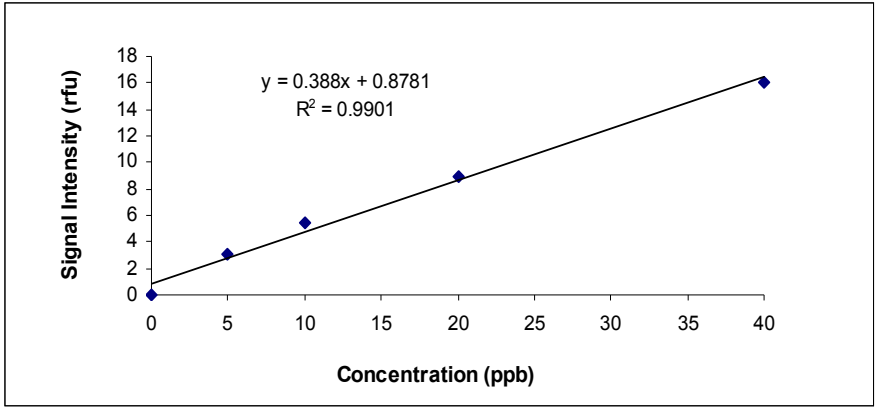


Fig. C2.5. Low range calibration curve of Phenanthrene

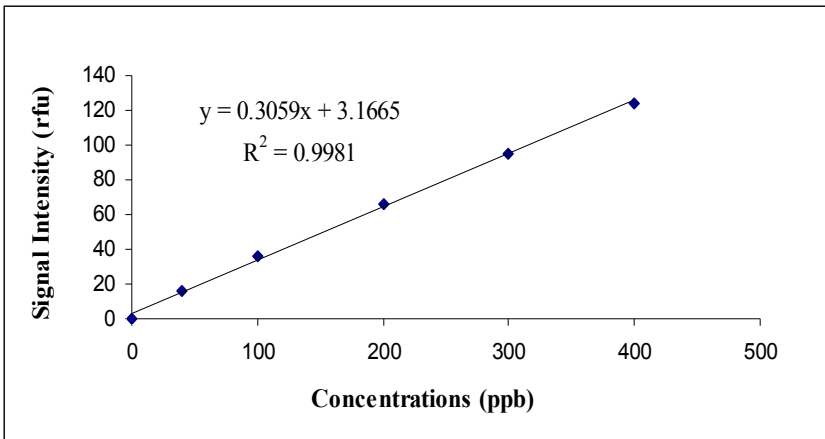


Fig. C2.6. High range calibration curve of Phenanthrene

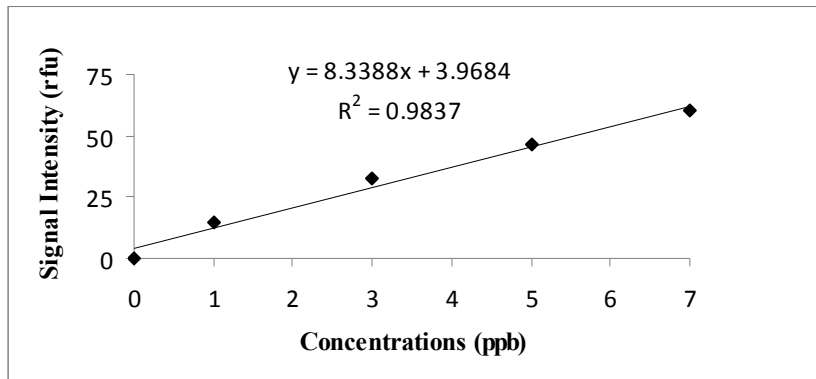


Fig. C2.7. Low range calibration curve of Pyrene

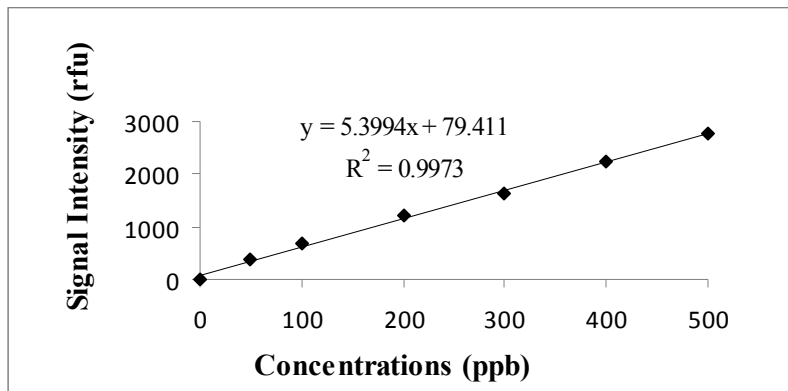


Fig. C2.8. High range calibration curve of Pyrene

**Table C3.1. CMC determination of CTABr by conductivity meter with 1.25% ethanol**

<b>CTABr(mM)</b>	<b>Conductivity (<math>\mu</math>S/cm)</b>
0	17.87
0.2	36
0.4	57.6
0.6	72
0.8	81.7
1	97.7
1.5	111.9
2	130
3	154.7
4	183.7
5	201
6	226

**Table C3.2. Equilibrium experiment of Fluorene**

<b>Hour (h)</b>	<b>Permeate side (M)</b>
2	0.000302
4	0.000517
6	0.000734
8	0.000822
12	0.000978
18	0.00105
24	0.00107

## Appendix D

### Additional data for chapter-6

*Table D1.1. CMC determination of SDS with 1.25% ethanol*

SDS (mM)	Conductivity ( $\mu\text{S}/\text{cm}$ )
20	875
18	821
16	773
14	720
12	662
10	621
8	545
6	426
4	293
3	222
2	160.3
1	92.1
0	20.4

*Table D1.2. CMC determination of SOL with 1.25% ethanol*

SOL(mM)	Conductivity ( $\mu\text{S}/\text{cm}$ )
40	1960
35	1768
30	1614
25	1439
20	1178
15	906
10	604
5	315
0	11.2

***Table D1.3. Equilibrium expt. of Pyrene in SDS (fluorescence measurement)***

<b>Hour (h)</b>	<b>Pyrene Conc. (permeate side)</b>
1	1.29 E-08
12	2.19 E-08
18	2.70 E-08
24	2.97 E-08

***Table D1.4. Equilibrium expt. of SOL***

<b>Hour (h)</b>	<b>Permeate side (M)</b>
1	0.00444
2	0.00740
4	0.00972
6	0.0117
8	0.0123
12	0.0123